ILMATIETEEN LAITOS
METEOROLOGISKA INSTITUTET
FINNISH METEOROLOGICAL INSTITUTE

145
CONTRIBUTIONS

# MODELLING CIRCULATION DYNAMICS IN THE NORTHERN BALTIC SEA

**ANTTI WESTERLUND**

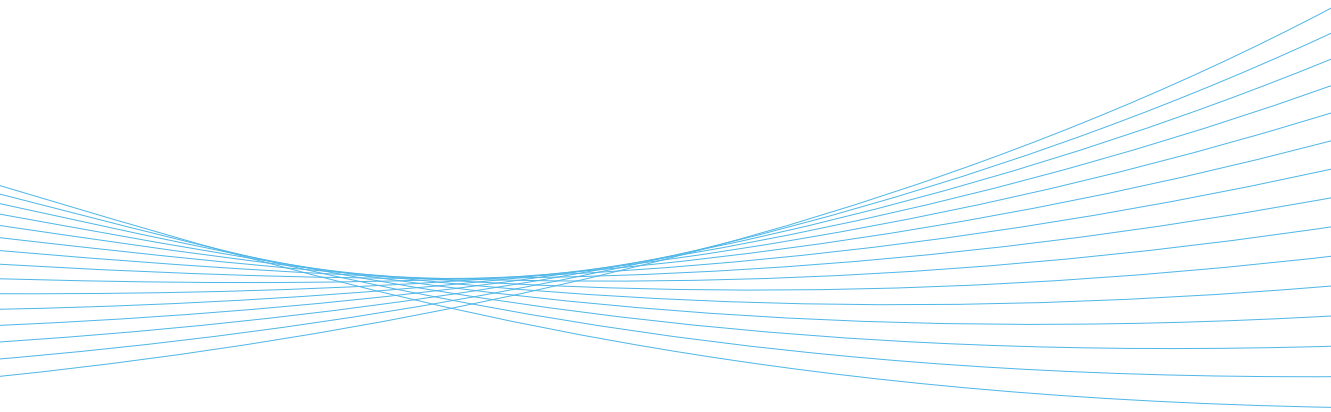

FINNISH METEOROLOGICAL INSTITUTE
CONTRIBUTIONS
No. 145

# Modelling circulation dynamics in the northern Baltic Sea

Antti Westerlund

Institute for Atmospheric and Earth System Research
Faculty of Science
University of Helsinki
Helsinki, Finland

ACADEMIC DISSERTATION

To be presented with the permission of the Faculty of Science of the University of Helsinki for public examination and criticism in auditorium D101 of the Physicum building (Gustaf Hällströmin katu 2, Helsinki) on the 23rd of November, 2018, at 12 o'clock noon.

Finnish Meteorological Institute
Helsinki, 2018

Supervisor Dr Laura Tuomi
Marine Research
Finnish Meteorological Institute
Helsinki
Finland

Pre-examiners Assoc. Prof. Lars Arneborg
University of Gothenburg and
the Swedish Meteorological and Hydrological Institute
Norrköping
Sweden

Dr Vladimir Ryabchenko
P.P. Shirshov Institute of Oceanology
Russian Academy of Sciences
St. Petersburg
Russia

Opponent Dr Andreas Lehmann
GEOMAR Helmholtz Centre for Ocean Research
Kiel
Germany

Custos Prof. Petteri Uotila
Institute for Atmospheric and Earth System Research
Faculty of Science
University of Helsinki
Helsinki
Finland

ISBN 978-952-336-054-9 (paperback)
ISSN 0782-6117
Erweko Oy
Helsinki 2018

ISBN 978-952-336-055-6 (pdf)
Helsinki 2018

FINNISH METEOROLOGICAL INSTITUTE

Published by
Finnish Meteorological Institute
(Erik Palménin aukio 1), P.O. Box 503
FIN-00101 Helsinki, Finland

Series title, number and report code of publication
Finnish Meteorological Institute Contributions 145,
FMI-CONT-145
Date
November 2018

Author(s)
Antti Westerlund

Title
Modelling circulation dynamics in the northern Baltic Sea

Abstract

Circulation and surface layer dynamics are of significant importance, for example, when considering how hazardous substances or nutrients are transported in the sea. The earliest studies mapping circulation patterns in the northern Baltic Sea were done before the Second World War and were based on lightship observations. Although the number of available observation points was low, these studies showed that there is a cyclonic long-term surface circulation pattern in the northern sub-basins.

Even today, there are considerable research gaps and uncertainties in knowledge. For example, observational data still has insufficient coverage, descriptions of processes in numerical models need tuning to the conditions of the Baltic Sea and model forcing data can have large uncertainties. With modern analysis methods and new observational datasets, gaps in the current understanding of Baltic Sea circulation patterns can be identified and analyzed.

In this thesis, circulation dynamics were investigated in the northern Baltic Sea with numerical hydrodynamic modelling. The complex dynamics of the brackish Baltic Sea put hydrodynamic models to the test. Several different model configurations were applied and developed further, including a high-resolution configuration of the NEMO (Nucleus for European Modelling of the Ocean) model for the Gulf of Finland (GoF). Methods such as machine learning algorithms, new data from automated observational platforms and ensemble forecasting were applied. Circulation patterns in the GoF were investigated with the self-organizing map (SOM) algorithm.

The cyclonic circulation pattern visible in earlier studies was not seen in the GoF in the overall means calculated from the model results for the studied periods 2007–2013 and 2012–2014. SOM analysis of currents in the GoF revealed that they are highly variable and complex. There was significant inter-annual and intra-annual variability in the circulation patterns. A connection between wind forcing and the characteristic patterns from the SOM analysis was found. Analysis emphasized the estuary-like nature of the GoF. The results showed that circulation in the GoF changes rapidly between normal estuarine circulation and reverse estuarine circulation. The fact that the dominant wind direction is from the southwest supports this reversal. The cyclonic mean circulation pattern seems to appear only if the normal estuarine circulation is common enough for it to emerge during the averaging period. Small changes to wind direction distribution can have a significant effect on the long-term circulation patterns. Upwelling events on a timescale of days to weeks can also affect long-term circulation patterns.

The NEMO model proved to be a suitable tool for the studies of circulation in the northern sub-basins of the Baltic Sea. It quality seems comparable to other models commonly used in the GoF and Bothnian Sea.

The GoF is still a challenging environment for circulation modelling. Salinity gradients in the GoF are still not reproduced in a satisfactory manner by the models. More information is required on how well the models reproduce true circulation patterns and, for example, upwelling frequency and intensity. The need for accurate model inputs, especially wind forcing, was demonstrated. The value of observations (especially the better spatial coverage of current measurements) was once again emphasized. Furthermore, the results highlighted that care must be taken to make sure that models and observations represent the same thing when they are compared.

Publishing unit
Finnish Meteorological Institute, Marine Research

Classification (UDC)
551.46

Keywords
Baltic Sea; Gulf of Finland; Bothnian Sea;
hydrodynamic modelling; circulation modelling

ISSN and series title
0782-6117 Finnish Meteorological Institute Contributions

ISBN
978-952-336-054-9 (paperback)
978-952-336-055-6 (pdf)

Language
English

Pages
141

ILMATIETEEN LAITOS


| | | |
|---|---|---|
| Julkaisija | Ilmatieteen laitos<br>(Erik Palménin aukio 1)<br>PL 503, 00101 Helsinki | Julkaisun sarja, numero ja raporttikoodi<br>Finnish Meteorological Institute Contributions 145,<br>FMI-CONT-145<br>Päiväys<br>marraskuu 2018 |



Tekijä(t)
Antti Westerlund


Nimeke
Itämeren pohjoisosien kiertoliikkeen dynamiikan mallintamisesta

Tiivistelmä


Meren virtausolot ja pintakerroksen dynamiikka ovat merkittäviä tekijöitä esimerkiksi silloin, kun selvitetään haitallisten aineiden tai ravinteiden kulkeutumista. Varhaisimmat Itämeren yleistä kiertoliikettä kartoittaneet tutkimukset tehtiin ennen toista maailmansotaa, ja ne perustuivat majakkalaivahavaintoihin. Vaikka havaintoja oli tuolloin käytössä vain vähän, Itämeren pohjoisissa altaissa voitiin pitkällä aikavälillä havaita sykloninen pintavirtauskuvio (ts. pohjoisella pallonpuoliskolla vastapäivään).

Sittemmin Itämeren pohjoisosien kiertoliikettä on tutkittu lisää, mutta edelleen tiedoissa on puutteita ja epävarmuustekijöitä. Esimerkiksi havaintoaineistoja on yhä melko vähän ja mittauspisteet ovat harvassa. Lisäksi monet numeeristen mallien prosessikuvauksista perustuvat valtamerillä tehtyyn tutkimukseen, ja mallien syötteenä käytetyissä pakoteaineistoissa – esimerkiksi säätiedoissa – on epätarkkuuksia. Moderneilla analyysimenetelmillä ja uusilla havaintoaineistoilla näitä puutteita pystytään tunnistamaan ja analysoimaan.

Tässä tutkimuksessa tutkittiin Itämeren pohjoisosien virtausolosuhteita hydrodynaamisen mallinnuksen avulla. Itämeri on murtovesiallas, ja sen dynamiikka on monimutkaista. Tämä tekee sen numeerisesta mallintamisesta haastavaa. Työssä käytettiin useita mallinnuskonfiguraatioita ja niitä myös kehitettiin kuvaamaan Itämeren olosuhteita aiempaa paremmin. Näihin lukeutui korkean resoluution Suomenlahti-konfiguraatio, joka perustuu NEMO-malliin (Nucleus for European Modelling of the Ocean). Tutkimuksessa käytettiin myös koneoppimismenetelmiä, automaattisten mittalaitteiden tuottamia havaintoaineistoja ja parviennusteita. Suomenlahden virtauskentän ominaispiirteitä analysoitiin itseorganisoituvilla kartoilla eli Kohosen kartoilla (self-organizing map, SOM).

Kun Suomenlahden mallinnetuista pintavirtauskentistä laskettiin keskiarvot koko tutkituilta ajanjaksoilta 2007–2013 ja 2012–2014, tuloksissa ei näkynyt aiemmissa tutkimuksissa havaittua syklonista virtauskuviota. Aineistoa SOM-menetelmällä analysoitaessa Suomenlahden virtaukset osoittautuivat hyvin vaihteleviksi ja monimutkaisiksi. Virtauksissa havaittiin paljon sekä vuosien välistä että niiden aikana tapahtuvaa vaihtelua. Mallin tuulipakotteen ja SOM-analyysin tuottamien karakteristisiten virtauskenttien välille löydettiin yhteys. Analyysin tulokset korostivat Suomenlahden samankaltaisuutta estuaarien eli jokisuulahtien kanssa. Aineistossa kiertoliike Suomenlahdella vaihteli nopeasti normaalin estuaarikiertoliikkeen ja käänteisen estuaarikiertoliikkeen välillä. Suomenlahdella vallitsevat lounaistuulet tukivat käänteistä kiertoliikettä. Mallinnusaineiston perusteella näyttää siltä, että sykloninen pintavirtauskuvio tulee näkyviin vain, jos tutkimusjakson aikana normaali estuaarikiertoliike esiintyy riittävän usein. Pienetkin muutokset tuulten suuntajakaumassa voivat vaikuttaa virtauskentän pitkän aikavälin keskiarvoihin merkittävästi. Myös kumpuaminen, joka näkyy päivien ja viikkojen aikaskaalalla, vaikuttaa virtausdynamiikkaan.

NEMO-malli soveltui hyvin virtausten tutkimiseen Itämeren pohjoisosissa. Sen tulosten laatu oli samankaltainen kuin aikaisemmin alueella käytettyjen numeeristen mallien.

Tässä tutkimuksessa saavutetusta edistyksestä huolimatta Suomenlahti on edelleen haastava alue virtausmallinnukselle. Malleilla on yhä vaikeuksia tuottaa Suomenlahden voimakkaita vertikaali- ja horisontaaligradientteja sisältävä suolaisuuskenttä. Tutkimuksessa kävi ilmi, että mallien syötteiden – erityisesti tuulipakotteen – tarkkuudella on suuri merkitys mallien tuloksille. Myös havaintojen merkitys mallikehitykselle korostui. Jatkossa tarvitaan kattavampia havaintoaineistoja, jotta voidaan arvioida mallien kykyä tuottaa virtauskenttä ja esimerkiksi kumpuamistapausten taajuus ja voimakkuus. Varsinkin virtaushavaintojen parempi alueellinen kattavuus olisi tärkeää. Tutkimuksessa kävi myös ilmi, miten tärkeää on malleja ja havaintoja vertailtaessa huolehtia siitä, että ne ovat vertailukelpoisia.



Julkaisijayksikkö
Ilmatieteen laitos, merentutkimus

| Luokitus (UDK) | Asiasanat |
|---|---|
| 551.46 | Itämeri; Suomenlahti; Selkämeri; hydrodynaaminen mallinnus; kiertoliikkeen mallinnus |

ISSN ja avainnimeke
0782-6117 Finnish Meteorological Institute Contributions

| ISBN | Kieli | Sivumäärä |
|---|---|---|
| 978-952-336-054-9 (nid.)<br>978-952-336-055-6 (pdf) | englanti | 141 |

# Preface

This book tries to make some sense of an intrinsically complex and chaotic system: the sea. The long road leading to this book has itself been complex and at times chaotic, yet serendipitous. I have to wonder where would I be if I had not almost randomly chosen to be a physics major at the University of Helsinki at the end of the last century? What if I had not accepted what was supposed to be a brief summer job at the Finnish Institute of Marine Research (FIMR) in 2002? At that time I did not even know there was such a thing as physical oceanography. What if I had not started this PhD project – ten years later – at the Finnish Meteorological Institute (FMI)? Or what if my PhD project had not received funding in 2015?

I want to thank a number of people for their crucial impact along the way. In school, a long time ago, I had some wonderful teachers who explained the significance of the scientific method. At the FIMR, Tapani Stipa introduced me to ocean science. Later at the FMI, Jari Haapala managed to convince me to enrol as a PhD student. His help and vision have been very significant for this project, especially early on. My supervisor Laura Tuomi provided highly valuable guidance numerous times. It has been a privilege to work with a scientist of her skill and ability. I also want to thank my co-authors, who have given me the opportunity to work with them and learn from them. During this thesis project, I have been fortunate enough to benefit from the experience of such insightful oceanographers as Pekka Alenius, Kai Myrberg, Robinson Hordoir and Roman Vankevich, to name but a few.

I would also like to extend my deepest gratitude to the Maj and Tor Nessling Foundation for their financial support. Without them, this project would have taken many more years, or perhaps forever. The impact of their support has been substantial.

Furthermore, I would also like to thank Professors Matti Leppäranta and Petteri Uotila at the university, pre-examiners Lars Arneborg and Vladimir Ryabchenko, my employer the FMI, my fellow PhD students and other colleagues at the FMI and elsewhere. It is not possible to name here every colleague who has helped me, but I make an exception for Simo Siiriä, who has helped me numerous times over the years, both directly and indirectly.

This book most certainly would not exist without my family. Mother, Father, Brother: thank you, for everything, from the very beginning. Petra: you are the sense in this chaos. I owe so much to you. And Otso: you have walked with me during the final years of this endeavour, bringing smiles and caring. Nothing makes me happier than sharing the wonder you feel when we observe the world together, when we ponder where the sun has gone for the night, when we gaze at the stars together or when we discuss whether the Earth has always been so blue. A scientist is not that different from a small child.

Antti Westerlund
Helsinki, September 2018

*Quid enim violentius mari ventisve et turbinibus ac procellis?*

— Gaius Plinius Secundus, Naturalis Historia, 31.1

*The sea is everything. It covers seven-tenths of the terrestrial globe. Its breath is pure and healthy. It is an immense desert, where man is never lonely, for he feels life stirring on all sides. [...] Ah! sir, live – live in the bosom of the waters! There only is independence! There I recognise no masters! There I am free!*

— Captain Nemo, a fictional character in the novel 'Twenty Thousand Leagues Under the Sea' by Jules Verne (1870). (Translated by Lewis Mercier.)

# Contents

# List of original publications

This thesis consists of an introductory part followed by four research articles. In the introductory part, the articles are cited according to their Roman numerals.

**I** **Westerlund A.**, Tuomi L., 2016. Vertical temperature dynamics in the northern Baltic Sea based on 3D modelling and data from shallow-water Argo floats. *Journal of Marine Systems*, 158:34–44. http://dx.doi.org/10.1016/j.jmarsys.2016.01.006

**II** Roiha P., **Westerlund A.**, Haavisto N., 2016. Forecasting upwelling events with the monthly ensembles on the eastern coast of the Gulf of Bothnia, Baltic Sea. *Journal of Operational Oceanography*, 9 (2):115–125. http://dx.doi.org/10.1080/1755876X.2016.1248148

**III** **Westerlund A.**, Tuomi L., Alenius P., Miettunen E., Vankevich R. E., 2018. Attributing mean circulation patterns to physical phenomena in the Gulf of Finland. *Oceanologia*, 60 (1):16–31. https://doi.org/10.1016/j.oceano.2017.05.003

**IV** **Westerlund A.**, Tuomi L., Alenius P., Myrberg K., Miettunen E., Vankevich R. E., Hordoir R., 2018. Circulation patterns in the Gulf of Finland from daily to seasonal timescales. *Tellus*. (submitted)

## Author's contribution

The author was the principal investigator in Articles I, III and IV. In these Articles the author was responsible for the majority of experimental design, modelling, analysis and manuscript preparation. In Article II, the author was responsible for the majority of the modelling. The author also participated in the experimental design, analysis and preparation of the manuscript.

# List of abbreviations

| | |
|---|---|
| **3D** | three-dimensional |
| **ACM** | acoustic current meter |
| **AVHRR** | Advanced Very High Resolution Radiometer |
| **ADCP** | acoustic Doppler current profiler |
| **BACC** | BALTEX Assessment of climate change for the Baltic Sea region |
| **BALTSEM** | Baltic Sea Long-Term Large Scale Eutrophication Model |
| **BMU** | best matching unit |
| **CeCILL** | CEA CNRS INRIA Logiciel Libre |
| **CMEMS** | Copernicus Marine Environment Monitoring Service |
| **COHERENS** | Coupled Hydrodynamical Ecological Model for Regional Shelf Seas |
| **CORE** | Coordinated Ocean-ice Reference Experiments |
| **CTD** | conductivity, temperature and pressure |
| **DWR4** | Directional Waverider 4 |
| **ECMWF** | European Centre for Medium-Range Weather Forecasts |
| **EOF/PCA** | empirical orthogonal functions / principal component analysis |
| **ERA-Interim** | ECMWF Reanalysis Interim |
| **EURO4M** | European Reanalysis and Observations for Monitoring |
| **EuroGOOS** | European Global Ocean Observing System |
| **FIMR** | Finnish Institute of Marine Research |
| **FMI** | Finnish Meteorological Institute |
| **GoF** | Gulf of Finland |
| **GoF2014** | Gulf of Finland Year 2014 |
| **GoB** | Gulf of Bothnia |
| **HF** | high frequency |
| **HIRLAM** | High Resolution Limited Area Model |
| **HIROMB** | High Resolution Operational Model for the Baltic Sea |
| **ICES** | International Council for the Exploration of the Sea |
| **LIM3** | Louvain-la-Neuve Sea Ice Model 3 |
| **NEMO** | Nucleus for European Modelling of the Ocean |
| **NM** | nautical mile |
| **NWP** | numerical weather prediction |
| **NOAA** | National Oceanic and Atmospheric Administration |
| **OAAS** | Oleg Andrejev Alexander Sokolov |
| **OPA** | Océan Parallélisé |
| **OSTIA** | Operational Sea Surface Temperature and Sea Ice Analysis |
| **POM** | Princeton Ocean Model |
| **RaKi** | Programme to promote the recycling of nutrients and improve the ecological status of the Archipelago Sea |
| **RCO** | Rossby Centre Ocean Model |
| **SMHI** | Swedish Meteorological and Hydrological Institute |
| **SOM** | self-organizing map |
| **SST** | sea surface temperature |
| **SYKE** | Finnish Environment Institute |

In the introductory part of the thesis, acronyms that are very common or are commonly used like proper names (e.g. model, project and product names) are introduced in this list only. Other abbreviations are introduced also at first mention.

# 1 Introduction

Physical oceanography is a good example of a discipline that was born from practical needs, as oceanographic data collection and systematization began for navigational purposes (Apel, 1987). It also demonstrates the two complementary sides of natural science. On the one hand, science pushes the limits of what is known and research is motivated by new knowledge in itself. On the other hand, science also has practical applications, with clear benefits to society.

Nowadays, practical needs continue to drive theoretical considerations in oceanography. For example, the study of ocean physics is needed to understand climate change, oil spills and eutrophication. Circulation patterns and surface layer dynamics, the central themes of this thesis, are of significant importance, for example, when considering how hazardous substances or nutrients are transported in the sea, or how heat from the atmosphere is distributed.

A largely stable, urbanized population of 85 million people inhabit the catchment basin of the Baltic Sea (Ducrotoy and Elliott, 2008). Human activities put significant pressure on the environment, in part due to the natural sensitivity of the area (HELCOM, 2018). These factors affect not only the ecosystem but also human well-being. When the effects of climate change are taken into account, it is obvious that the already vulnerable Baltic Sea system is under considerable stress. In many cases, understanding these issues and their potential impact requires studying the physical processes of the system, including circulation dynamics (Stigebrandt, 2001; Leppäranta and Myrberg, 2009).

The main tool in this thesis is 3D hydrodynamic ocean modelling. In a way, numerical models are just another way to systematize knowledge of the oceans. Descriptions of the physics of the sea are codified in the models, which are then used to investigate and analyze the system further. Numerical modelling of the Baltic Sea started with the advent of computers in the 1950s. Today it is an important component of ocean science.

In this work, circulation dynamics are studied in the northern sub-basins of the Baltic Sea (see Fig. 1.1), namely the Gulf of Finland (GoF) and the Gulf of Bothnia (GoB). This section discusses the background information for this endeavour.

## 1.1 How to characterize circulation patterns

Instantaneous fields are often nothing like longer-term averages. An annual or seasonal mean circulation field does not necessarily tell that much about what happens in a timescale of, say, hours or days. It is common to average the circulation field, at least on some timescale. Averaging is also often done spatially.

In practice, long-term mean currents are a statistical property of the ocean system, and as such, they are not what is present in nature at any given moment. It can be useful to accompany averages with quantities describing the statistical properties of the field, for example, the persistency or stability of currents (e.g. Alenius et al., 1998).

Measurements most often involve (near-)instantaneous velocities at a certain

point, and data typically includes all short-term variability in the currents, such as tides and wind fluctuations. Furthermore, the point at which measurements are performed is not necessarily representative of the larger-scale current field. This means that the analysis and interpretation of current data requires processing and diligence. A vector field of currents as a function of time and space can be produced with 3D modelling of circulation patterns, but modelling has its limitations, such as finite resolution and incomplete descriptions of processes (see Section 1.4).

Although averaging and normal statistical calculations are the most common analysis methods for data about currents, other possibilities also exist. Like any other vector field, current fields can also be analyzed using standard mathematical methods. For example, methods such as empirical orthogonal functions / principal component analysis (EOF/PCA) can be used to describe the variability of a circulation field (e.g. Elken et al., 2011; Thomson and Emery, 2014). Another way of describing currents is through the concept of water age (Deleersnijder et al., 2001; Meier, 2005; Myrberg and Andrejev, 2006). Water transports can also be useful when discussing the relation of water budgets and circulation (e.g. Talley et al., 2011b). Also, clustering methods such as self-organizing maps (SOMs) can be used (see Section 3.3).

There are different ways of describing and visualizing the circulation patterns of the sea, which all have their own advantages and disadvantages. An obvious way to visualize them is to display vectors depicting current direction and speed for several points in the sea area. This visualization method was used in this study. For models, the vectors are typically displayed at model grid points. While this is an easy and intuitive way of describing the flow, it is not the only way (e.g. Apel, 1987). One can also show streamlines, for example. The routes of particles can be used to get a more Lagrangian view.

### 1.1.1 Definitions for a time-averaged circulation field

Since circulation and its timescales are important for the results presented in this thesis, it makes sense to spend some time defining the key concepts.

The term *mean circulation* is often used when describing the circulation field (e.g. Leppäranta and Myrberg, 2009; Andrejev et al., 2004). It is commonly not defined in context, but it is taken as an arithmetic mean over a 'sufficiently long' period of time to remove short-term variations. It is usually interchangeably used with *long-term average circulation* (e.g. Kullenberg, 1981). Also, *annual mean circulation* is used at times (e.g. Beletsky and Schwab, 2008), presumably to emphasize that the average has been taken over the whole year instead of just over some seasons for instance. *Climatological circulation* has also been used (e.g. Beletsky et al., 1999; Beletsky and Schwab, 2008). *General circulation*, on the other hand, is usually used to refer to the overall large-scale circulation scheme (e.g. Apel, 1987).

Asking what is a 'sufficiently long' averaging period is a good question. For example, Palmén (1930) used a period of five years to calculate mean currents from observations. Modelling studies have typically used mean circulation to refer

to whatever is the maximum time span of available data. For example, Andrejev et al. (2004) used a modelling period of five years, while Elken et al. (2011) and Lagemaa (2012) used two and three year spans. This issue is discussed further in Section 5.

In studies of estuaries, the term *residual circulation* is often referenced. It is usually defined in estuarine and coastal studies as the circulation field that is left when the periodic motions due to the tides are subtracted (e.g. MacCready and Banas, 2011). It has also been called *sub-tidal circulation*, *tidally averaged circulation* or *tidal residual current* (Naimie et al., 2001; Wei et al., 2004). Typically these terms mean the time-average of the velocity field taken over a sufficiently long time period to remove the tidal signal. In areas where the tides are a significant forcing factor, this is a useful definition. In the Baltic Sea, however, the tides are small and as such, this definition is less relevant.

In practice, *residual mean circulation* has been used as a synonym for a time-averaged circulation pattern (e.g. Meyers et al., 2007; Kikas and Lips, 2016). It has also been used to mean all current patterns remaining after time averaging, regardless of their origin (e.g. Carballo et al., 2009; Herrling and Winter, 2015), differentiating between the causes of the pattern where necessary (e.g. 'residual circulation induced by winds' or 'wind-driven residual circulation'). On the other hand, other sources use the term *residual* in the general sense (a quantity left over after any process; in this case, time-averaging) when describing circulation (e.g. Alenius et al., 1998; Myrberg, 1998; Beletsky et al., 1999; Beletsky and Schwab, 2001). Also, in Article III the long-term mean circulation was referenced in this manner (as residual), even though the patterns discussed in that article were not tide-induced. In the interests of clarity and to avoid confusion, in this introductory part of the thesis the term residual circulation is not used.

*Resultant current* has been used in the literature of Baltic Sea studies for a long time. Hela (1952) is an early English-language example of its use. Typically, resultant current is used interchangeably with *residual current*, *permanent flow* or *background flow* (Alenius et al., 1998). Hela (1952) defines permanent flow as the quantity which is obtained when drift currents are eliminated from actual current data.

## 1.2 Circulation dynamics in the northern Baltic Sea

### 1.2.1 Overview of the system

The Baltic Sea is a semi-enclosed, brackish water basin located in northern Europe. It is a small, shallow sea that has some unique properties that make it an interesting subject for circulation studies. The following overview of the system is based on Leppäranta and Myrberg (2009), Ehlin (1981), Kullenberg (1981) and Omstedt et al. (2014).

One of the things that make the Baltic Sea interesting is its horizontal and vertical gradients. Salinity decreases from the typical ocean values in the Danish Straits to almost zero in the eastern GoF and the northern Bay of Bothnia. Volu-

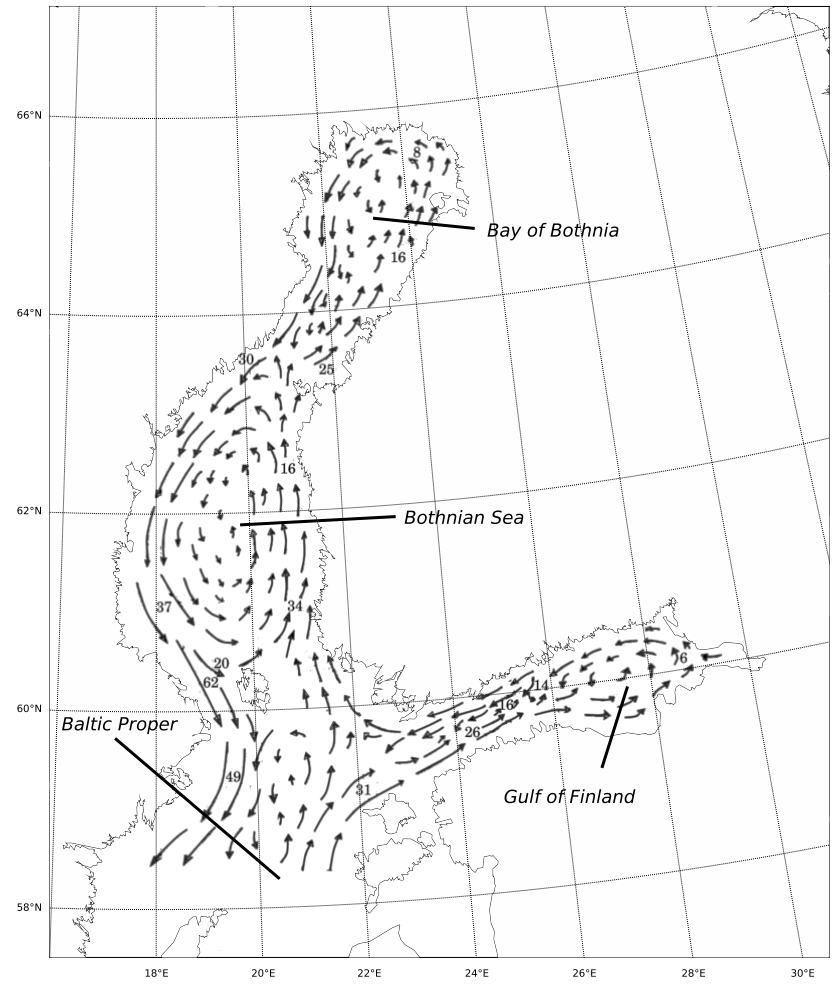


Figure 1.1: The northern sub-basins of the Baltic Sea. The vector overlay is an approximate reproduction of estimated long-term currents from Palmén (1930).

minous river runoffs from its large catchment area bring fresh water to the surface, while saline water inflow from the North Sea via the Danish Straits fills the deeps and replenishes the salinity of the whole system. This creates a permanent two-layer structure with the halocline usually located at a depth of 40–80 metres. There is also a seasonal thermocline from late spring to autumn, with the maximum depth of 10–30 m, typically occurring in August.

The Baltic Sea is a highly non-linear system. Wind stress, tidal forces, sea surface inclination and density differences all induce currents in the sea. Also, volume transport on the boundaries (e.g. river runoffs or transport in the straits) affects currents. The currents in the sea are then steered by topography, friction and Coriolis acceleration.

The overall long-term mean circulation pattern of the Baltic Sea is a combination of the wind-independent baroclinic circulation pattern and mean wind-driven circulation. The wind-independent circulation patterns arise from the density gradients in the system. The Baltic Sea has a positive freshwater balance, which results in a salinity gradient. Waters flowing into the system settle at a depth determined by their density. For fresh waters that means the surface. Roughly speaking, the circulation dynamics of the Baltic Sea can be thought of as a two-layer system, separated by the permanent halocline, wherein the upper and lower layer behave quite differently.

On a timescale of days, wind stress dominates surface currents. Long-term wind-driven mean circulation is weak due to the high variability of winds. But it does contribute to the overall mean in a meaningful way. The relative significance of this contribution depends on the timescale investigated. On a timescale of hours to days, periodic dynamical processes, such as seiches and inertial oscillations, are important. Tides in the Baltic Sea are small.

Overall, long-term surface mean circulation is weak, with average surface current speeds of around 5 cm/s. Cyclonic (counter-clockwise in the northern hemisphere) structures appear in the main basins, although these have varying persistency. Instantaneous drift currents can be of the order of tens of cm/s, reaching values as high as 50 cm/s during storms or even more in straits. In the lower layer, currents are steered by topography and sills limit flows from basin to basin.

Differences between the sub-basins become clear when they are compared more closely. The GoB is the northernmost basin of the Baltic Sea and consists of the Bay of Bothnia, the Bothnian Sea, the Archipelago Sea and the Åland Sea. In the south, the Bothnian Sea has shallow sills (c. 70 m and 100 m in the Åland Sea) and an archipelago to the Baltic Proper. There is also a sill (c. 25 m) in the Quark, which separates the Bothnian Sea from the Bay of Bothnia. These sills limit water exchange. Deepwater in the Bothnian Sea is mostly formed from cooling surface water from the Baltic Proper. The halocline is very weak and mixing is able to penetrate to deeper layers. Recent observations from Argo floats suggest seasonal variation can reach depths of almost 100 m (Haavisto et al., 2018). There is a cyclonic long-term circulation pattern.

The situation is different in the GoF. While the whole Baltic Sea can be thought of as estuary-like, this concept is especially useful for understanding circulation

patterns in the GoF, where there is large freshwater input from the Neva River at the eastern end (inflow c. 78 $km^3/a$) and free exchange of water with the Baltic Proper at the western end. Salinity gradients in the GoF are relatively strong, with near-zero salinities in the Neva Bay and values typically around 10 in the deeper layers near the boundary to the Baltic Proper. Estuarine circulation is established by freshwater forcing and density-driven currents (cf. e.g. Talley et al., 2011a). The fresh river waters from the head of the estuary in the east flow on the surface outwards towards the mouth of the estuary in the west. A compensating flow of saltier, denser water is transported in the opposite direction, deeper in the water column. This circulation pattern is then modified by other factors, such as wind forcing, topography and geostrophic effects. In the short-term, variable winds are the main driver of currents in the GoF. Overall, circulation patterns in the GoF are very complex and variable. While a cyclonic pattern has been reported in the literature (see Section 1.2.2), the persistency of currents is smaller than in the Bothnian Sea.

The differences between these two sub-basins also mean that the challenges for circulation modelling are different. Whereas in the Bothnian Sea, a 2 NM horizontal resolution appears to be enough to capture the essential features of the circulation field (cf. Article I), in the GoF a much higher resolution seems to be required to do the same.

A more detailed description of physics in the GoB can be found in Håkansson et al. (1996). For in-depth descriptions of the physical oceanography of the GoF, see, for example, Alenius et al. (1998), Soomere et al. (2008), Soomere et al. (2009), Leppäranta and Myrberg (2009) and Myrberg and Soomere (2013).

### 1.2.2 Early studies

There have been several studies that have mapped the circulation patterns in the northern Baltic Sea over the last hundred years or so. The works of Witting (1912), Palmén (1930) and Hela (1952) together formed an understanding of circulation patterns in the northern Baltic Sea, which served as the foundation for later studies.

While Stepan Makarov had already published a study of the hydrography and circulation in the GoF (Leppäranta and Myrberg, 2009) in 1894, the mapping of large-scale circulation patterns in the northern Baltic Sea became feasible after regular observations of current variations began (in Finland this was in 1907). Preceding decades had seen an international push for systematic ocean observations. As a part of that effort, more regular observations of the water body of the northern Baltic Sea were performed. In Finland, for example, the main focus up until then had been on the observation of ice conditions. Mälkki (2001) notes that, apart from scientific curiosity, this interest in oceanography was also motivated by the need to show independence of the Russian influence in the Grand Duchy of Finland.

Regular current observations were done from lightships (see Fig. 1.2) using a cross tied to a rope. Weights and floaters could be attached to the cross to control its depth. A compass was used for determining current direction. By combining the results from Swedish, Estonian and Finnish lightships, better spatial coverage could be achieved. These observations were first used by Witting (1912), who


Figure 1.2: Lightship Äransgrund, pictured most likely in 1893. This vessel was one of the ships stationed in the Gulf of Finland to guide seafarers. Regular scientific observations from Finnish lightships started in 1907 and were used in several studies, for example by Palmén (1930) in his study of northern Baltic Sea circulation patterns (Mälkki, 2001).

created long-term circulation maps based on them, originally for a book called *The Atlas of Finland*. However, the most notable pre-war contribution was by Palmén (1930), who presented a map of surface circulation for the northern basins of the Baltic Sea (see Fig. 1.1). The cyclonic mean circulation pattern visible in his results is still referred to as Palmén circulation. Palmén's maps show that average surface currents in the GoF have low stability and are only a fraction of the instantaneous velocities observed.

After the Second World War, political tensions made efforts to study the Baltic Sea as a whole more difficult (Alenius et al., 1998). Soon after the war the currents in the GoF were considered by Hela (1952), who also relied on the pre-war lightship observations. He concentrated on characteristic flows and drift currents, and the relationship between wind and currents.

The number of observation points in these early studies was low. The authors of these studies were well aware of the uncertainties involved. Palmén (1930) himself commented on this several times, at one point noting:

> *In order to get a better overview, I have tried to draw a map of surface currents based on these data. Of course, coming up with such a map requires a quite bold interpolation approach as the number of stations for current measurements is far too low to depict the details of the current features correctly.*[1]

Palmén also clearly notes the statistical nature of mean circulation patterns and comments on the significant seasonal and inter-annual variability of the currents.

[1] Passage translated from the original German by Andrea Gierisch, who is gratefully acknowledged.

## 1.3 Surface layer dynamics and circulation

Circulation patterns emerge as the sum of numerous different processes, which, in connection to and in interaction with each other, produce the flow field in a basin. The response of the system to forcing is non-linear. Therefore, improvements in understanding and modelling different processes will also affect the accuracy overall. Here, these interconnections are considered from two different perspectives when the effect of stratification and upwelling on circulation is discussed.

Stratification is one of the most important aspects characterising coastal seas and estuaries. In fact, because of its significant effect on dynamics, stratification has long been used to categorize estuaries (e.g. Stacey et al., 2011). Stratification is significant due to its effect on vertical mixing. A pycnocline effectively divides the water column into two, and there can be strong vertical shears and velocity differences at the boundary (e.g. Geyer and Ralston, 2011).

The water column can become stratified due to salinity and temperature variations. During the summer in the Baltic Sea, as discussed in Section 1.2.1, there can be two pycnoclines at different depths (or even more if secondary pycnoclines are taken into account). This is challenging for ocean models (e.g. Myrberg et al., 2010; Tuomi et al., 2012). In addition to the temporal variation there is also spatial variation. For example, the halocline in the GoB can be very weak (with a salinity difference of about 0.5 from surface to bottom). In the GoF, the halocline is more of an estuary-type salt wedge, with at times almost linear salinity gradients.

Through its significance for vertical mixing, stratification also affects a multitude of other issues, including the dynamics of all tracers in seawater, such as salt, oxygen and nutrients. Stratification affects the momentum transfer in the water column, and a pycnocline can effectively decouple the two layers from each other.

Wind-induced coastal upwelling is another example of the connections between stratification and currents. This phenomenon is prevalent in the Baltic Sea (Lehmann and Myrberg, 2008).

Wind stress acting on the ocean surface generates drift. According to the Ekman motion theory, net water transport is to the right of the wind direction (in the northern hemisphere). When wind blows alongshore and the coast is on the left, drift is directed offshore. This creates water depletion in the upper layers, which is replenished from below (e.g. Cushman-Roisin and Beckers, 2011). This is called upwelling. During the summer the water originating below the seasonal thermocline tends to be colder, more saline and richer in nutrients than surface waters. In addition to the Ekman transport of the surface layer, other currents are also associated with the event. In a stratified elongated basin, the coastal upwelling current is accompanied by a downwelling current on the opposite coast. Also, an alongshore current is produced on both coasts.

Stratification and wind affect the formation of the upwelling event. For example, if stratification is strong, weaker winds can induce upwelling. If stratification is weak, wind energy will be mixed deeper in the water column and stronger winds are required for an upwelling event to take place. Based on data from the GoF, Haapala (1994) suggested that in an unstratified situation, a wind impulse of

roughly double the size is required to trigger an upwelling event when compared to the stratified case. Also, the wind impulse alone does not determine the magnitude of the upwelling event (Kikas and Lips, 2016). This means that inaccuracies in the depth or steepness of the thermocline can lead to inaccuracies in modelled upwelling events.

An upwelling event tilts pycnoclines across the basin and mixes surface waters with waters originating from deeper layers. Their contribution to the vertical mixing in basins such as the GoF seems to be significant (Lips et al., 2009). Overall, it is obvious that in relatively small areas (such as the GoF and the GoB), where upwelling events take place quite frequently, the effect of the phenomenon on the hydrography, and subsequently on circulation fields, is significant.

## 1.4 Model studies of circulation patterns in the northern Baltic Sea

Hydrodynamic ocean modelling is used to understand the physical processes of the sea. The basics of ocean modelling are reviewed in a number of textbooks (e.g. Cushman-Roisin and Beckers, 2011).

Many 3D hydrodynamic models have been implemented for the Baltic Sea and its sub-basins over the years. Earlier modelling efforts have been reviewed for example by Leppäranta and Myrberg (2009) and Myrberg (1997, 1998). Some more recent modelling studies have been discussed by Omstedt et al. (2014). In the last two decades, fruitful investigations of the northern Baltic Sea have been carried out with models such as HIROMB (e.g. Elken et al., 2011), RCO (e.g. Meier, 2005, 2007), OAAS (e.g. Andrejev et al., 2004; Myrberg and Andrejev, 2006), POM (e.g. Zhurbas et al., 2008; Ryabchenko et al., 2010) and COHERENS (e.g. Tuomi et al., 2012, 2018a). (There are many more examples of models and model studies. The list is inevitably incomplete and does not do justice to the large amount of work that has gone into modelling efforts.)

Baltic Sea circulation patterns have been investigated with numerical models since the 1970s. These early models were often severely limited in several ways, but could already describe some fundamental aspects of Baltic Sea circulation patterns. For example, in 1975, Sarkisiyan et al. first modelled the cyclonic circulation pattern including the GoF (cited by Leppäranta and Myrberg, 2009). A few years later, Kielmann (1981) modelled wind-driven circulation with different idealized scenarios and also included maps for the northern sub-basins. The models around this time still very much needed further improvements. Kielmann, for instance, described the quality of his results as unsatisfactory. As time passed, 3D modelling of the Baltic Sea slowly started to reach a resolution and accuracy sufficient for in-depth investigations of long-term mean circulation. One can cite Krauss and Brügge (1991) or Lehmann (1995) as examples of developments in the 1990s.

Baltic Sea–wide circulation studies showed cyclonic surface current patterns for the northern sub-basins (e.g. Lehmann and Hinrichsen, 2000). Andrejev et al. (2004) modelled the GoF's mean circulation for the five-year period 1987–1992. They found a cyclonic circulation pattern that was mostly in line with previous

studies. They also found the circulation field in the GoF to have numerous mesoscale features, such as eddies.

While there have been several studies concentrating specifically on the GoF, there have been far fewer specifically for the GoB. Myrberg and Andrejev (2006) modelled the mean circulation in the GoB. Based on a 10-year barotropic model run they found the expected cyclonic mean circulation pattern in the Bothnian Sea. This agrees with results from Baltic Sea–wide studies (Omstedt et al., 2014; Meier, 2007).

Recent modelling studies of the circulation in the GoF have shown more variability in the results. For example, Maljutenko et al. (2010) and Soomere et al. (2011) did not find the traditional cyclonic circulation pattern. On the other hand, Elken et al. (2011) modelled the GoF's mean circulation for 2006–2008 and found a cyclonic surface circulation pattern. However, this run was extended for 2010–2011 by Lagemaa (2012); for these years, the results showed anticyclonic loops and no clear cyclonic pattern.

Much of the difference between modelling studies can be explained by interannual variability and differences in model configurations. However, it is interesting that several studies have lately shown similar anticyclonic features. It is at the moment difficult to be certain how much of the variability visible in these models is a feature of those models and not of nature. It is possible that models deviate more from observations now than they perhaps once did, perhaps due to problems common to these models or to their forcing. Or it is also possible that they indicate some true changes in circulation patterns. Observational data does not provide a clear answer, as many of these studies are based on moored current measurements and have too low spatiotemporal coverage to form an overall view of the circulation field in the basin. More work is required to study this issue.

In this study the primary tool is NEMO, which is a community 3D ocean model developed by a consortium and published under the CeCILL open source licence (Madec and the NEMO team, 2008). It has been used widely in global climate applications (e.g. Flato et al., 2013) and also in operational oceanography (Blockley et al., 2014) and regional applications (e.g. Guihou et al., 2018; Tranchant et al., 2016). It originally grew from the OPA model. It also includes components for sea ice and biogeochemistry.

The NEMO model has been successfully applied to regional applications for many areas, including the Baltic Sea. A configuration called NEMO Nordic has been specifically made for studying the Baltic Sea (Hordoir et al., 2013, 2015, 2018). This configuration originated from the Swedish Meteorological and Hydrological Institute (SMHI). Several adaptations have been made to ensure that the model works well in this area. These include, of course, appropriate bathymetry and forcing data, but also adjustments to bottom friction and turbulence schemes, for example. Different versions of the basin-wide configuration exists, for example versions for long-term and short-term studies. In addition to the NEMO Nordic configuration, which covers the whole Baltic Sea and also the North Sea, there is also a high-resolution configuration for the GoF. This configuration is based on the work by Vankevich et al. (2015, 2016).

## 1.5 Applications for Baltic Sea circulation studies

### 1.5.1 Circulation dynamics and the living sea

Understanding the ecology and biogeochemistry in the Baltic Sea requires the understanding of two things: on the one hand, the ecological and biogeochemical processes, on the other hand, the physical transport system. Circulation dynamics determine much about the boundary conditions experienced by ecosystems.

As Stigebrandt (2001) puts it, 'the physical transport system of the Baltic Sea is composed of currents and mixing processes'. This means that currents and mixing — in other words advective and diffusive processes — are the effects that move all the tracers in the sea around, including nutrients, salt and oxygen.[2] If circulation patterns change, large-scale tracer distributions can also change, which will have an effect on the ecosystems.

For example, nutrients such as nitrogen and phosphorus are central to the issue of eutrophication. They have numerous sinks and sources, and understanding them requires advanced knowledge about biogeochemistry. But they are also transported in the sea by physical processes, so an understanding of the whole system is required.

Eutrophication can be defined as an increase in the rate of supply of organic matter to an ecosystem (Nixon, 1995). The consequences of eutrophication include harmful algal blooms and hypoxia. It has long been a problem in the Baltic Sea. While the problem has been identified for decades, its significance had not been fully recognized earlier (HELCOM, 2009, 2014). Lately it has been estimated that in the GoF the situation has been bad since the 1970s (Andersen et al., 2017). Significant resources have been devoted to the studying the issue in the area. Large-scale efforts, such as the Gulf of Finland Year 1996 and Gulf of Finland Year 2014 (GoF2014) have on the one hand brought scientists together with other stakeholders, and on the other hand, they have assisted in the creation of observational datasets that make further investigations possible (Raateoja and Setälä, 2016).[3] In the GoB, the ecological status of the area has been much better, but lately signs of deterioration have also been observed (e.g. HELCOM, 2014; Fleming-Lehtinen et al., 2015; Lundberg et al., 2009).

Another issue quite obviously connected to the large-scale physical transport system is how hazardous substances are transported when they enter the sea. These substances — be they oil spills, chemicals or radioactive substances — are, like other tracers, moved by currents and mixed by turbulent diffusion. Similar examples can be given for other tracers, for example oxygen.

[2] Note that different definitions for an ocean tracer exist (e.g. Talley et al., 2011c; Jenkins, 2014; Klymak and Nash, 2009). Some definitions include active tracers, like salt and temperature, while others only include passive tracers.

[3] http://www.gulfoffinland.fi/

### 1.5.2 Changing climate and circulation

Climate change also affects the Baltic Sea. Many projected changes have potential side effects on circulation fields. For example, changes in wind forcing and salinity can be expected to affect circulation. Understanding and quantifying these effects requires the study of circulation dynamics. Some of the key changes are briefly reviewed here, mainly based on the BACC II report (BACC II Author Team, 2015).

The Baltic Sea area has variable weather conditions. Westerly winds are dominant, but all other winds directions are also observed. Future changes in winds remain uncertain.

In the last century the maximum sea ice extent has decreased and the length of the ice season has become shorter. Sea ice cover is projected to diminish considerably in all climate scenarios, although some seasonal ice cover is still expected in the future in northern parts of the Baltic Sea.

The salinity dynamics of the Baltic Sea are rather poorly known and large uncertainties remain. No clear trend in the salinity of the Baltic Sea has been observed. The salinity of the Baltic Sea is dependent on the frequency and intensity of inflows of saline water from the Danish Straits. Major Baltic inflows only take place under specific and quite rare circumstances (e.g. Leppäranta and Myrberg, 2009). In the future, the salinity may very well change. Current estimates expect it to lower (Meier et al., 2011, 2012), but it is still uncertain if it will in fact do the opposite. The uncertainties are still large and it is impossible to say what will happen with confidence.

The question of salinity is also linked to precipitation. No long-term trend has been observed in precipitation or river runoff so far, but precipitation is projected to increase across the whole region during the winter. Evaporation is projected to increase with rising temperatures. Changes to annual runoff are unclear, but the yearly cycle is expected to change.

The waters and the atmosphere are warming in the Baltic Sea region, with the largest increases in Bay of Bothnia and the GoF. Seasonal changes have also been observed. An additional sea surface temperature (SST) increase of several degrees is projected for the coming decades, depending on the climate scenario and the geographical area. The largest increases are expected in the north.

The cascading effects of all these changes are hard to evaluate. Changes in runoffs, winds, salinity, stratification, etc., can have far-reaching and unexpected consequences, which may include consequences to circulation dynamics. Large uncertainties remain, and as the effects of these changes on ecosystems depends heavily on the extent of changes to physical parameters, it is extremely important that these processes, including circulation dynamics, are understood as well as possible.

### 1.5.3 Operational oceanography and decision support

Another area where the accurate description of circulation dynamics is necessary is the field of operational oceanography. While no official definition exists for it,

European Global Ocean Observing System (EuroGOOS), for example, defines operational oceanography as 'the activity of systematic and long-term routine measurements of the seas and oceans and atmosphere, and their rapid interpretation and dissemination'.[4] In practice, this means (near) real-time measurements of the seas and ocean forecasting.

Operational oceanography in the Baltic Sea already began in the 19th century with real-time information of ice conditions (Leppäranta and Myrberg, 2009). Numerical ice forecasts began in 1977. Nowadays, forecasts that include ocean currents are done by several institutes. Co-operation between different actors is routine. For example, institutes co-operate under the umbrella of the European Copernicus Marine Environment Monitoring Service (CMEMS).[5]

One of the major motivators for the study of high-resolution regional hydrodynamic models is their application in the field of operational oceanography. In recent years, societies have come to rely on routine forecasts of the oceans in increasing amounts. For example, the FMI has a legal obligation to produce oceanographic forecasts, including information on currents and drifting (Laki ilmatieteen laitoksesta 6.4.2018/212 § 2).[6] The study of circulation dynamics is central to this mission.

Another way in which ocean science can serve society is by giving support to the management of the seas. By providing current and up-to-date information on the state of the sea and on the projected impacts of decisions, oceanographers can promote science-based governance. This can, hopefully, lead to more sustainable choices for both the environment and society. In this effort, oceanographic models can be used as a part of a decision support system. Here, a realistic description of physical processes is needed as a foundation for fact-based decision-making. In the Baltic Sea, examples of this include the Nest decision support system (Wulff et al., 2013), which includes the BALTSEM model (Savchuk et al., 2012). The Nest system has been used to estimate the effect of possible nutrient reductions. Another example is the RaKi Nutrient Cycling project (Lignell et al., 2016), which developed a decision support system for the Archipelago Sea, including a hydrodynamic component (Tuomi et al., 2018a).

[4] http://eurogoos.eu/about-eurogoos/what-is-operational-oceanography/
[5] http://marine.copernicus.eu/
[6] http://www.finlex.fi/fi/laki/alkup/2018/20180212

# 2 Objectives and scope of the study

As discussed in Section 1, much has been done to advance understanding of circulation patterns in the northern Baltic Sea over the last 100 years or so. Yet, there are still considerable gaps and uncertainties in knowledge. In relation to circulation modelling in the Baltic Sea and the applications discussed in Section 1.5, the existing research gaps involve such issues as incomplete descriptions of the structures and processes appearing at various spatiotemporal scales, insufficient understanding of their variability and how changes in forcing affect circulation dynamics. More complete descriptions would make it easier to assess the impact of environmental problems such as climate change.

Filling knowledge gaps involves first removing the obstacles that prevent advancement. To highlight the objectives of this study, some of the obstacles preventing modelling progress are discussed.

From the point of view of circulation modelling, *observational datasets* remain sparse, both in time and in space. Observations are the bedrock on which science is built. Due to the complexities of Baltic Sea dynamics (cf. Section 1), the number of observations required to draw conclusions on the dynamics in the area is relatively high (when compared to many other areas in the open oceans). For example, many interesting studies of circulation features in the GoF have been published based on acoustic Doppler current profiler (ADCP) data (recent examples include Lagemaa et al., 2010; Suursaar, 2010; Liblik and Lips, 2012; Lilover et al., 2017; Lips et al., 2017; Suhhova et al., 2018). But an increase in the number of ADCP stations would make basin-scale circulation studies much easier. Furthermore, due to practical considerations — such as limited resources — the locations or deployment times of the ADCP installations can be suboptimal for circulation studies. It can also be difficult to determine how well the observations represent general circulation features in the area, rather than local small-scale features. For example, the local topographic steering of currents can significantly affect the current direction distribution seen by the instrument.

Because of the poor availability of direct current measurements, other measurements have been used as a proxy for currents. Salinity observations have been used for this purpose in the Baltic Sea, especially in the GoF. But even salinity observations lack coverage at times. Regular monitoring observations are only done a couple of times each year and for a limited number of stations. While measurement campaigns can provide better coverage, they are infrequent and expensive. Methods, such as Ferryboxes installed aboard ships of opportunity, vastly improve temporal coverage (e.g. Kikas and Lips, 2016), but they do not provide full profiles and are only available from major shipping routes. There are also issues with the observational methods that limit their usability. For example, the near-surface layers are often interesting for the study of dynamics, but this information tends to be unusable in ADCP data. In a situation where observations are not as complete as they could be, it is difficult to formulate and verify (or falsify) theoretical considerations.

*Forcing datasets and other model inputs* are still incomplete and inaccurate

(see e.g. Tuomi, 2014). For example, as wind forcing has a significant effect on the circulation patterns in the GoF, it is vital that the atmospheric model data used to force the oceanic circulation models is as high quality as possible. Also, other forcing datasets have issues. For example, river runoff data can be incomplete and hydrological models have their own uncertainties (e.g. Donnelly et al., 2016). When model resolutions improve, the need for accurate bathymetric information becomes even more important. But even when this information exists, it may be unavailable for scientific study for various reasons (e.g. for political or commercial reasons). Therefore, it is important to also quantify the remaining uncertainties. Careful analysis and uncertainty quantification can mitigate some of the problems associated with incomplete understanding of the dynamics of the system.

*The Comparison of models and observations* continues to be arduous. Observational data is often noisy as it holds evidence of a multitude of different processes at numerous different scales. This makes the post-processing of observations challenging. Filtering the data can remove features that were not intended to be removed or even introduce artefacts not previously present in the data. As models can only depict some of those processes at limited spatiotemporal resolutions, the output of the model can be representative of something quite different than the observation, even when at first glance they seem to be the same thing. So, a point measurement of currents often does not represent the same thing as instantaneous current reported by a 3D model supposedly at the same coordinates. New approaches are needed to process, analyze and compare existing modelling and observational datasets.

The *increasing complexity* of the modelling systems also poses challenges. When incomplete forcing and validation data is used to model the Baltic Sea system, errors can accumulate through non-intuitive and non-linear processes in unexpected ways (as discussed in Section 1). It is therefore important also to improve the description of processes (e.g. stratification and upwelling) from the point of view of circulation studies. For example, seemingly small inaccuracies in the depth of the seasonal thermocline can affect the distribution of momentum in the water column, therefore leading to inaccuracies in the modelled currents. These non-linear interactions are also hard to analyze when models and their outputs continue to grow. There is a clear need to develop ways to deal with this complexity.

*The objective* of this thesis is to contribute to the work aimed at responding to these challenges. In that spirit, this thesis addresses the following topics (Table 2.1 highlights the connection of these questions to the presented challenges):

- The analysis of currents. The circulation patterns of the GoF are analyzed with several modelling configurations at different resolutions (Article III), in different seasons and with a machine learning method used for feature extraction (Article IV). Connections between wind forcing and circulation patterns are also analyzed.
- The application of new observation methods to model validation. The ability of a hydrodynamic model to depict the mixed layer in the GoB is evaluated, including the response of the mixed layer to wind forcing. The bene-

fits of automated observational platforms are shown by applying data from autonomous Argo floats to evaluate model performance (Article I).

- Quantifying and dealing with remaining uncertainty. The ability of an ensemble forecasting system to forecast upwelling events in the GoB is discussed (Article II). The usefulness of uncertainty information from the system is demonstrated. The sensitivity of the circulation patterns to changes in river runoff are studied (Article III).

The spatiotemporal scales of the investigated phenomena, the intrinsic limitations of methods and existing research gaps also affect the scope of this thesis. The spatial scales of the investigation are from the lower limits of model resolution (around 500 m) to basin-wide scales. The temporal focus is on motions ranging from the daily scale to the decadal scale.

Table 2.1: A summary of some of the current challenges in hydrodynamic modelling of the Baltic Sea and the possible paths forward demonstrated in this thesis.

| **Challenge** | | **Path forward** | **Article(s)** |
|---|---|---|---|
| Increasing complexity, growing data flows | → | Automated analysis methods and feature extraction | IV |
| Insufficient observational data coverage for model validation | → | Automated observations | I |
| Uncertainty in model inputs and incomplete process descriptions in models | → | The quantification of uncertainty and its effects | II, III |

# 3 Materials and methods

## 3.1 Modelling

### 3.1.1 NEMO ocean model

Several configurations of the NEMO 3D ocean model (V3.6) were used and developed in this study. For the whole Baltic Sea, a North Sea–Baltic Sea grid with a 2 NM horizontal resolution was used in Articles I and III. The model domain covered the Baltic Sea and the North Sea. In Article I, the open boundary condition in the North Sea was configured to include tidal surface height contribution, while in Article III the boundary condition was upgraded to use data from the CMEMS Global Ocean Reanalysis product (Ferry et al., 2016).

For the GoF, two versions of a configuration with a 0.25 NM or roughly 500 m horizontal resolution were used. The main differences between these two configurations were in the atmospheric forcing, boundary conditions and the bathymetry. The configuration used in Article III had a domain extending to 23.5° E in the west. The boundary condition was obtained from the coarser 2 NM configuration. The model run was analyzed for the years 2012–2014.

The GoF configuration used in Article IV had a slightly larger domain, extending to the Vormsi–Kimitoön line across the GoF at roughly 23° E in the west. The bathymetry was also updated. The boundary condition for this setup was obtained from a Baltic Sea reanalysis run by the SMHI. The model ran from the beginning of 2006 to the end of 2013. The results from 2006 were considered as the initialisation of the model and the years 2007–2013 were chosen for closer analysis. The model saved the daily mean values of the temperature, salinity and current fields.

Both GoF configurations had 94 z-coordinate (with partial step) vertical layers. The topmost vertical layers were 1 m thick, and the layer thickness slightly increased with depth, being about 1.08 m at the lower bound of the z-axis. Ice model LIM3 was included in these configurations (Vancoppenolle et al., 2009). As the computational requirements of the configuration were high, the ice model was only run with a thermodynamic formulation.

Several forcing datasets were used in this study. Forecasts from the HIRLAM numerical weather prediction system (HIRLAM-B, 2015) of the FMI were used in Articles I and III. The domain of the model covers the European region with a horizontal resolution of 0.15° (V73 and earlier; before 2012-03-06) or 0.068° (V74; after 2012-03-06). Vertically the domain is divided into 60 (V73) or 65 (V74) terrain-following hybrid levels, the lowest level being about 12 m above the sea surface. The forecasts are run four times a day (00, 06, 12 and 18 UTC) using boundary conditions from the Boundary Condition Optional Project of the European Centre for Medium-Range Weather Forecasts (ECMWF). Each day of forcing was extracted from the 00 forecast with the highest available temporal resolution in the model archive, varying from one to six hours. Forcing taken from the HIRLAM includes the two-metre air temperature, total cloud cover, mean sea-level pressure and 10-metre winds, and either the two-metre dew point temperature or relative humidity, depending on the availability in the model archive. Forcing was

read into the NEMO run with CORE bulk formulae (Large and Yeager, 2004).

In Article IV, the EURO4M regional reanalysis product (Dahlgren et al., 2016; Landelius et al., 2016) was used as atmospheric forcing, both in the 0.25 NM GoF configuration and in the coarser configuration that provided the boundary condition. This product has the approximate horizontal resolution of 22 km, and its domain is centred in Europe. Longwave and shortwave radiation, humidity, 10-metre wind, two-metre air temperature and precipitation fields at three-hour intervals were used. The reanalysis was produced with HIRLAM numerical weather prediction (NWP) model version 7.3. It was constrained with the ERA-Interim product (Dee et al., 2011) on lateral boundaries and also via data assimilation.

### 3.1.2 Ensemble modelling system

Ensemble forecasting means that instead of producing one deterministic model simulation for a time period, a series of simulations is performed (e.g. Leutbecher and Palmer, 2008). Each of the simulations differs from the others in some way. For example, they can have slightly perturbed forcing, initial conditions or parameter values. The ensemble formed by these simulations then enables a statistical parameter and error estimation.

The theory of ensemble weather forecasting began to be developed in the late 1960s and early 1970s. Operational forecasting began in December 1992, in both Europe and the United States (Molteni et al., 1996). Ocean ensemble forecasts are also becoming more commonplace. There are also several examples from the Baltic Sea (e.g. Roiha et al., 2010; Golbeck et al., 2015).

Ensemble forecasting was used in Article II. Due to the heavy computational requirements of ensemble forecasting, the forecasting system was based on a more robust modelling configuration. This system was based on the MITgcm model core (Marshall et al., 1997a,b), with the domain covering the Baltic Sea at 6 NM horizontal resolution and with 21 vertical levels. Ensembles were created by running the model with 50 different perturbed forcing sets from the monthly forecasting system of the ECMWF, in addition to the deterministic forecast.

## 3.2 Observations and measurements

### 3.2.1 CTD, moorings, tide gauges and satellite data

In Article I, CTD monitoring data for the Bothnian Sea was obtained from International Council for the Exploration of the Sea (ICES) for the years 2012 and 2013. This data consisted of temperature and salinity profiles that originated from the *R/V Aranda*.

In Article III, the GoF2014 dataset was used. Temperature measurements for 2012–2014 were taken for some of the more frequently visited stations in the area. Furthermore, gridded CTD data from three different one-week surveys (done in June 2013, June 2014 and September 2014) were used. This gridded dataset had approximately 4 NM resolution across the GoF and around 9 NM resolution along the GoF. Each survey had more than 80 stations.

In Article IV, salinity and temperature data from three monitoring stations in the GoF were used for model validation. This dataset from the Haapasaari, Länsi-Tonttu and Längden stations typically had 1–3 data points each month during the ice-free season.

In Article I, temperature measurements from wave buoys were used for model validation in the Bay of Bothnia, the Bothnian Sea and the Northern Baltic Proper. Data from the FMI's Directional Waverider buoys and the SMHI's Finngrundet buoy was used.

SST measurements from 2008 and 2009 were also used in Article II, where data from Northern Baltic wave buoy was used to analyze the performance of the forecasting system.

In Article II, tide gauge SST data was also used from eight sites along the shore of the GoB in 2008 and 2009.

Satellite data for 2008 and 2009 was employed in Article II, where SST observations were used to identify upwelling events. Data from the AVHRR was used. This dataset from National Oceanic and Atmospheric Administration (NOAA) was processed by Finnish Environment Institute (SYKE).[7]

### 3.2.2 Weather Stations

Wind measurements from the Kalbådagrund coastal weather station, operated by the FMI, were used in Articles III and IV. This station can be considered representative of open sea weather conditions in the GoF. Wind measurements at the station are made at 32 m height, and the main meteorological parameters are recorded at 10-minute intervals.

### 3.2.3 Autonomous observational systems

In Article I, data from autonomous Argo floats were used. The floats used in the paper operated in the Bothnian Sea during two missions in 2012 and 2013. These missions lasted approximately six months and four months respectively and collected altogether around 300 profiles of temperature and salinity.

The Argo project as a whole consists of several thousand automatic profiling floats around the world (Roemmich et al., 2009). These buoys drift with ocean currents and measure the CTD profiles of the upper ocean. The profiles are then transmitted to public databases. Data from Argo floats has been used for many purposes, for example to estimate the heat content of the world ocean, which is of high importance for climate research.

In the Baltic Sea, Argo floats were first tested in 2011 and have successfully operated since 2012 (Article I; Purokoski et al., 2013; Roiha et al., 2018; Haavisto et al., 2018; Siiriä et al., 2018). Since the Baltic Sea is brackish and very shallow compared to the oceans, applying the floats has required special efforts. However, the Baltic Sea Argo float deployments have been very successful.

[7] www.syke.fi/earthobservation

## 3.3 Machine learning and the self-organizing map

Traditionally, oceanography has been a 'data-poor' science. Often scientists have had to make their conclusions from limited datasets. While the ocean is, for the large-part, still not adequately sampled, the situation has nevertheless changed. The amount of data that needs to be processed and analyzed is rapidly increasing. On the one hand, there are automated measurement platforms and satellites providing continuous data streams for the scientist. On the other hand, numerical models are used to fill the gaps in the data with their estimates of the state of the ocean.

In this situation it is no longer possible for a scientist to manually analyze all the available data. Automated methods can help. In particular, algorithms originating from the field of machine learning and artificial intelligence have, in recent years, become more common in environmental science (Hsieh, 2009).

There are some reasons that have limited the uptake of these algorithms in the field of geosciences. For one, the success of traditional methods based on direct calculations from the laws of physics has meant that the benefits of machine learning have not been as apparent as perhaps they have been in other fields where equally successful approaches have not been available. As machine learning methods are at heart statistical in nature, they do not adapt that well to unexpected situations, such as extreme cases that are not already present in their inputs.

However, applications of value can be found for these algorithms. For example, one successful approach is to develop tools to aid the exploration and interpretation of the huge datasets created by numerical models or automated measurement platforms in order to find features of interest and to limit the dimensionality of that data. This was the application most relevant for the present study.

The machine learning algorithm chosen for the analysis of current fields in Article IV was the SOM, also known as the Kohonen Map. It is an unsupervised learning algorithm based on artificial neural networks (Kohonen, 1982, 2001). It can be used as a way to extract features and reduce the dimensionality of a dataset, in a manner similar to classical EOF/PCA. It can be used to visualize and analyze high-dimensional data. The algorithm sorts input data into a predefined number of clusters or nodes, and enables the extraction of characteristic patterns describing the clusters. A time series of best matching units (BMUs) is produced, which describes the node that best describes the input data for each time. States considered to be similar by the algorithm are near each other on the map.

Compared to other machine learning methods, SOM analysis has been used in oceanography relatively often (e.g. Liu and Weisberg, 2011; Thomson and Emery, 2014; Liu and Weisberg, 2005; Hisaki, 2013; Falcieri et al., 2014; Fraysse et al., 2014; Liu et al., 2016).

As with any other algorithm, there are pros and cons with a SOM. Unlike EOF/PCA, a SOM is a non-linear method, which makes it better suited for asymmetric patterns. Also, missing data values are easier to handle in SOM analysis. Furthermore, the temporal mean does not have to be removed prior to applying the algorithm, which makes the output easier to visualize (Liu and Weisberg, 2005; Liu et al., 2006). A problem with the SOM algorithm is that the user predefines

the map dimensions. This always involves striking a balance between the easy interpretability of the output and the accuracy of mapping.

# 4 Results

## 4.1 Circulation patterns in the GoF

### 4.1.1 Mean circulation fields

Circulation patterns in the GoF were modelled for two periods: 2012–2014 (Article III) and 2007–2013 (Article IV). The mean circulation field was calculated for both of the studied periods. When the results were averaged over the whole study period, neither the 2007–2013 run nor the 2012–2014 run showed the traditional cyclonic pattern (cf. Section 1). While the overall pattern for both time periods was similar, there were also differences. The 2007–2013 period showed smaller current speeds near the northern coast. There were also stronger alongshore currents in the north-eastern corner of the domain. The differences between the two runs can most likely be attributed to inter-annual variability, a change in forcing and different lengths of averaging periods.

For 2012–2014 (Article III), annual mean circulation maps were produced. These emphasized the significance of the inter-annual variability of the mean circulation field. For 2012 the result most resembled the traditional circulation pattern, with an outflow from the GoF near the northern coast. The years 2013 and 2014 differed notably, as no outflow was visible near the northern coast.

Mean circulation maps for 2007–2008 and 2010–2011 (Fig. 4.1) show notable inter-annual variability in circulation patterns in the GoF during the investigation period of Article IV. The pattern for 2007–2008 has more in common with the traditional cyclonic view of the GoF's mean circulation, with clear outflowing currents along the northern coast. The 2010–2011 period does not show a clear current westwards in this area. Both maps show an alongshore current near the southern coast, just west of Narva Bay. Mean currents seem to be slightly stronger in 2007–2008 overall.

In Article IV, seasonal mean circulation maps were presented. Distinctly different structures appeared from one season to another. Generally speaking, autumn and winter showed stronger currents than spring and summer. Perhaps the most notable differences are in the outflowing current near the northern coast. In summer and winter, there is a clear outflowing current. In autumn, such a current is not visible. In spring, there is a weak outflowing current. The location of this current pattern seems to vary from one season to another. Also, the location of the inflowing current near the centre line of the GoF changes.

The sensitivity to river runoff was investigated (Article III) for the 2012–2014 run by first turning of the river runoff entirely, then doubling its original values. It was found that these changes mainly affected the magnitude of the near-surface currents rather than their direction.

As the 2012–2014 run was performed with two different configurations with different resolutions (2 NM and 0.25 NM) it was possible to compare the effect of increased resolution. It was seen that the overall mean circulation pattern was mostly similar in both runs, although the finer grid showed much more detail and simulated higher current speeds.

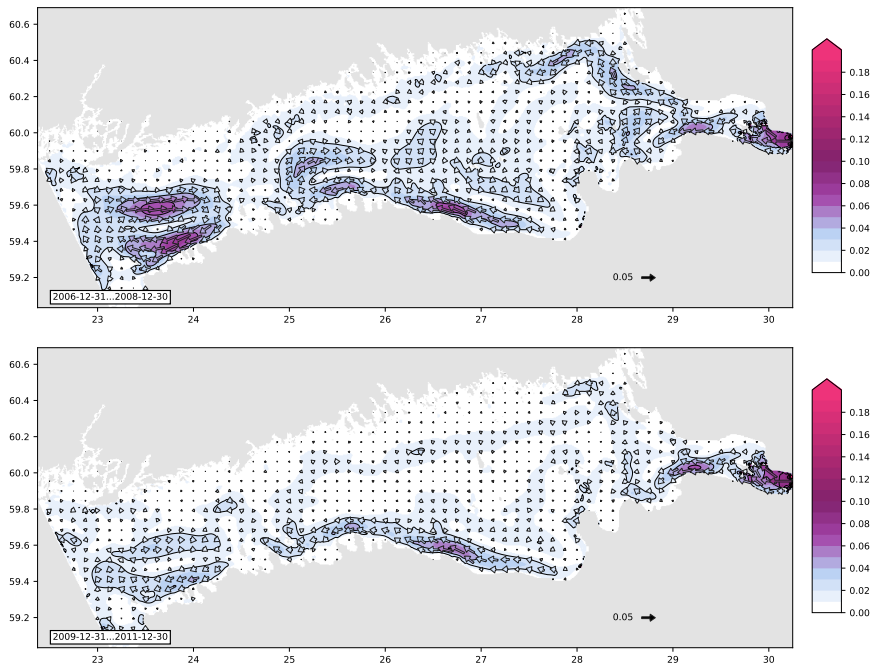


Figure 4.1: Mean circulation maps for 2007–2008 (top) and 2010–2011 (bottom), produced with the GoF 0.25 NM NEMO configuration using EURO4M reanalysis forcing and averaged from 0 m to 7.5 m depth. Velocities are in m/s. Vector arrows are drawn for every 15th grid point in the longitudinal direction and every 13th grid point in the latitudinal direction.

### 4.1.2 Analysis of daily circulation patterns and wind

The effect of winds on the mean circulation fields was studied for 2012–2014 based on wind distributions at the Kalbådagrund weather station (Article III). This analysis revealed differences between the years but could not conclusively relate winds to the circulation pattern.

The results of the wind analysis, along with the mean circulation field computations, prompted the need for additional analysis in order to understand the reasons why these results emerged. For 2007–2013 daily circulation fields were analyzed with one-dimensional SOM analysis (Article IV). Daily current fields were clustered into five nodes for seven north–south sections in the GoF. Each of these nodes represents several daily current fields that the algorithm has determined to belong to the same cluster. The patterns are topologically ordered so that patterns next to each other represent clusters that the algorithm considers similar.

The resulting maps of characteristic patterns consistently showed a node with a pattern where the zonal component of the surface current was mostly towards the west at one end. At the other end there was a node where zonal surface currents were mostly towards the east. These were identified as depicting normal estuarine circulation and reversed estuarine circulation (illustrated in Fig. 4.2). The analysis showed that these circulation patterns were both roughly as commonly found in the modelled data. Throughout the modelling period, there was significant variability in the BMU time series. This means that circulation states sometimes changed rather quickly (on a timescale of days) from estuarine circulation to its reversal, and vice versa.

Overall, nodes representing normal estuarine circulation displayed a more heterogeneous structure than nodes depicting reversed estuarine circulation. The nodes representing normal estuarine circulation were determined to provide a significant contribution to the horizontal structures visible in the seasonal means. A comparison of circulation patterns from west to east showed that circulation patterns in the eastern, wider, shallower part of the GoF generally have a more complex structure.

When the results of the SOM analysis were compared to prevailing wind conditions during the study period, it was found that reversal of the estuarine circulation was related to westerlies and southwesterlies (Fig. 4.3). As this is the dominant wind direction in the area, reversals take place relatively often. Normal estuarine circulation was more common with other wind directions.

When the seasonality of different circulation patterns was investigated, no clear way of dividing the year into different circulation regimes emerged. The BMU hit count was calculated for each day of the year and for each SOM node (Fig. 4.4). This analysis calculated how many times each particular node was the BMU, summed over the modelled time period. It was found that the relative frequency of a node being the BMU changed from one season to another. Overall in this dataset, fully developed reversed estuarine circulation was more common early and late in the year, while the transitional nodes were the more frequent in the middle of the year. There was also a period later in the year when normal estuarine circulation was more common. Transitional nodes were relatively rare from September to

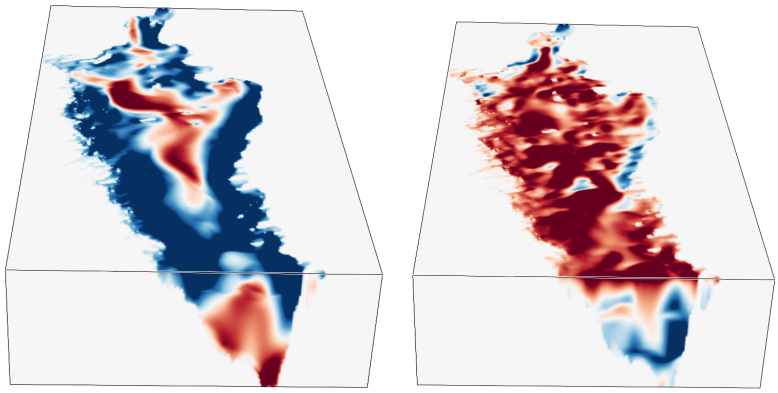

Figure 4.2: A schematic diagram of circulation in the GoF with examples of estuarine circulation (left) and reversed estuarine circulation (right). Zonal velocity is shown for the surface and a section at 24.04° E. The head of the estuary at the eastern end is at the top of the image. Red hues indicate flows towards the head of the estuary, blue indicates outward flows. This diagram was drawn based on Fig. 9 of Article IV, with modelled January and December 2013 situations shown. Please refer to the original for quantitative estimates, axes and colour scale.

March, but from March to September they were common.

The SOM analysis also provided an intuitive way of demonstrating how the long-term salinity field of the GoF emerges from shorter-term circulation patterns and how tracer distribution is affected by the currents. Analysis of salinity differences across the GoF revealed how the expected salinity field with slanted salinity gradients and lower salinities along the northern coast compared to the southern coast seems to require frequent enough normal estuarine circulation to emerge.

## 4.2 Surface layer dynamics and circulation

### 4.2.1 Upwelling

Coastal upwelling was studied in Articles II and III.

The importance of accurately modelling upwelling intensity and frequency from the point of view of circulation patterns came into focus in Article III. When the mean circulation field of the 0.25 NM NEMO configuration was analyzed, it was found that upwelling events contributed significantly to some of the features visible in the mean circulation patterns in the GoF. A relatively small number of high-velocity events near the southern coast were found to induce alongshore currents strong enough to be clearly seen in the long-term means. This highlighted how any uncertainty in the modelled intensity or the frequency of these events would also have an effect on mean currents. It also made apparent the need to better validate the upwelling events.

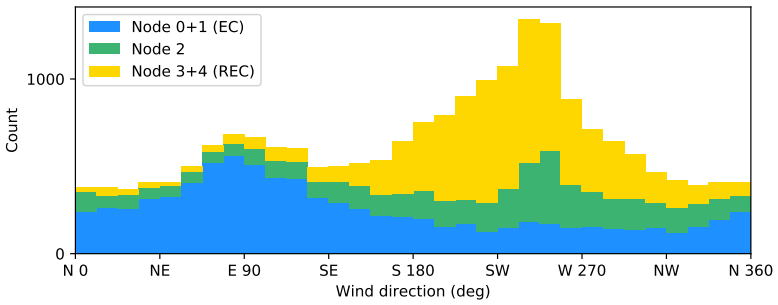


Figure 4.3: Wind direction distribution for the BMUs of SOM nodes as a stacked histogram for the 2007–2013 run of the 0.25 NM GoF NEMO configuration. Wind direction is taken from the model forcing at the Kalbådagrund station. The BMU is taken from the analysis for the section at 24.04° E. Redrawn and modified from Article IV.

It is quite difficult to get a comprehensive understanding of the ability of a model to reproduce coastal upwelling. While there are some upwelling events for which enough observational data exists for in-depth comparison, for most events this is not the case. Satellite observations are often blocked by clouds, CTD sampling is too sparse for meaningful analysis and current measurements are performed only occasionally. On the one hand, these results highlight the importance of the upwelling phenomenon for circulation dynamics. On the other hand, they demonstrate the need to further develop observational, analysis and forecasting methods.

In Article II, ensemble forecasting and analysis methods were used to demonstrate how upwelling forecasts could be developed to quantify uncertainties and mitigate the limits of modelling systems. Using a modelling system with 50 ensemble members, the ability of the system to forecast upwelling events in the GoB was studied. Ensemble verification methods were used to demonstrate some areas of improvement for the forecasting system. While the resolution of the modelling system was only moderate (6 NM), it was still able to produce many upwelling events in the study area.

### 4.2.2 Mixed layer depth

Mixed layer depth, vertical temperature dynamics and the response of the mixed layer to wind forcing were studied with the NEMO model (Article I). The study focused on the Bothnian Sea. Profiles obtained from Argo floats in the area in the summers of 2012 and 2013 were used to estimate the ability of the NEMO model to depict the evolution of the seasonal thermocline. As the Argo float sampled the water column on a nearly daily basis, it was possible to compare this time series to a virtual float time series sampled from NEMO model results.

The 2 NM NEMO model configuration was able to reproduce the general fea-

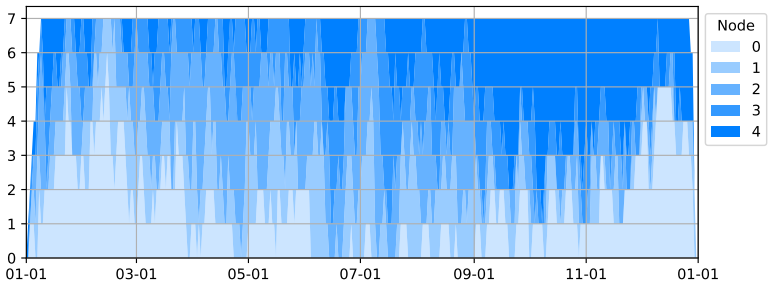


Figure 4.4: The BMU hit count in the SOM analysis of the 2007–2013 period for each node, for each day of the year. Node 0 was identified as normal estuarine circulation, Node 4 as reversed estuarine circulation. Nodes 1, 2 and 3 are transitional states between the two.

tures of seasonal temperature development in the study area, and overall the evolution of the seasonal thermocline was in line with expectations. The modelled temperature gradients were gentler than in reality. The dicothermal ('old winter water') layer was not as pronounced in the model as it was in the measurements.

The effect of vertical mixing schemes on vertical temperature structure was analyzed by testing the $k$-$\varepsilon$ and $k$-$\omega$ mixing schemes, but neither scheme proved superior. The sea surface temperature was better simulated with the $k$-$\omega$ scheme, but the thermocline depth was better reproduced with the $k$-$\varepsilon$ scheme. Importantly, it was discovered that the so-called Craig and Banner parameterization for breaking waves clearly improved the representation of thermocline depth. This hints at the importance of wave breaking for vertical mixing, and the importance of correctly describing air–sea interaction in general.

An investigation of a wind-induced mixing event in August 2012 revealed that the model was not as sensitive to forcing as it should be. While the mixed layer showed deepening during the wind event, it did not capture it in full. Also, while the surface temperature in the model did show a drop, the observations showed a larger one.

Overall, this investigation revealed that the ability of the model to reproduce mixed layer depth and vertical temperature structure was satisfactory, but several areas of improvement were also identified. Most notably, the quality of atmospheric forcing was once again found to be significant. The results showed how central correctly estimating momentum transfer from the atmosphere to the sea is, including realistically quantifying wave effects.

# 5 Discussion

## 5.1 Baltic Sea circulation dynamics and modelling

The results presented in this thesis deepen our understanding of circulation dynamics in the northern basins of the Baltic Sea and help to improve the hydrodynamic models that are used to describe them.

Circulation studies in the GoF revealed new aspects of the circulation field in this basin. Analysis of daily circulation fields emphasized the estuary-like nature of the GoF. A connection between the dominant southwesterly winds and the reversal of estuarine circulation in the basin was demonstrated.

While there was considerable inter-annual variability, long-term means of circulation patterns in the GoF did not show the traditional cyclonic circulation pattern. It is important to note that although several model studies have reported similar results, it does not necessarily mean that such a pattern is no longer there. Rather, it may as well be that, for one reason or another, multiple models these days have similar biases or errors that lead to suppression of the cyclonic mean circulation pattern. If this is the case, our results may serve as a step in the work of identifying these modelling problems. To better comprehend how these modelling results relate to reality, more work is needed on analyzing the existing observational data and obtaining new measurements. For example, it might be fruitful to analyze wind and runoff forcing biases in greater depth in order to understand if they relate to errors that are common to different modelling studies.

Furthermore, the role of certain model components, such as the ice model, needs to be better understood. One source of uncertainty in this study relates to the fact that, due to the high computational requirements of the GoF configuration, the LIM3 ice model was run with a thermodynamic formulation. When this is the case, the ice model transfers atmospheric stresses directly to the ocean. In reality or when the full dynamic ice model is used, ice cover makes the momentum flux into the ocean smaller. However, at the same time, the forcing datasets used in this study were produced with atmospheric models that take sea ice concentration and SST as inputs. In the atmospheric models, the ice cover increases surface roughness and often induces a stable boundary layer, reducing wind speeds. This makes it difficult to estimate the cumulative effect of the ice model formulation on the currents. Also, any quality issues in the sea ice data used in the atmospheric models could potentially be reflected in our results. For the EURO4M dataset and for our study period, sea ice and SST data originated from the OSTIA satellite analysis product (Dahlgren et al., 2016; Dee et al., 2011; Donlon et al., 2012). OSTIA is a global product, not specifically designed for the Baltic Sea area. These sources of uncertainty should be kept in mind when assessing the results of the model calculations, in particular as far as intra-annual variability of the currents is concerned. It would be beneficial to study this issue further when runs with a full ice model become feasible.

It is also possible that the models are in fact revealing something previously unknown about the circulation in these basins, something not seen in earlier con-

figurations. As noted in Section 2, existing observational datasets are not necessarily representative of the overall circulation field in the study area. For instance, in the past, current measurements have been performed more often during the ice-free season, when the weather is typically relatively calm. The results in this thesis on the seasonality of the circulation patterns hint that this might lead to the under-representation of fully developed reversed estuarine circulation in the observational data.

A noteworthy question that can be contemplated based on these results is how the projected changes to the climate (see Section 1.5) will affect circulation patterns in the GoF. In particular, changes to wind, freshwater forcing and salinity distribution are important for circulation. Ice cover is projected to diminish all over the Baltic Sea. Due to such changes in ice cover, wind speeds may increase in the winter. Momentum flux to the sea may also change. This can further strengthen situations with reverse estuarine circulation in the winter. The signal for wind changes is less clear for other seasons. Nevertheless, at least some models also project increases in wind speed in the summer, which might have similar effects. However, again, the uncertainties are large.

Also, the yearly cycle of runoff is expected to change. If spring floods occur earlier in the year and are smaller in magnitude, this might weaken the stability of standard estuarine circulation at that time, favouring reversal situations. An increase in temperature might strengthen seasonal stratification. Stronger stratification in the summer might mean that transitional nodes between the two extremes become less frequent. The question of future Baltic Sea salinity is also an important one for the dynamics of the GoF, but it is a question that is still without a definite answer. The strengthening of salinity gradients in the gulf would most likely support standard estuarine circulation, while their weakening might support its reversal.

Modelling the vertical temperature structure and mixed layer depth are important elements of successfully modelling circulation patterns in the sea. The 2 NM NEMO–based configuration in this study was, overall, able to depict large-scale features of the seasonal thermocline in the Bothnian Sea, suggesting the adequate parameterization of vertical mixing for circulation studies. But at the same time, this study revealed that many aspects of vertical mixing parameterizations are crude approximations at best and the response of the model to wind-mixing situations was not completely correct. Sustained effort is required to improve the ability of models to depict both mixing in the ocean and air–sea interaction. For these tasks, the Baltic Sea is an excellent natural laboratory, with strong gradients that are difficult for all current mixing parameterizations. The on-going efforts to improve wave effect descriptions in hydrodynamic models (e.g. Alari et al., 2016) should be continued.

Upwelling is a challenging phenomenon to study for several reasons. For one, the observational data of upwelling events is often incomplete. At times, it is possible to spot upwelling events from satellite images, but often cloud cover prevents the use of this data source. The upwelling studies in this thesis also demonstrated how a phenomenon visible on timescales of days to weeks can affect long-term

means. This emphasizes the need to consider the connections between different timescales adequately.

The results in this thesis raise the question of what is a 'sufficiently long' averaging period for mean currents in the Baltic Sea. Based on the amount of interannual variability in the results, it is recommended that the averaging period should be at least significantly longer than those used in most studies published so far. One starting point could be the use of a normal climate averaging period of 30 years, like the one routinely used in meteorology (WMO, 2017). The challenge in this is that at the same time a relatively high resolution is also required from the model.

Spatiotemporally this study only covered a part of the range of ocean movements. The focus of this work was spatially from the mesoscale to the basin-wide scale, and temporally from a daily scale to a decadal scale. One of the directions for future work is to extend these limits so that the connections between different scales can be further investigated. The need for wider timescales was already discussed. Also, there are opportunities spatially. For example, it could be interesting to extend these studies to the sub-mesoscale range with the existing tools in order to study how circulation patterns are related to sub-mesoscale features. Earlier studies show some potential paths forward (e.g. Zhurbas et al., 2008; Vankevich et al., 2015, 2016; Väli et al., 2018).

## 5.2 Tools and analysis methods

Methods developed in this thesis are useful for future projects. These include the modelling configurations that have been applied and further developed.

The main tool of this thesis is 3D hydrodynamic modelling. The NEMO model — which was used in Articles I, III and IV — demonstrated its worth for the northern sub-basins of the Baltic Sea. The high-resolution GoF configuration, originally by Vankevich et al. (2016), was further developed and validated in this thesis. Improvements included an extended domain, updated bathymetry, changes to boundary conditions and new forcing data. This configuration is now ready to be applied to further research projects. Examples of future study topics could include coupling the configuration to a biogeochemical model or a trajectory model.

The horizontal resolution of this configuration is around 500 m. It is expected that the users of these types of models will want even higher resolutions in the future. However, we need to acknowledge the limits of our current tools. The hydrostatic approximation, for one, sets boundaries to the applicability of models based on that approximation. NEMO is one of those models. Also, models based on unstructured grids should be considered closely. As higher resolutions become commonplace, a sober evaluation of our tools is needed in order to see where the current approach is just not enough anymore.

It is obvious that in the future, the sizes of observational and modelling datasets will only continue to increase. This in turn will increase the need for efficient analysis, feature extraction and data exploration methods. This study demonstrated how simple applications of machine learning methods can efficiently assist ocean modelling. A feature extraction and clustering method based on the SOM algorithm

was applied to the circulation of the GoF. This approach clearly demonstrated how machine learning methods can complement traditional approaches and produce interesting insights into datasets.

The difficult part of the work of applying machine learning methods is finding applications for these algorithms that produce meaningful results. It is not enough to blindly push datasets into an algorithm and expect revelations. It is recommended that the work of finding applications for machine learning in oceanography is continued. The results of this thesis raise several new questions worthy of further study. For example, it could be beneficial to extend the SOM analysis of circulation patterns by incorporating more observational data from, say, ADCPs or Ferryboxes (cf. e.g. Kikas and Lips, 2016). Such an analysis could yield additional information about the estuarine dynamics of the basin. Another area where there is a need for new ways forward is how modelling and observations are used together. An important part of this work is to find enough time to take advantage of existing datasets, as well as new ones.

This work also has implications for practical applications. For example, as computing power continues to increase, it will become possible to combine the ensemble forecasting methods presented in this thesis with high resolution modelling. Together they will allow for improved estimates of uncertainties, for example, they will allow for better quantification of what is known and what is uncertain. In turn, this will allow for better operational forecasts.

## 5.3 Role of observations and forcing

A notable weakness in circulation modelling in the Baltic Sea, and one that is not easily addressed in the near term, are the issues related to atmospheric forcing. These forcing datasets are of utmost importance for the quality of ocean models, but at the same time they are most often based on atmospheric models which themselves have limitations, often because of the same issues as oceanographic models (e.g. limited resolution, computational capacity, a lack of observations, or too simplistic parameterizations). It might also be the case that there could be more communication and co-operation between the two modelling communities on how to improve the situation. While increasing resolution is useful, it is not a silver bullet. A recent example from the Archipelago Sea demonstrated that, while higher resolution of atmospheric data did improve the results of a hydrodynamic model of the area, it alone was not enough to significantly improve circulation patterns (Tuomi et al., 2018a). On-going dialogue and co-operation between atmospheric and ocean modellers is the only way to address this. The outputs of this co-operation could include improved parameterizations of air–sea interaction for example, or more sophisticated coupled modelling systems with both atmospheric and oceanic components.

One thing clearly highlighted by the results of this thesis is that observations are paramount for successful modelling efforts. In many cases observations, or the lack thereof, were the defining factor when the applicability of model results was considered. Furthermore, even when observational data does exist, it is not

always possible or practical to compare it to model simulations. For example, relatively little can be done at the moment to validate the full circulation patterns produced by the circulation model with existing observations. There are a number of existing, and even unpublished, datasets from the area that could be used more extensively. This includes both earlier (e.g. Alenius et al., 1998) and recent (e.g. Tuomi et al., 2018b) ADCP and drifter data. It is therefore more important than ever to continue developing new observational methods and to continue the work to compare existing observations with modelling data. The need for co-operation between modellers and observational oceanographers is once again re-iterated.

The use of robotics is becoming more widespread in virtually every sector. Autonomous observational methods are gaining ground in marine sciences. Increasingly sophisticated measurement platforms are being deployed, also in the Baltic Sea. As they become more affordable over time, they represent one of the more realistic approaches to expanding the current observational network, as resource limitations may place many traditional approaches (such as extended research cruises) out of reach.

The method developed to validate model results with Argo float data was very useful. It has already been applied to new cases, including its application in the validation of the official NEMO Nordic configuration for the North Sea–Baltic Sea system (Hordoir et al., 2018).

In addition to Argo floats, there are also other autonomous systems which could be used for the kind of studies presented here. Gliders have already been used in the Baltic Sea (e.g. Karstensen et al., 2014; Alenius et al., 2014; Rudnick, 2016). A glider has more manoeuvrability than an Argo float. The vehicle achieves this vertically by modifying its buoyancy and horizontally with the use of wings. Typically they also have more sophisticated sensors than Argo floats. The higher cost of the system means that fewer units are typically deployed than is the case with Argo floats.

There are also other developments in the observational domain that could potentially be useful for modelling efforts. For example, the FMI has recently procured Datawell Directional Waverider 4 (DWR4) buoys with acoustic current meter (ACM) sensors (H. Petterson, pers. comm., 2018-05-09).[8] These buoys can measure near-surface currents simultaneously with wave measurements, which also opens up possibilities for more extensive and routine validation of modelled currents than before. Another possible method for surface current mapping is high frequency (HF) radar. Unfortunately, low salinity limits their usability (Gurgel et al., 1999). Relatively high costs, combined with the limited range, have so far prevented their use in the northern Baltic Sea (T. Purokoski, pers. comm., 2018-05-17). Currents could, in theory, also be indirectly measured by satellites, but satellite observations are very difficult (Dohan and Maximenko, 2010). Satellite salinity observations have not yet reached usable quality in the Baltic Sea.

This investigation highlighted how difficult — but also how important for circulation dynamics — it is to model upwelling events correctly. To further improve

[8] http://datawell.nl/Portals/0/Documents/Brochures/datawell_brochure_dwr4_acm_b-38-07.pdf

how the intensity and frequency of these events are modelled, more observational data is needed. It would be especially useful to have more multi-sensor datasets of upwelling events, like the dataset presented by Suursaar and Aps (2007), as these can be combined with hindcasts of these events to estimate how well they are captured in the model.

# 6 Conclusions

In this thesis, circulation dynamics were investigated in the northern Baltic Sea with numerical hydrodynamic modelling. The results of this work can be summarized as follows:

- The overall mean circulation fields in this study did not show the traditional cyclonic pattern in the GoF. Analysis of currents in the GoF revealed that they are highly variable and complex. There is significant inter-annual and intra-annual variability in the circulation patterns. Circulation features in the GoF often move or change direction from season to season. Long-term averages can hide or damp circulation patterns that are visible in the shorter term.

- SOM analysis of the currents emphasized the estuary-like nature of the GoF. Circulation in the GoF changes rapidly between normal estuarine circulation and reverse estuarine circulation. The dominant wind direction being from the southwest supports this reversal. The emergence of the cyclonic mean circulation pattern seems to require that standard estuarine circulation is common enough for it to emerge during the averaging period.

- There are numerous non-linear connections between different processes at different timescales. For example, the SOM analysis demonstrated how sensitive long-term circulation patterns in the GoF are to small changes in wind direction distribution. Upwelling events on timescales of days to weeks can have a notable effect on long-term circulation patterns. Relatively small changes in mixed-layer depth can affect the distribution of momentum in the water column, which in turn affects current speeds.

- The GoF is still a challenging environment for circulation modelling. Model configurations have differences in their abilities. Salinity gradients in the GoF are still not reproduced in a satisfactory manner by the models. More information is required on how well the models reproduce true circulation patterns and, for example, upwelling frequency and intensity.

- The NEMO model is a suitable tool for the studies of circulation in the northern sub-basins of the Baltic Sea. Its quality seems comparable to other commonly used models in the area. However, as the needs for accurate information about coastal processes increase, it will become necessary to evaluate alternative modelling strategies, such as unstructured grids and non-hydrostatic models.

- Model inputs are a significant source of uncertainty. Forcing data remains unreliable or unavailable in many cases. The role of wind forcing is especially important. There is also still a need to develop other forcing data such as river runoff forcing, for example.

- There are also notable uncertainties related to model parameterizations and simplifications. For instance, the GoF configuration in this study did not include a full dynamic ice model for computational reasons. This means that the momentum transfer from the atmosphere might not be accurate in the model during the ice-covered season, which could affect the results of this analysis, in particular when it comes to intra-annual variability.
- Observations are a necessity for any successful model development efforts. More observations, especially in the form of better spatial coverage of current measurements, would benefit circulation modelling in the northern Baltic Sea. Even when observational datasets are available, comparing them to models can be tricky. Care must be taken to make sure that the models and observations represent the same thing when they are compared.

Finally, as difficult and laboursome as these investigations of the non-linearities of the hydrodynamics of the oceans can be, this work also, in a small way, demonstrates how necessary it is. Environmental changes such as climate change can have complicated effects – also in the northern Baltic Sea. If circulation patterns change significantly, the cascading effects can be unexpected. Further study is needed.

# References


Alari, V., Staneva, J., Breivik, Ø., Bidlot, J.-R., Mogensen, K., Janssen, P., 2016. Surface wave effects on water temperature in the Baltic Sea: simulations with the coupled NEMO-WAM model. Ocean Dynamics 66 (8), 917–930. https://doi.org/10.1007/s10236-016-0963-x

Alenius, P., Myrberg, K., Nekrasov, A., 1998. The physical oceanography of the Gulf of Finland: a review. Boreal Environment Research 3 (2), 97–125. http://www.borenv.net/BER/pdfs/ber3/ber3-097-125.pdf

Alenius, P., Tikka, K., Barrera, C., 2014. Gliders for studies of multi-scale variability in the Baltic Sea. In: 2014 IEEE/OES Baltic International Symposium (BALTIC). pp. 1–6.

Andersen, J. H., Carstensen, J., Conley, D. J., Dromph, K., Fleming-Lehtinen, V., Gustafsson, B. G., Josefson, A. B., Norkko, A., Villnäs, A., Murray, C., 2017. Long-term temporal and spatial trends in eutrophication status of the Baltic Sea. Biological Reviews 92 (1), 135–149. http://dx.doi.org/10.1111/brv.12221

Andrejev, O., Myrberg, K., Alenius, P., Lundberg, P. A., 2004. Mean circulation and water exchange in the Gulf of Finland – a study based on three-dimensional modelling. Boreal Environment Research 9 (1), 1–16. http://www.borenv.net/BER/pdfs/ber9/ber9-001.pdf

Apel, J. R., 1987. Principles of ocean physics. Vol. 38 of International Geophysics Series. Academic Press.

BACC II Author Team, 2015. Second assessment of climate change for the Baltic Sea basin. Springer. http://dx.doi.org/10.1007/978-3-319-16006-1

Beletsky, D., Saylor, J. H., Schwab, D. J., 1999. Mean circulation in the Great Lakes. Journal of Great Lakes Research 25 (1), 78–93. https://doi.org/10.1016/S0380-1330(99)70718-5

Beletsky, D., Schwab, D., 2008. Climatological circulation in Lake Michigan. Geophysical Research Letters 35 (21). https://doi.org/10.1029/2008GL035773

Beletsky, D., Schwab, D. J., 2001. Modeling circulation and thermal structure in Lake Michigan: Annual cycle and interannual variability. Journal of Geophysical Research: Oceans 106 (C9), 19745–19771. http://dx.doi.org/10.1029/2000JC000691

Blockley, E. W., Martin, M. J., McLaren, A. J., Ryan, A. G., Waters, J., Lea, D. J., Mirouze, I., Peterson, K. A., Sellar, A., Storkey, D., 2014. Recent development of the Met Office operational ocean forecasting system: an overview and assessment of the new global FOAM forecasts. Geoscientific Model Development 7 (6), 2613–2638. https://doi.org/10.5194/gmd-7-2613-2014

Carballo, R., Iglesias, G., Castro, A., 2009. Residual circulation in the Ría de Muros

(NW Spain): A 3D numerical model study. Journal of Marine Systems 75 (1), 116–130.
https://doi.org/10.1016/j.jmarsys.2008.08.004

Cushman-Roisin, B., Beckers, J.-M., 2011. Introduction to geophysical fluid dynamics: physical and numerical aspects. Vol. 101 of International Geophysics Series. Academic Press.

Dahlgren, P., Landelius, T., Kållberg, P., Gollvik, S., 2016. A high-resolution regional reanalysis for Europe. Part 1: Three-dimensional reanalysis with the regional HIgh-Resolution Limited-Area Model (HIRLAM). Quarterly Journal of the Royal Meteorological Society 142 (698), 2119–2131.
http://dx.doi.org/10.1002/qj.2807

Dee, D. P., Uppala, S. M., Simmons, A. J., Berrisford, P., Poli, P., Kobayashi, S., Andrae, U., Balmaseda, M. A., Balsamo, G., Bauer, P., Bechtold, P., Beljaars, A. C. M., van de Berg, L., Bidlot, J., Bormann, N., Delsol, C., Dragani, R., Fuentes, M., Geer, A. J., Haimberger, L., Healy, S. B., Hersbach, H., Hólm, E. V., Isaksen, L., Kållberg, P., Köhler, M., Matricardi, M., McNally, A. P., Monge-Sanz, B. M., Morcrette, J.-J., Park, B.-K., Peubey, C., de Rosnay, P., Tavolato, C., Thépaut, J.-N., Vitart, F., 2011. The ERA-Interim reanalysis: configuration and performance of the data assimilation system. Quarterly Journal of the Royal Meteorological Society 137 (656), 553–597.
http://dx.doi.org/10.1002/qj.828

Deleersnijder, E., Campin, J.-M., Delhez, E. J., 2001. The concept of age in marine modelling: I. Theory and preliminary model results. Journal of Marine Systems 28 (3), 229–267.
https://doi.org/10.1016/S0924-7963(01)00026-4

Dohan, K., Maximenko, N., 2010. Monitoring ocean currents with satellite sensors. Oceanography 23 (4), 94–103.
https://doi.org/10.5670/oceanog.2010.08

Donlon, C. J., Martin, M., Stark, J., Roberts-Jones, J., Fiedler, E., Wimmer, W., 2012. The operational sea surface temperature and sea ice analysis (OSTIA) system. Remote Sensing of Environment 116, 140–158.
http://dx.doi.org/10.1016/j.rse.2010.10.017

Donnelly, C., Andersson, J. C., Arheimer, B., 2016. Using flow signatures and catchment similarities to evaluate the E-HYPE multi-basin model across Europe. Hydrological Sciences Journal 61 (2), 255–273.
https://doi.org/10.1080/02626667.2015.1027710

Ducrotoy, J.-P., Elliott, M., 2008. The science and management of the North Sea and the Baltic Sea: Natural history, present threats and future challenges. Marine Pollution Bulletin 57 (1), 8–21, eMECS 7/ECSA 40, Caen (France), May 2006.
https://doi.org/10.1016/j.marpolbul.2008.04.030

Ehlin, U., 1981. Hydrology of the Baltic Sea. In: Voipio, A. (Ed.), The Baltic Sea. Vol. 30 of Elsevier Oceanography Series. Elsevier, pp. 123 – 134.
https://doi.org/10.1016/S0422-9894(08)70139-9

Elken, J., Nõmm, M., Lagemaa, P., 2011. Circulation patterns in the Gulf of Finland derived from the EOF analysis of model results. Boreal environment research 16 (suppl. A), 84–102.
http://www.borenv.net/BER/pdfs/ber16/ber16A-084.pdf

Falcieri, F. M., Benetazzo, A., Sclavo, M., Russo, A., Carniel, S., 2014. Po river plume pattern variability investigated from model data. Continental Shelf Research 87 (Supplement C), 84 – 95, oceanography at coastal scales.
https://doi.org/10.1016/j.csr.2013.11.001

Ferry, N., Parent, L., Masina, S., Storto, A., Zuo, H., Balmaseda, M., 2016. Global ocean physics reanalysis Glorys2V3. Tech. rep., EU Copernicus Marine Service.
http://marine.copernicus.eu/documents/PUM/CMEMS-GLO-PUM-001-009-011-017.pdf

Flato, G., Marotzke, J., Abiodun, B., Braconnot, P., Chou, S. C., Collins, W. J., Cox, P., Driouech, F., Emori, S., Eyring, V., et al., 2013. Evaluation of climate models. In: Climate change 2013: the physical science basis. Vol. 5. Cambridge University Press, pp. 741–866.
http://www.ipcc.ch/report/ar5/wg1/

Fleming-Lehtinen, V., Andersen, J. H., Carstensen, J., Łysiak-Pastuszak, E., Murray, C., Pyhälä, M., Laamanen, M., 2015. Recent developments in assessment methodology reveal that the Baltic Sea eutrophication problem is expanding. Ecological Indicators 48, 380–388.
https://doi.org/10.1016/j.ecolind.2014.08.022

Fraysse, M., Pairaud, I., Ross, O. N., Faure, V. M., Pinazo, C., 2014. Intrusion of Rhone River diluted water into the Bay of Marseille: Generation processes and impacts on ecosystem functioning. Journal of Geophysical Research: Oceans 119 (10), 6535–6556.
http://dx.doi.org/10.1002/2014JC010022

Geyer, W., Ralston, D., 2011. The dynamics of strongly stratified estuaries. In: Wolanski, E., McLusky, D. (Eds.), Treatise on Estuarine and Coastal Science. Academic Press, Waltham, pp. 37–51.
https://doi.org/10.1016/B978-0-12-374711-2.00206-0

Golbeck, I., Li, X., Janssen, F., Brüning, T., Nielsen, J. W., Huess, V., Söderkvist, J., Büchmann, B., Siiriä, S.-M., Vähä-Piikkiö, O., Hackett, B., Kristensen, N. M., Engedahl, H., Blockley, E., Sellar, A., Lagemaa, P., Ozer, J., Legrand, S., Ljungemyr, P., Axell, L., 2015. Uncertainty estimation for operational ocean forecast products—a multi-model ensemble for the North Sea and the Baltic Sea. Ocean Dynamics 65 (12), 1603–1631.
https://doi.org/10.1007/s10236-015-0897-8

Guihou, K., Polton, J., Harle, J., Wakelin, S., O'Dea, E., Holt, J., 2018. Kilometric scale modeling of the North West European Shelf seas: Exploring the spatial and temporal variability of internal tides. Journal of Geophysical Research: Oceans 123 (1), 688–707.
http://dx.doi.org/10.1002/2017JC012960

Gurgel, K.-W., Essen, H.-H., Kingsley, S., 1999. High-frequency radars: physical limitations and recent developments. Coastal Engineering 37 (3), 201–218. https://doi.org/10.1016/S0378-3839(99)00026-5

Haapala, J., 1994. Upwelling and its influence on nutrient concentration in the coastal area of the Hanko Peninsula, entrance of the Gulf of Finland. Estuarine, Coastal and Shelf Science 38 (5), 507–521. https://doi.org/10.1006/ecss.1994.1035

Haavisto, N., Tuomi, L., Roiha, P., Siiriä, S.-M., Alenius, P., Purokoski, T., 2018. Argo floats as a novel part of the monitoring the hydrography of the Bothnian Sea. Frontiers in Marine Science 5, 324. https://doi.org/10.3389/fmars.2018.00324

Håkansson, B., Alenius, P., Brydsten, L., 1996. Physical environment in the Gulf of Bothnia. Ambio (Special report Number 8), 5–12.

Hela, I., 1952. Drift currents and permanent flow. Soc. Scient. Fenn., Comm. Phys.-Math. XVI (14).

HELCOM, 2009. Eutrophication in the Baltic Sea — an integrated thematic assessment of the effects of nutrient enrichment and eutrophication in the Baltic Sea region. Vol. 115B of Baltic Sea Environment Proceedings. HELCOM. http://www.helcom.fi/Lists/Publications/BSEP115B.pdf

HELCOM, 2014. Eutrophication status of the Baltic Sea 2007–2011 A concise thematic assessment. Vol. 143 of Baltic Sea Environment Proceedings. HELCOM. http://www.helcom.fi/Lists/Publications/BSEP143.pdf

HELCOM, 2018. State of the Baltic Sea — Second holistic assessment 2011–2016. Vol. 155 of Baltic Sea Environment Proceedings. HELCOM. http://stateofthebalticsea.helcom.fi

Herrling, G., Winter, C., 2015. Tidally- and wind-driven residual circulation at the multiple-inlet system East Frisian Wadden Sea. Continental Shelf Research 106, 45 – 59. https://doi.org/10.1016/j.csr.2015.06.001

HIRLAM-B, 2015. System documentation. Tech. rep., HIRLAM consortium. http://www.hirlam.org/

Hisaki, Y., 2013. Classification of surface current maps. Deep Sea Research Part I: Oceanographic Research Papers 73 (Supplement C), 117 – 126. https://doi.org/10.1016/j.dsr.2012.12.001

Hordoir, R., Axell, L., Höglund, A., Dieterich, C., Fransner, F., Gröger, M., Liu, Y., Pemberton, P., Schimanke, S., Andersson, H., Ljungemyr, P., Nygren, P., Falahat, S., Nord, A., Jönsson, A., Lake, I., Döös, K., Hieronymus, M., Dietze, H., Löptien, U., Kuznetsov, I., Westerlund, A., Tuomi, L., Haapala, J., 2018. Nemo-Nordic: A NEMO based ocean model for Baltic & North Seas, research and operational applications. Geoscientific Model Development Discussions 2018, 1–29. https://doi.org/10.5194/gmd-2018-2

Hordoir, R., Axell, L., Löptien, U., Dietze, H., Kuznetsov, I., 2015. Influence of sea level rise on the dynamics of salt inflows in the Baltic Sea. Journal of Geophysical Research: Oceans 120 (10), 6653–6668.
http://dx.doi.org/10.1002/2014JC010642

Hordoir, R., Dieterich, C., Basu, C., Dietze, H., Meier, H., 2013. Freshwater outflow of the Baltic Sea and transport in the Norwegian current: A statistical correlation analysis based on a numerical experiment. Continental Shelf Research 64, 1–9.
http://dx.doi.org/10.1016/j.csr.2013.05.006

Hsieh, W. W., 2009. Machine Learning Methods in the Environmental Sciences: Neural Networks and Kernels, 1st Edition. Cambridge University Press, New York, NY, USA.

Jenkins, W. J., 2014. Tracers of ocean mixing. In: Holland, H. D., Turekian, K. K. (Eds.), Treatise on Geochemistry, 2nd Edition. Elsevier, Oxford, pp. 235–257.
https://doi.org/10.1016/B978-0-08-095975-7.00608-2

Karstensen, J., Liblik, T., Fischer, J., Bumke, K., Krahmann, G., 2014. Summer upwelling at the Boknis Eck time-series station (1982 to 2012) — a combined glider and wind data analysis. Biogeosciences 11 (13), 3603–3617.
https://doi.org/10.5194/bg-11-3603-2014

Kielmann, J., 1981. Grundlagen und Anwendung eines numerischen Modells der geschichteten Ostsee. Ph.D. thesis, Institut für Meereskunde, in German, with English summary.
http://oceanrep.geomar.de/21892/1/IFM-BER_87.pdf

Kikas, V., Lips, U., 2016. Upwelling characteristics in the Gulf of Finland (Baltic Sea) as revealed by ferrybox measurements in 2007–2013. Ocean Science 12 (3), 843–859.
http://dx.doi.org/10.5194/os-12-843-2016

Klymak, J., Nash, J., 2009. Estimates of mixing. In: Steele, J. H. (Ed.), Encyclopedia of Ocean Sciences, 2nd Edition. Academic Press, Oxford, pp. 288–298.
https://doi.org/10.1016/B978-012374473-9.00615-9

Kohonen, T., 1982. Self-organized formation of topologically correct feature maps. Biological cybernetics 43 (1), 59–69.

Kohonen, T., 2001. Self-Organizing Maps. Physics and astronomy online library. Springer Berlin Heidelberg.

Krauss, W., Brügge, B., 1991. Wind-produced water exchange between the deep basins of the Baltic Sea. Journal of Physical Oceanography 21 (3), 373–384.
https://doi.org/10.1175/1520-0485(1991)021<0373:WPWEBT>2.0.CO;2

Kullenberg, G., 1981. Physical oceanography. In: Voipio, A. (Ed.), The Baltic Sea. Vol. 30 of Elsevier Oceanography Series. Elsevier, pp. 135 – 181.
https://doi.org/10.1016/S0422-9894(08)70140-5

Lagemaa, P., 2012. Operational forecasting in Estonian marine waters. TUT Press, Marine Systems Institute at Tallinn University of Technology, Tallinn.

http://digi.lib.ttu.ee/i/?714

Lagemaa, P., Suhhova, I., Nõmm, M., Pavelson, J., Elken, J., 2010. Comparison of current simulations by the state-of-the-art operational models in the Gulf of Finland with ADCP measurements. In: Baltic International Symposium (BALTIC), 2010 IEEE/OES US/EU. IEEE, pp. 1–11.

Landelius, T., Dahlgren, P., Gollvik, S., Jansson, A., Olsson, E., 2016. A high-resolution regional reanalysis for Europe. Part 2: 2D analysis of surface temperature, precipitation and wind. Quarterly Journal of the Royal Meteorological Society 142 (698), 2132–2142.
http://dx.doi.org/10.1002/qj.2813

Large, W. G., Yeager, S. G., 2004. Diurnal to decadal global forcing for ocean and sea-ice models: the data sets and flux climatologies. NCAR Technical Note, NCAR/TN-460+STR, CGD Division of the National Center for Atmospheric Research.
http://dx.doi.org/10.5065/D6KK98Q6

Lehmann, A., 1995. A three-dimensional baroclinic eddy-resolving model of the Baltic Sea. Tellus A 47 (5), 1013–1031.
https://doi.org/10.1034/j.1600-0870.1995.00206.x

Lehmann, A., Hinrichsen, H.-H., 2000. On the thermohaline variability of the Baltic Sea. Journal of Marine Systems 25 (3), 333–357.
http://doi.org/10.1016/S0924-7963(00)00026-9

Lehmann, A., Myrberg, K., 2008. Upwelling in the Baltic Sea – a review. Journal of Marine Systems 74, S3–S12.
https://doi.org/10.1016/j.jmarsys.2008.02.010

Leppäranta, M., Myrberg, K., 2009. Physical oceanography of the Baltic Sea. Springer Verlag.
https://doi.org/10.1007/978-3-540-79703-6

Leutbecher, M., Palmer, T., 2008. Ensemble forecasting. Journal of Computational Physics 227 (7), 3515–3539, predicting weather, climate and extreme events.
https://doi.org/10.1016/j.jcp.2007.02.014

Liblik, T., Lips, U., 2012. Variability of synoptic-scale quasi-stationary thermohaline stratification patterns in the Gulf of Finland in summer 2009. Ocean Science 8 (4), 603–614.
https://www.ocean-sci.net/8/603/2012/

Lignell, R., Miettunen, E., Ropponen, J., Huttunen, M., Korppoo, M., Kuosa, H., Lehtoranta, J., Lukkari, K., Peltonen, H., Piiparinen, J., Attila, J., Tikka, K., Tuomi, L., Puttonen, I., 2016. Saaristomeren valuma-alueen kokonaiskuormitusmallin kehittäminen. Tech. rep., SYKE, in Finnish.
http://www.syke.fi/download/noname/%7B042BDB02-D6F2-4954-AC70-BA7DDCFA7B64%7D/121616

Lilover, M.-J., Elken, J., Suhhova, I., Liblik, T., 2017. Observed flow variability along the thalweg, and on the coastal slopes of the Gulf of Finland, Baltic Sea. Estuarine, Coastal and Shelf Science 195, 23–33.

https://doi.org/10.1016/j.ecss.2016.11.002

Lips, I., Lips, U., Liblik, T., 2009. Consequences of coastal upwelling events on physical and chemical patterns in the central Gulf of Finland (Baltic Sea). Continental Shelf Research 29 (15), 1836–1847.
https://doi.org/10.1016/j.csr.2009.06.010

Lips, U., Laanemets, J., Lips, I., Liblik, T., Suhhova, I., Ülo Suursaar, 2017. Wind-driven residual circulation and related oxygen and nutrient dynamics in the Gulf of Finland (Baltic Sea) in winter. Estuarine, Coastal and Shelf Science 195, 4–15.
https://doi.org/10.1016/j.ecss.2016.10.006

Liu, Y., Weisberg, R. H., 2005. Patterns of ocean current variability on the West Florida Shelf using the self-organizing map. Journal of Geophysical Research: Oceans 110 (C6), c06003.
http://dx.doi.org/10.1029/2004JC002786

Liu, Y., Weisberg, R. H., 2011. A review of self-organizing map applications in meteorology and oceanography. In: Mwasiagi, J. I. (Ed.), Self Organizing Maps — Applications and Novel Algorithm Design. IntechOpen, Rijeka, Ch. 13, pp. 253–272.
https://doi.org/10.5772/13146

Liu, Y., Weisberg, R. H., He, R., 2006. Sea surface temperature patterns on the West Florida Shelf using growing hierarchical self-organizing maps. Journal of Atmospheric and Oceanic Technology 23 (2), 325–338.
https://doi.org/10.1175/JTECH1848.1

Liu, Y., Weisberg, R. H., Vignudelli, S., Mitchum, G. T., 2016. Patterns of the loop current system and regions of sea surface height variability in the eastern Gulf of Mexico revealed by the self-organizing maps. Journal of Geophysical Research: Oceans 121 (4), 2347–2366.
https://doi.org/10.1002/2015JC011493

Lundberg, C., Jakobsson, B.-M., Bonsdorff, E., 2009. The spreading of eutrophication in the eastern coast of the Gulf of Bothnia, northern Baltic Sea–an analysis in time and space. Estuarine, Coastal and Shelf Science 82 (1), 152–160.
https://doi.org/10.1016/j.ecss.2009.01.005

MacCready, P., Banas, N., 2011. Residual circulation, mixing, and dispersion. In: Wolanski, E., McLusky, D. (Eds.), Treatise on Estuarine and Coastal Science. Academic Press, Waltham, pp. 75–89.
https://doi.org/10.1016/B978-0-12-374711-2.00205-9

Madec, G., the NEMO team, 2008. NEMO ocean engine. Institut Pierre-Simon Laplace (IPSL), France, note du Pôle de modélisation, No 27.
https://www.nemo-ocean.eu/bibliography/documentation/

Maljutenko, I., Laanemets, J., Raudsepp, U., 2010. Long-term high-resolution hydrodynamical model simulation in the Gulf of Finland. In: Baltic International Symposium (BALTIC), 2010 IEEE/OES US/EU. IEEE, pp. 1–7.

Marshall, J., Adcroft, A., Hill, C., Perelman, L., Heisey, C., 1997a. A finite-volume

incompressible Navier Stokes model for studies of the ocean on parallel computers. Journal of Geophysical Research 102 (C3), 5753–5766.
https://doi.org/10.1029/96JC02775

Marshall, J., Hill, C., Perelman, L., Adcroft, A., 1997b. Hydrostatic, quasi-hydrostatic, and non-hydrostatic ocean modeling. Journal of Geophysical Research 102 (C3), 5733–5752.
https://doi.org/10.1029/96JC02776

Meier, H. E. M., 2005. Modeling the age of Baltic seawater masses: Quantification and steady state sensitivity experiments. Journal of Geophysical Research: Oceans 110 (C2).
http://dx.doi.org/10.1029/2004JC002607

Meier, H. E. M., 2007. Modeling the pathways and ages of inflowing salt- and freshwater in the Baltic Sea. Estuarine, Coastal and Shelf Science 74 (4), 610–627.
https://doi.org/10.1016/j.ecss.2007.05.019

Meier, H. E. M., Andersson, H. C., Eilola, K., Gustafsson, B. G., Kuznetsov, I., Müller-Karulis, B., Neumann, T., Savchuk, O. P., 2011. Hypoxia in future climates: A model ensemble study for the Baltic Sea. Geophysical Research Letters 38 (24).
https://doi.org/10.1029/2011GL049929

Meier, H. E. M., Müller-Karulis, B., Andersson, H. C., Dieterich, C., Eilola, K., Gustafsson, B. G., Höglund, A., Hordoir, R., Kuznetsov, I., Neumann, T., Ranjbar, Z., Savchuk, O. P., Schimanke, S., 2012. Impact of climate change on ecological quality indicators and biogeochemical fluxes in the Baltic Sea: a multi-model ensemble study. Ambio 41 (6), 558–573.
https://doi.org/10.1007/s13280-012-0320-3

Meyers, S. D., Luther, M. E., Wilson, M., Havens, H., Linville, A., Sopkin, K., 2007. A numerical simulation of residual circulation in Tampa Bay. Part I: Low-frequency temporal variations. Estuaries and Coasts 30 (4), 679–697.
https://doi.org/10.1007/BF02841965

Molteni, F., Buizza, R., Palmer, T. N., Petroliagis, T., 1996. The ECMWF ensemble prediction system: Methodology and validation. Quarterly Journal of the Royal Meteorological Society 122 (529), 73–119.
http://dx.doi.org/10.1002/qj.49712252905

Myrberg, K., 1997. Sensitivity tests of a two-layer hydrodynamic model in the Gulf of Finland with different atmospheric forcings. Geophysica 33 (2), 69–98.
http://www.geophysica.fi/pdf/geophysica_1997_33_2_069_myrberg.pdf

Myrberg, K., 1998. Analysing and modelling the physical processes of the Gulf of Finland in the Baltic Sea. Monographs of the Boreal Environment Research 10. Finnish Institute of Marine Research.
http://hdl.handle.net/10138/39317

Myrberg, K., Andrejev, O., 2006. Modelling of the circulation, water exchange and water age properties of the Gulf of Bothnia. Oceanologia 48 (S), 55–74.

http://www.iopan.gda.pl/oceanologia/48Smyrbe.pdf

Myrberg, K., Ryabchenko, V., Isaev, A., Vankevich, R., Andrejev, O., Bendtsen, J., Erichsen, A., Funkquist, L., Inkala, A., Neelov, I., Rasmus, K., Medina, M. R., Raudsepp, U., Passenko, J., Söderkvist, J., Sokolov, A., Kuosa, H., Anderson, T., Lehmann, A., Skogen, M., 2010. Validation of three-dimensional hydrodynamic models of the Gulf of Finland. Boreal Environmental Research 15 (5), 453–479. http://www.borenv.net/BER/pdfs/ber15/ber15-453.pdf

Myrberg, K., Soomere, T., 2013. The Gulf of Finland, its hydrography and circulation dynamics. In: Preventive Methods for Coastal Protection. Springer, pp. 181–222.
https://doi.org/10.1007/978-3-319-00440-2_6

Mälkki, P., 2001. Oceanography in Finland 1918–2000. Geophysica 37 (1-2), 225–259.
http://www.geophysica.fi/pdf/geophysica_2001_37_1-2_225_malkki.pdf

Naimie, C. E., Blain, C. A., Lynch, D. R., 2001. Seasonal mean circulation in the Yellow Sea — a model-generated climatology. Continental Shelf Research 21 (6), 667–695.

Nixon, S. W., 1995. Coastal marine eutrophication: A definition, social causes, and future concerns. Ophelia 41 (1), 199–219.
https://doi.org/10.1080/00785236.1995.10422044

Omstedt, A., Elken, J., Lehmann, A., Leppäranta, M., Meier, H., Myrberg, K., Rutgersson, A., 2014. Progress in physical oceanography of the Baltic Sea during the 2003–2014 period. Progress in Oceanography 128 (0), 139 – 171.
http://dx.doi.org/10.1016/j.pocean.2014.08.010

Palmén, E., 1930. Untersuchungen über die Strömungen in den Finnland umgebenden Meeren. Soc. Scient. Fenn., Comm. Phys.-Math. V (12), in German.

Purokoski, T., Aro, E., Nummelin, A., 2013. First long-term deployment of Argo float in Baltic Sea. Sea technology 54 (10), 41–44.

Raateoja, M., Setälä, O. (Eds.), 2016. The Gulf of Finland assessment. Reports. Finnish Environment Institute.
http://hdl.handle.net/10138/166296

Roemmich, D., Johnson, G. C., Riser, S., Davis, R., Gilson, J., Owens, W. B., Garzoli, S. L., Schmid, C., Ignaszewski, M., 2009. The Argo program: Observing the global ocean with profiling floats. Oceanography 22 (2), 34–43.
https://doi.org/10.5670/oceanog.2009.36

Roiha, P., Siiriä, S.-M., Haavisto, N., Alenius, P., Westerlund, A., Purokoski, T., 2018. Estimating currents from Argo trajectories in Bothnian Sea, Baltic Sea. Frontiers in Marine Science 5, 308.
https://doi.org/10.3389/fmars.2018.00308

Roiha, P., Westerlund, A., Nummelin, A., Stipa, T., 2010. Ensemble forecasting of harmful algal blooms in the Baltic Sea. Journal of Marine Systems 83 (3), 210–

220.
https://doi.org/10.1016/j.jmarsys.2010.02.015

Rudnick, D. L., 2016. Ocean research enabled by underwater gliders. Annual Review of Marine Science 8 (1), 519–541.
https://doi.org/10.1146/annurev-marine-122414-033913

Ryabchenko, V., Dvornikov, A., Haapala, J., Myrberg, K., 2010. Modelling ice conditions in the easternmost Gulf of Finland in the Baltic Sea. Continental Shelf Research 30 (13), 1458–1471.
https://doi.org/10.1016/j.csr.2010.05.006

Savchuk, O. P., Gustafsson, B. G., Müller-Karulis, B., 2012. BALTSEM: A marine model for decision support within the Baltic Sea region. Tech. rep., Baltic Nest Institute.
http://www.balticnest.org/balticnest/research/publications/publications/baltsemamarinemodelfordecisionsupportwithinthebalticsearegion.5.d4ae509138dcbba8a2158.html

Siiriä, S.-M., Roiha, P., Tuomi, L., Purokoski, T., Haavisto, N., Alenius, P., 2018. Applying area-locked, shallow Argo floats in the Baltic Sea monitoring. Journal of Operational Oceanography(submitted).

Soomere, T., Delpeche, N., Viikmäe, B., Quak, E., Meier, H. E. M., Doos, K., 2011. Patterns of current-induced transport in the surface layer of the Gulf of Finland. Boreal environment research 16 (suppl. A), 49–63.
http://www.borenv.net/BER/pdfs/ber16/ber16A-049.pdf

Soomere, T., Leppäranta, M., Myrberg, K., 2009. Highlights of the physical oceanography of the Gulf of Finland reflecting potential climate changes. Boreal environment research 14 (1), 152–165.
http://www.borenv.net/BER/pdfs/ber14/ber14-152.pdf

Soomere, T., Myrberg, K., Leppäranta, M., Nekrasov, A., 2008. The progress in knowledge of physical oceanography of the Gulf of Finland: a review for 1997–2007. Oceanologia 50 (3), 287–362.
https://www.iopan.pl/oceanologia/503myrbe.pdf

Stacey, M., Rippeth, T., Nash, J., 2011. Turbulence and stratification in estuaries and coastal seas. In: Wolanski, E., McLusky, D. (Eds.), Treatise on Estuarine and Coastal Science. Academic Press, Waltham, pp. 9–35.
https://doi.org/10.1016/B978-0-12-374711-2.00204-7

Stigebrandt, A., 2001. Physical oceanography of the Baltic Sea. In: Wulff, F. V., Rahm, L. A., Larsson, P. (Eds.), A systems analysis of the Baltic Sea. Springer, pp. 19–74.
https://doi.org/10.1007/978-3-662-04453-7

Suhhova, I., Liblik, T., Madis-Jaak, L., Urmas, L., 2018. A descriptive analysis of the linkage between the vertical stratification and current oscillations in the Gulf of Finland. Boreal Environmental Research 23, 83–103.
http://www.borenv.net/BER/pdfs/ber23/ber23-083-103.pdf

Suursaar, Ü., 2010. Waves, currents and sea level variations along the Letipea-

Sillamäe coastal section of the southern Gulf of Finland. Oceanologia 52 (3), 391–416.
https://www.iopan.pl/oceanologia/523suurs.pdf

Suursaar, Ü., Aps, R., 2007. Spatio-temporal variations in hydro-physical and-chemical parameters during a major upwelling event off the southern coast of the Gulf of Finland in summer 2006. Oceanologia 49 (2), 209–228.
https://www.iopan.pl/oceanologia/492suurs.pdf

Talley, L. D., Pickard, G. L., Emery, W. J., Swift, J. H., 2011a. Gravity waves, tides, and coastal oceanography: Supplementary materials. In: Talley, L. D., Pickard, G. L., Emery, W. J., Swift, J. H. (Eds.), Descriptive Physical Oceanography, 6th Edition. Academic Press, Boston, pp. 1–31.
https://doi.org/10.1016/B978-0-7506-4552-2.10020-4

Talley, L. D., Pickard, G. L., Emery, W. J., Swift, J. H., 2011b. Mass, salt, and heat budgets and wind forcing. In: Talley, L. D., Pickard, G. L., Emery, W. J., Swift, J. H. (Eds.), Descriptive Physical Oceanography, 6th Edition. Academic Press, Boston, pp. 111–145.
https://doi.org/10.1016/B978-0-7506-4552-2.10005-8

Talley, L. D., Pickard, G. L., Emery, W. J., Swift, J. H., 2011c. Physical properties of seawater. In: Talley, L. D., Pickard, G. L., Emery, W. J., Swift, J. H. (Eds.), Descriptive Physical Oceanography, 6th Edition. Academic Press, Boston, pp. 29–65.
https://doi.org/10.1016/B978-0-7506-4552-2.10003-4

Thomson, R. E., Emery, W. J., 2014. The spatial analyses of data fields. In: Thomson, R. E., Emery, W. J. (Eds.), Data Analysis Methods in Physical Oceanography, 3rd Edition. Elsevier, Boston, pp. 313–424.
https://doi.org/10.1016/B978-0-12-387782-6.00004-1

Tranchant, B., Reffray, G., Greiner, E., Nugroho, D., Koch-Larrouy, A., Gaspar, P., 2016. Evaluation of an operational ocean model configuration at 1/12° spatial resolution for the Indonesian seas (NEMO2.3/INDO12) – part 1: Ocean physics. Geoscientific Model Development 9 (3), 1037–1064.
http://dx.doi.org/10.5194/gmd-9-1037-2016

Tuomi, L., 2014. On modelling surface waves and vertical mixing in the Baltic Sea. Ph.D. thesis, Finnish Meteorological Institute Contributions 103.
http://urn.fi/URN:ISBN:978-951-697-810-2

Tuomi, L., Miettunen, E., Alenius, P., Myrberg, K., 2018a. Evaluating hydrography, circulation and transport in a coastal archipelago using a high-resolution 3D hydrodynamic model. Journal of Marine Systems 180, 24–36.
https://doi.org/10.1016/j.jmarsys.2017.12.006

Tuomi, L., Myrberg, K., Lehmann, A., 2012. The performance of the parameterisations of vertical turbulence in the 3D modelling of hydrodynamics in the Baltic Sea. Continental Shelf Research 50, 64–79.
https://doi.org/10.1016/j.csr.2012.08.007

Tuomi, L., Vähä-Piikkiö, O., Alenius, P., Björkqvist, J.-V., Kahma, K. K., Jan

2018b. Surface stokes drift in the Baltic Sea based on modelled wave spectra. Ocean Dynamics 68 (1), 17–33.
https://doi.org/10.1007/s10236-017-1115-7

Vancoppenolle, M., Fichefet, T., Goosse, H., Bouillon, S., Madec, G., Maqueda, M. A. M., 2009. Simulating the mass balance and salinity of Arctic and Antarctic sea ice. 1. Model description and validation. Ocean Modelling 27 (1), 33–53.
https://doi.org/10.1016/j.ocemod.2008.10.005

Vankevich, R. E., Sofina, E. V., Eremina, T. E., Ryabchenko, V. A., Molchanov, M. S., Isaev, A. V., 2016. Effects of lateral processes on the seasonal water stratification of the Gulf of Finland: 3-D NEMO-based model study. Ocean Science 12 (4), 987–1001.
http://dx.doi.org/10.5194/os-12-987-2016

Vankevich, R. E., Sofina, E. V., Ryabchenko, V. A., 2015. Modelling the spring-summer evolution of the thermohaline structure in the Gulf of Finland on the basis of a three-dimensional hydrodynamic model of high resolution. Fundamentalnaya i prikladnaya gidrofizika 8 (2), 3–9, (in Russian, with English abstract).
http://hydrophysics.info/?p=2643&lang=en

Väli, G., Zhurbas, V. M., Laanemets, J., Lips, U., 2018. Clustering of floating particles due to submesoscale dynamics: a simulation study for the Gulf of Finland, Baltic Sea. Fundamentalnaya i prikladnaya gidrofizika 11 (2), 21–35.
http://hydrophysics.info/?p=3685&lang=en

Wei, H., Hainbucher, D., Pohlmann, T., Feng, S., Suendermann, J., 2004. Tidal-induced Lagrangian and Eulerian mean circulation in the Bohai Sea. Journal of Marine Systems 44 (3), 141–151, analysis and Modelling of the Bohai Sea Ecosystem.
https://doi.org/10.1016/j.jmarsys.2003.09.007

Witting, R., 1912. Zusammenfassende Uebersicht der Hydrographie des Bottnischen und Finnischen Meerbusens und der Nördlichen Ostsee nach den Untersuchungen bis Ende 1910. Soc. Scient. Fenn., Finländische Hydr.-Biol. Untersuchungen (7), in German.

WMO, 2017. WMO Guidelines on the Calculation of Climate Normals. WMO-No. 1203. World Meteorological Organization.
https://library.wmo.int/opac/doc_num.php?explnum_id=4166

Wulff, F., Sokolov, A., Savchuk, O., 2013. Nest – a decision support system for management of the Baltic Sea. Tech. rep., Baltic Nest Institute.
http://www.balticnest.org/download/18.416c425f13e06f977b15bec/1381789016966/TR+10+-+Nest+user+manual.pdf

Zhurbas, V., Laanemets, J., Vahtera, E., 2008. Modeling of the mesoscale structure of coupled upwelling/downwelling events and the related input of nutrients to the upper mixed layer in the Gulf of Finland, Baltic Sea. Journal of Geophysical Research: Oceans 113 (C5).
https://doi.org/10.1029/2007JC004280

# Licences and permissions

*Articles* — Article I is reproduced with the permission of Elsevier, B.V. Article II is reproduced with the permission of the Taylor & Francis Group. Article III is reproduced under the Creative Commons BY-NC-ND 4.0 International Licence (http://creativecommons.org/licenses/by-nc-nd/4.0/). Article IV is reproduced under the Creative Commons BY 4.0 Licence (http://creativecommons.org/licenses/by/4.0/).

*Figures* — Fig. 1.2: National Archives of Finland (Luotsi- ja majakkalaitoksen arkisto, Uaab:139); http://digi.narc.fi/digi/view.ka?kuid=24767256. No copyright restrictions apply to the use of this photo.

*Data* — Finngrundet wave buoy data was obtained from the SMHI open data service (http://opendata-download-ocobs.smhi.se/explore/), licensed under the Creative Commons CC-BY-2.5 licence. Argo data were collected and made freely available by the International Argo Program and the national programs that contribute to it (http://www.argo.ucsd.edu, http://argo.jcommops.org). The Argo program is part of the Global Ocean Observing System. Parts of the CTD monitoring data were extracted from the ICES Dataset on Ocean Hydrography (The International Council for the Exploration of the Sea, Copenhagen, 2014, http://ices.dk). The satellite SST data in Article II is available under the Creative Commons BY 4.0 International license and is processed by Finnish Environment Institute (SYKE). This study has been conducted using E.U. Copernicus Marine Service Information. The Gulf of Finland Year 2014 data providers include Estonian Marine Institute (EMI); Marine Systems Institute (MSI); Finnish Environment Institute (SYKE); Uusimaa and South-East Finland Centres for Economic Development, Transport and the Environment (UUDELY and KASELY); City of Helsinki Environment Centre (HELSINKI); and North-West Interregional Territorial Administration for Hydrometeorology and Environmental Monitoring (HYDROMET). The bathymetric data in Article IV was obtained from the Finnish Inventory Programme for the Underwater Marine Environment (VELMU) depth model (Finnish Environment Institute, http://www.syke.fi/en-US/Open_information/Spatial_datasets) and the Baltic Sea Bathymetry Database (Baltic Sea Hydrographic Commission, 2013) version 0.9.3, downloaded from http://data.bshc.pro on 25 Aug 2014. VELMU data is licensed under the Creative Commons BY 4.0 licence and Baltic Sea Bathymetry Database (BSBD) data is licensed under the Creative Commons BY 3.0 licence. The CTD monitoring data in Article IV was provided by Finnish Environment Institute (SYKE) and Centres for Economic Development, Transport and the Environment (ELY), and is licensed under the Creative Commons BY 4.0 licence, see http://www.syke.fi/en-US/Open_information. To view a copy of these licenses, visit http://creativecommons.org/licenses or send a letter to Creative Commons, PO Box 1866, Mountain View, CA 94042, USA.

I

Journal of Marine Systems 158 (2016) 34–44

Contents lists available at ScienceDirect

Journal of Marine Systems

journal homepage: www.elsevier.com/locate/jmarsys

# Vertical temperature dynamics in the Northern Baltic Sea based on 3D modelling and data from shallow-water Argo floats

Antti Westerlund *, Laura Tuomi

*Finnish Meteorological Institute, Marine Research, Erik Palménin aukio 1, P.O. Box 503, FI-00101 Helsinki, Finland*

ARTICLE INFO

*Article history:*
Received 15 July 2015
Received in revised form 14 January 2016
Accepted 20 January 2016
Available online 28 January 2016

*Keywords:*
Vertical mixing
Hydrodynamics
Modelling
Temperature profiles
Baltic Sea
Bothnian Sea

ABSTRACT

3D hydrodynamic models often produce errors in the depth of the mixed layer and the vertical density structure. We used the 3D hydrodynamic model NEMO to investigate the effect of vertical turbulence parameterisations on seasonal temperature dynamics in the Bothnian Sea, Baltic Sea for the years 2012 and 2013. We used vertical profiles from new shallow-water Argo floats, operational in the area since 2012, to validate our model. We found that NEMO was able to reproduce the general features of the seasonal temperature variations in the study area, when meteorological forcing was accurate. The $k$-$\varepsilon$ and $k$-$\omega$ schemes were selected for a more detailed analysis. Both schemes showed clear differences, but neither proved superior. While sea surface temperature was better simulated with the $k$-$\omega$ scheme, thermocline depth was clearly better with the $k$-$\varepsilon$ scheme. We investigated the effect of wave-breaking on the mixing of the surface layer. The Craig and Banner parameterisation clearly improved the representation of thermocline depth. However, further tuning of the mixing parameterisations for the Baltic Sea is needed to better simulate the vertical temperature structure. We found the autonomous Baltic Sea Argo floats valuable for model validation and performance evaluation.

© 2016 Elsevier B.V. All rights reserved.

## 1. Introduction

Vertical and horizontal density gradients are an essential part of ocean dynamics. To be considered good, a hydrodynamic model must be able to faithfully reproduce them. Several studies have shown that 3D hydrodynamic models often produce considerable errors in mixed layer depths and in vertical temperature structure that can be related to the parameterisations of vertical turbulence. These errors can be especially pronounced in areas with complex hydrography, such as coastal seas, where parameterisations that have been proven to work well in the World Ocean may fail. Although their performance can be improved by tuning the parameterisations (Meier, 2001), the models still struggle to produce the stratification with sufficient accuracy.

Accurate simulation of density stratification is important not only for the model performance per se, but also for several applications that use model results. For example, in biogeochemical models the accuracy of nutrient concentrations in the surface mixed layer strongly depends on the density stratification of the hydrodynamic model. As upward transport of nutrients is mainly physically driven (e.g. Reissmann et al., 2009), problems with density stratification can lead to incorrect estimates of nutrient concentrations in the mixed layer. This has a direct effect on the representation of the primary production in the euphotic zone. Furthermore, biogeochemical model parameters have been shown to exhibit high dependence on the chosen turbulence closure (Burchard et al., 2006). Other relevant applications include the calculation of sound speed in the sea, which is based on temperature and salinity profiles (e.g. Apel, 1987).

The Baltic Sea is a semi-enclosed brackish water basin with specific horizontal and vertical stratification conditions compared to those of the World Ocean. The density stratification in the Baltic Sea is mostly determined by salinity. The water body of the Baltic Sea has a permanent two-layer structure as a result of saline water inflow from the Danish Straits filling the deeps, and of voluminous river runoffs bringing fresh water to the surface. The halocline is usually at a depth of 40–80 m. The seasonal thermocline starts to develop in late spring and reaches its maximum depth of 10–30 m typically in late August. In the autumn the thermocline vanishes due to convection caused by the cooling and wind-induced mixing. The location of thermocline and halocline at different depths produces stratification conditions that are challenging for the present ocean models, as was shown e.g. by Myrberg et al. (2010) and Tuomi et al. (2012), who suggested further effort to develop modelling methods for vertical mixing with particular relevance for the Baltic Sea.

Our study area, the Bothnian Sea (Fig. 1), is a semi-enclosed basin in the Gulf of Bothnia, Baltic Sea. Gulf of Bothnia consists of the Archipelago Sea, the Åland Sea, the Bothnian Sea and the Bothnian Bay. The Gulf of Bothnia has sills and archipelagos in the south to the Baltic Proper. The hydrography of the Gulf of Bothnia differs considerably from that of the other basins of the Baltic Sea. The salinity stratification in the Bothnian Sea depends on the water exchange between the Baltic Proper and the Bothnian Sea through the Åland Sea and the Archipelago Sea

* Corresponding author.
*E-mail address:* antti.westerlund@fmi.fi (A. Westerlund).

http://dx.doi.org/10.1016/j.jmarsys.2016.01.006
0924-7963/© 2016 Elsevier B.V. All rights reserved.

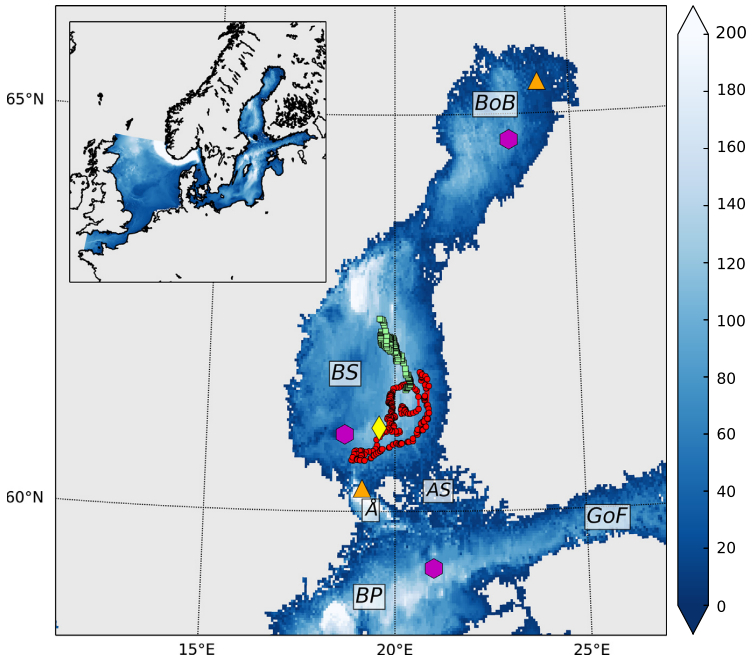


**Fig. 1.** Model bathymetry (in metres) in the study area. BoB: Bay of Bothnia, BS: Bothnian Sea, BP: Baltic Proper, GoF: Gulf of Finland, AS: Archipelago Sea, Å: Åland Sea. Locations of the Argo profiles are marked with red circles (2012) and green squares (2013). The magenta hexagons show from north to south the locations of the Bay of Bothnia wave buoy, the Finngrundet wave buoy in the Bothnian Sea, and the Northern Baltic Proper wave buoy. The orange triangles show from north to south the locations of Kemi I and Märket weather stations. The yellow diamond shows the location of the SR5 monitoring station. The inset in the upper corner of the map shows the whole model domain and bathymetry. (For interpretation of the references to colour in this figure legend, the reader is referred to the web version of this article.)

and on the river runoff. The sill in the Åland Sea towards the Baltic Proper is shallow (c. 70 m), thus only the water above the halocline (with salinity of c. 6.5–7 PSU) penetrates to the Bothnian Sea forming the bottom water of the basin. The halocline in the Bothnian Sea is at the depth of 60–80 m. The surface salinity varies between 4–6 PSU decreasing towards the north. Overall, the stratification in the Bothnian Sea is rather weak and mixing is able to penetrate also to deeper layers. A more detailed description of the Baltic Sea and its hydrography can be found e.g. in Leppäranta and Myrberg (2009), and of the Gulf of Bothnia specifically e.g. in Håkansson et al. (1996).

In many ways, the Gulf of Bothnia is one of the least investigated sub-basins of the Baltic Sea, as noted by e.g. Omstedt and Axell (2003). It has had good ecological status and extended monitoring has not been a key priority unlike in other, more eutrophicated areas of the Baltic Sea. There has been a renewed interest in the Gulf of Bothnia, as ecosystem health indicators and eutrophication-related parameters have shown a decline in the eutrophication status of the area (HELCOM, 2014; Fleming-Lehtinen et al., 2015; Lundberg et al., 2009). Warming trends in surface air and sea temperatures seem stronger in the Gulf of Bothnia than elsewhere in the Baltic Sea (BACC II Author Team, 2015; Lehmann et al., 2011), but relatively large uncertainties remain in terms of the impact of climate change on the biogeochemistry of the area (e.g. Meier et al., 2012). In addition to monitoring, evaluations based on model studies are also needed. Unfortunately, comparisons of physical-biogeochemical models have found that typical model performance in the area is poor. There are problems in the representation of both biogeochemistry and physics (Eilola et al., 2011).

One notable factor that has previously limited process and modelling studies of the northernmost Baltic Sea has been the limited amount of observational data. In Baltic Sea off-shore areas, temperature and salinity profiles are measured mainly at monitoring stations that are visited 2–4 times a year. In order to improve the performance of hydrodynamic models, observations need to have sufficient spatial and temporal coverage. New measurement techniques that are already frequently used in the oceans, such as Argo floats and gliders, give the opportunity to collect new data for model validation and development. The Finnish Meteorological Institute (FMI) together with Aalto University have been developing Argo floats that can also be operated in shallow seas (Purokoski et al., 2013). The first tests were made in 2011 and since then Argo floats have been operated first in the Bothnian Sea and later also in the Baltic Proper. This new dataset is well suited for evaluating the capability of hydrodynamic models to produce the vertical structure of temperature and salinity. It provides a time series of profiles from the area of interest with good temporal resolution, showing the dynamics of temperature and salinity in the water column throughout the summer.

State-of-the-art 3D ocean models, such as NEMO (Madec and the NEMO team, 2008), provide a good basis for implementing and further developing model applications for coastal and shelf seas. However, similar to other models originally developed for oceans, several adaptations are required, including adjusting bottom friction and tuning the turbulence schemes. A specific configuration of NEMO, named NEMO Nordic, has been made for the Baltic Sea studies by Hordoir et al. (2013a,b, 2015). This configuration has been previously used to study e.g. air–sea coupling (Gröger et al., 2015) and degradation of dissolved organic matter (Fransner et al., 2015). By studying the performance of this model configuration in the Bothnian Sea, we can gain further understanding of its capabilities and also of any improvements that may be required. We focus our studies on the vertical structure of temperature in the Bothnian Sea, from which new observations from autonomous Baltic Sea Argo floats are available. With this new data we can evaluate the ability of 3D models to produce vertical temperature profiles and mixed layer depths in the area with unprecedented temporal detail. We also validate the model against other observations and examine different vertical mixing options.

## 2. Materials and methods

### 2.1. NEMO ocean model

NEMO 3D ocean model version 3.6 has been set up at FMI for the Baltic Sea, based on the NEMO Nordic configuration by Hordoir et al. (2013a,b, 2015). The model has been discretised on a Baltic Sea–North Sea grid with two nautical mile horizontal resolution and 56 z-coordinate vertical layers. The topmost vertical layer is 3 m, and the vertical resolution gradually increases with depth, being about 13 m at 150 m depth. The deepest point in the domain is in the Norwegian Trench in the North Sea at around 720 m depth and 22 m layer thickness. Our study area, the Bothnian Sea, is mostly less than 150 m deep. The time step of the model was 360 s. Model domain and bathymetry are shown in Fig. 1.

The NEMO Nordic configuration uses the TVD advection scheme (Leclair and Madec, 2009) for both tracers and momentum. Lateral mixing in NEMO Nordic uses Laplacian isopycnal diffusion. Isopycnal viscosity was set to 50 $m^2\ s^{-1}$ above the depth of 30 m, and to $10^{-3}\ m^2\ s^{-1}$ below. Isopycnal diffusivity was set to 10% of viscosity. The model was configured with the LIM3 sea ice model (Vancoppenolle et al., 2009).

The model was run for the years 2012 and 2013. Temperature data from the model was saved as 3-h averages for surface fields and daily averages for full profiles. Initial conditions for both runs were taken from the FMI operational ocean model HBM-FMI (Berg and Poulsen, 2012), which provides a daily model output for roughly the same domain as the NEMO Nordic configuration.

#### 2.1.1. Surface fluxes, forcing and lateral boundary conditions

Forecasts from FMI's numerical weather prediction (NWP) system HIRLAM (HIRLAM-B, 2015) were used as atmospheric forcing. Its domain covers the European region with a horizontal resolution of 0.15 degrees (V73 and earlier; before 6 March 2012) or 0.068 degrees (V74; after 6 March 2012). Vertically the domain is divided into 60 (V73) or 65 (V74) terrain-following hybrid levels, the lowest level being about 12 m above the sea surface. A forecast is run four times a day (00, 06, 12, and 18 UTC) using boundary conditions from the Boundary Condition Optional Project of the ECMWF. Each day of forcing was extracted from the 00 forecast cycles with the highest available temporal resolution in the model archive, varying from 1 to 6 h.

Forcing taken from HIRLAM includes the 2-metre air temperature, total cloud cover, mean sea-level pressure and 10-metre winds, and either the 2-metre dew point temperature or relative humidity, depending on the availability in the model archive. Forcing was read into the NEMO run with the CORE bulk formulae (Large and Yeager, 2004). Precipitation and river runoffs were climatological (as described by Hordoir et al., 2013a, 2015). The two open boundaries in the model, in the English Channel and between Scotland and Norway, were configured as in Hordoir et al. (2015), but with only tidal boundary surface height contribution and no storm surge model.

#### 2.1.2. Vertical turbulence schemes in NEMO

In order to find the optimal vertical turbulence scheme for simulating the vertical temperature structures in the area, different schemes and settings available in the NEMO vertical mixing package were compared. The following model test runs are referenced later in this article:

- GLS/$k$-$\varepsilon$, with CB parameterisation ("k-e")
- GLS/$k$-$\omega$, with CB parameterisation ("k-w")
- GLS/$k$-$\varepsilon$, no CB parameterisation ("k-e, CB off")

Here GLS/$k$-$\varepsilon$ and GLS/$k$-$\omega$ refer to the Generic Length Scale (GLS) turbulence model (Umlauf and Burchard, 2003, 2005) implemented in NEMO, which reduces to $k$-$\varepsilon$ (Rodi, 1987) and $k$-$\omega$ (Wilcox, 1988) models with a choice of constants. These were selected for closer investigation as both are frequently used in the Baltic Sea (e.g. Omstedt et al., 2014) and the $k$-$\varepsilon$ model in particular has a long history in Baltic Sea modelling community (e.g. Svensson, 1979). The CB parameterisation refers to the Craig and Banner (1994) parameterisation of wave-breaking induced turbulence, which was used to study the effect of wave-induced mixing. We used $\alpha_{CB} = 100$ for the wave-age related parameter, as suggested by Craig and Banner (1994). For Charnock's constant we used the default NEMO Nordic value of $\beta = 7.0 \cdot 10^4$.

More information of the turbulence parameterisations in NEMO can be found in Reffray et al. (2015), and a review of some issues encountered in numerical modelling of coastal ocean turbulence in Burchard et al. (2008).

### 2.2. Measurements

#### 2.2.1. Baltic Sea Argo floats

Observations from autonomous Argo floats operating in the Baltic Sea were used to study the accuracy of the model results. Data were collected during two separate missions in 2012 and 2013. The first mission lasted approximately six months from 17 May 2012 to 5 Dec. 2012, during which time around 200 vertical profiles of temperature and salinity were collected. The second mission lasted approximately four months from 13 Jun. 2012 to 2 Oct. 2013 with over 100 acquired profiles. Argo tracks and locations of the profiles are shown in Fig. 1.

#### 2.2.2. Moored buoys

Surface temperature measured at FMI's Directional Waveriders (locations shown in Fig. 1) was used to validate the model. Waveriders have a temperature sensor in the mooring eye at the bottom of the buoy and the measurement depth is c. 0.4 m below the sea surface. Temperature measurements are provided every 30 min, excluding the ice season, when the buoys do not perform measurements. Temperature data from FMI's wave buoy in the Bothnian Sea could not be used as the temperature sensor in the buoy did not measure within the specifications during the study period and was eventually replaced in 2014. Instead, data from Swedish Meteorological and Hydrological Institute's (SMHI) Finngrundet wave buoy were used for the Bothnian Sea. This buoy measures SST at 0.5 m depth (http://www.smhi.se/kunskapsbanken/oceanografi/en-vagboj-finngrundet-1.22076) and the data is provided at 1-h intervals.

#### 2.2.3. Monitoring data

Temperature and salinity profiles from monitoring cruises to the Bothnian Sea in 2012 and 2013 were collected from the ICES (International Council for the Exploration of the Sea) Dataset on Ocean Hydrography. A total of 55 profiles were obtained for 2012 and 82 for 2013. All these profiles originated from the *R/V Aranda*.

### 2.3. Statistical methods

The model performance was evaluated using statistical analysis based on the following equations. The mean of a dataset (observations or model) was defined as:

$$\bar{x} = \frac{1}{N}\sum_{i=1}^{N} x_i \tag{1}$$

where $N$ is the number of data points and $x_i$ are the data points.

The bias of a dataset was defined as

$$B = \bar{y} - \bar{x} \tag{2}$$

where $\bar{y}$ and $\bar{x}$ are the means of the datasets being compared. In this case $y$ refers to the observations and $x$ to the model data.

The root-mean-square error was defined as

$$RMSE = \sqrt{\frac{1}{N}\sum_{i=1}^{N}(x_i - y_i)^2}. \quad (3)$$

and the correlation coefficient as

$$R = \frac{\sum_{i=1}^{n}[(x_i - \overline{x})(y_i - \overline{y})]}{(N-1)\sigma_x\sigma_y} \quad (4)$$

where the standard deviation $\sigma$ is defined as

$$\sigma_x = \sqrt{\frac{\sum_{i=1}^{n}\left[(x_i - \overline{x})^2\right]}{N-1}}. \quad (5)$$

## 3. Results

### 3.1. Validation

The model configuration used in the study has been previously validated by Hordoir et al. (2013a, 2013b, 2015), who showed that generally the configuration performs in a satisfactory manner. The emphasis of these previous validations has been on salinity dynamics, while validation performed by the present authors concentrated on the seasonal temperature variations in the model. The $k$-$\varepsilon$ vertical mixing scheme with the CB parameterisation was chosen here for closer examination, since it is the parameterisation used in the NEMO Nordic configuration.

This study focused on the summers 2012 and 2013, periods for which there was Argo data available for the study area. Both summers had roughly average air temperatures in the area based on long term data from the area (Pirinen et al., 2012). May 2012 was some degrees warmer compared to the 30-year average (1981–2010), while May 2013 was colder than average. This is in line with data from FMI's ice charts, according to which the ice season ended in the Baltic Sea approximately two weeks earlier in 2012 (15 May) than in 2013 (30 May). There were also a number of interesting wind-induced mixing events during the period in question. Overall, these two summers proved interesting test cases for the model.

#### 3.1.1. Meteorological forcing

As the performance of any 3D hydrodynamic model is highly dependent on the accuracy of the atmospheric forcing, the FMI-HIRLAM forcing was evaluated against data from coastal weather stations Märket and Kemi I (locations shown in Fig. 1). Both stations can be considered generally representative of open sea conditions. The comparison showed that the forcing wind speed was fairly well represented by HIRLAM. The air temperature was forecast with good accuracy except for the beginning of June 2013. During this period there was a technical problem in the SST assimilation of the NWP system, which caused a cold bias in air temperature over the Baltic Sea lasting at least four days (Fig. 2).

#### 3.1.2. Sea surface temperature

The statistical analysis of the modelled sea surface temperature (SST) in the northernmost sub-basins of the Baltic Sea (Table 1) shows that the SST was generally well reproduced by NEMO. Bias and RMS error are typically less than 1 °C in all the areas. The largest RMS error, of 3.31 °C with a bias of 2.95 °C, is for summer 2013 in the Bay of Bothnia. This resulted from incorrectly timed melting of ice cover in the model. In addition, the aforementioned problem with meteorological forcing increased the error. Furthermore, the late deployment of the wave buoy in that area on 11 June 2013 means that the number of available data points for the summer period was slightly lower than in the other stations.

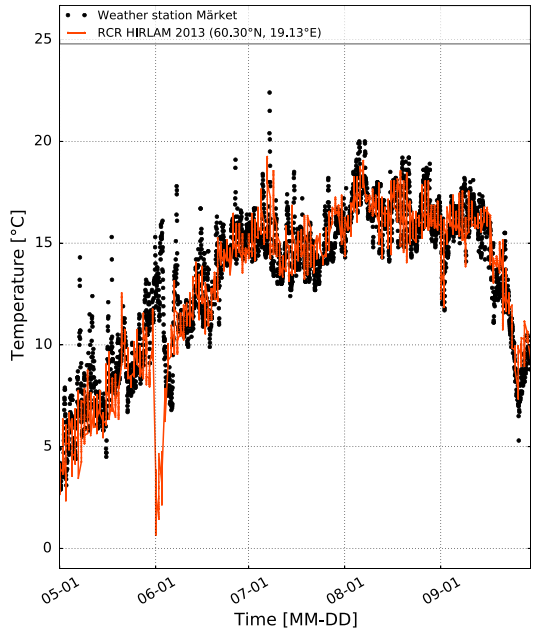


**Fig. 2.** Two metre air temperature measured at the Märket weather station in summer 2013 compared to FMI-HIRLAM forcing used for the NEMO model. The drop in modelled air temperature in early June 2013 was due to a technical problem in the NWP system, see Section 3.1.1.

In addition to the statistics, the time series of modelled and measured SST from Finngrundet (located in the Bothnian Sea, location shown in Fig. 1) is shown in Fig. 3. In both years, the model followed the seasonal cycle of SST well. In 2013 the model slightly underestimated the SST throughout the summer as was already shown in the statistical analysis in Table 1. In both years the cooling of the surface layer in autumn was slower in the model than in the measurements. The above-mentioned problem in meteorological forcing in June 2013 can be seen as a drop in modelled SST. Furthermore, the measured data shows higher temporal variation than the modelled data, due to modelled SST data being

**Table 1**
Modelled daily SST averages from NEMO compared against wave buoy observations in 2012 and 2013 for the study area and adjacent basins. Model RMS errors, biases (°C) and correlation coefficients R shown for spring, summer, autumn and all three seasons combined. N/A means that observation data was not available for that time, or there were too few observation data points for statistical comparison.

| | Baltic Proper | | | Bothnian Sea | | | Bay of Bothnia | | |
|---|---|---|---|---|---|---|---|---|---|
| | RMSE | Bias | R | RMSE | Bias | R | RMSE | Bias | R |
| *2012* | | | | | | | | | |
| Mar–May | 0.60 | <0.01 | 0.98 | 0.74 | −0.18 | 0.87 | N/A | N/A | N/A |
| Jun–Aug | 0.70 | 0.23 | 0.98 | 0.78 | 0.33 | 0.98 | 1.07 | −0.09 | 0.97 |
| Sep–Nov | 0.39 | 0.075 | 0.99 | 0.63 | −0.46 | 0.99 | 0.64 | −0.39 | 0.99 |
| Mar–Nov | 0.57 | 0.11 | 0.99 | 0.71 | −0.08 | 0.99 | 0.89 | −0.23 | 0.98 |
| *2013* | | | | | | | | | |
| Mar–May | 0.94 | 0.68 | 0.97 | N/A | N/A | N/A | N/A | N/A | N/A |
| Jun–Aug | 0.97 | 0.65 | 0.97 | 1.48 | 1.09 | 0.96 | 3.31 | 2.95 | 0.92 |
| Sep–Nov | 0.42 | 0.21 | 0.99 | 0.57 | −0.27 | 0.99 | 0.80 | 0.25 | 0.99 |
| Mar–Nov | 0.80 | 0.49 | 0.99 | 1.18 | 0.47 | 0.96 | 2.50 | 1.72 | 0.86 |

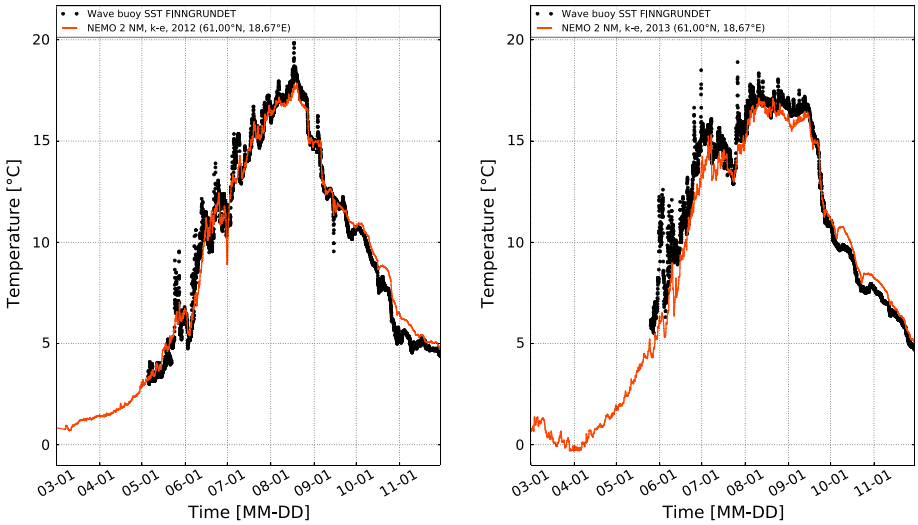


**Fig. 3.** Modelled SST from NEMO compared to measured SST in 2012 and 2013 for the Finngrundet wave buoy in the Bothnian Sea (location shown in Fig. 1).

saved as temporal averages (as 3-h averages) and observations being instantaneous data.

*3.1.3. Temperature and salinity from ship observations*

We validated the model results against CTD monitoring data from the Bothnian Sea. The dataset was relatively sparse both in space and time. Many stations were sampled only once during the study period. Most frequently visited monitoring stations were sampled three or four times a year.

Comparison of temperature profiles showed that the model could reproduce seasonal variations as expected in the study area. Comparison of salinity showed that the model results were sensible for the purposes of this study for the Bothnian Sea. Due to its sparseness, only limited conclusions about salinity or temperature dynamics could be drawn from this data. An example of typical results is shown in Fig. 4, where all salinity and temperature profiles taken at the SR5 monitoring station (location shown in Fig. 1) in 2012 are shown. In the southern Baltic Sea outside our study area, the model showed some overestimation of salinity below the permanent halocline.

*3.2. Profiles from Argo floats*

Figs. 5 and 6 show measured and modelled ($k$-$\varepsilon$ with CB parameterisation) temperature profiles during Argo measurement campaigns in the Bothnian Sea in 2012 and 2013. In both years, the seasonal thermocline developed in the spring, as expected, and the surface mixed layer reached its maximum depth and temperature in August.

NEMO was able to reproduce the vertical structure of temperature near the surface, when the atmospheric forcing was sufficiently accurate. The deepening of the thermocline as well as the temperature gradient was well represented by the model. The response of the surface layer to forcing was similar in measurements and model data. However, the warming of the surface layer in spring was slower in the modelled than in the measured profiles. Moreover, the layers below thermocline had a warm bias, and the dicothermal layer or the old winter water layer was not as pronounced as in the measurements. The most probable reason behind this is the combination of initial conditions, limited vertical resolution, and over-mixing in the deeper layers. Overall, temperature gradients in the model were gentler than measured and some fine-scale features were not correctly reproduced. For example, when secondary thermocline developed in the mixed layer during calmer periods, their structure in the model was smoother than in reality.

Argo salinity profiles from these two campaigns (not shown) did not reveal notable features with respect to the subject of this study, presenting a picture similar to the CTD profiles in Fig. 4.

*3.2.1. Near-surface temperature and thermocline depth*

Next, we further investigated measured and modelled temperatures near the surface along the Argo float route and the depth of the mixed layer for the three tested parameterisations listed in Section 2.1.2. We defined near-surface temperature as the model data point that has been sampled at the depth of the topmost data point in the Argo data (typically around 4 m, depending on the profile). In our modelled data this was in most cases very close to the sea surface temperature (mean difference around 0.1 °C), but at single locations the difference was larger (up to 3 °C). Overall, when compared to the sea surface temperature of the model at the same points, the near-surface temperature time series was very similar but slightly smoother. Thermocline depth was defined as the location of the maximum temperature gradient with depth.

Figs. 7 and 8 show measured and modelled near-surface temperatures, along with estimated thermocline depths. Modelled near-surface temperature captured the overall seasonal heating and cooling. However, in spring 2013 heating was slower than in the measurements with most mixing schemes, with the exception being the run with no wave-breaking parameterisation. All schemes were able to produce the near-surface temperatures in late July/August 2013.

Thermocline depths were fairly well reproduced by the model when the $k$-$\varepsilon$ scheme was used together with the wave-breaking parameterisation. The representation of the thermocline depth was sensitive to the selected turbulence scheme and especially at the beginning of summer to whether the wave-breaking parameterisation was applied or not. The $k$-$\varepsilon$ scheme in 2012 was better overall than $k$-$\omega$ scheme at producing the correct thermocline depth, while the $k$-$\omega$ scheme was slightly better at producing surface temperatures. The $k$-$\omega$ scheme underestimated thermocline depth throughout the summer of 2013.

The $k$-$\varepsilon$ scheme slightly underestimated temperatures during the warming phase. During cooling the difference was less noticeable. In 2013 the $k$-$\varepsilon$ scheme underestimated temperatures during the warming phase more than the previous year. In addition, the $k$-$\omega$ scheme underestimated surface temperatures at that time. These problems in

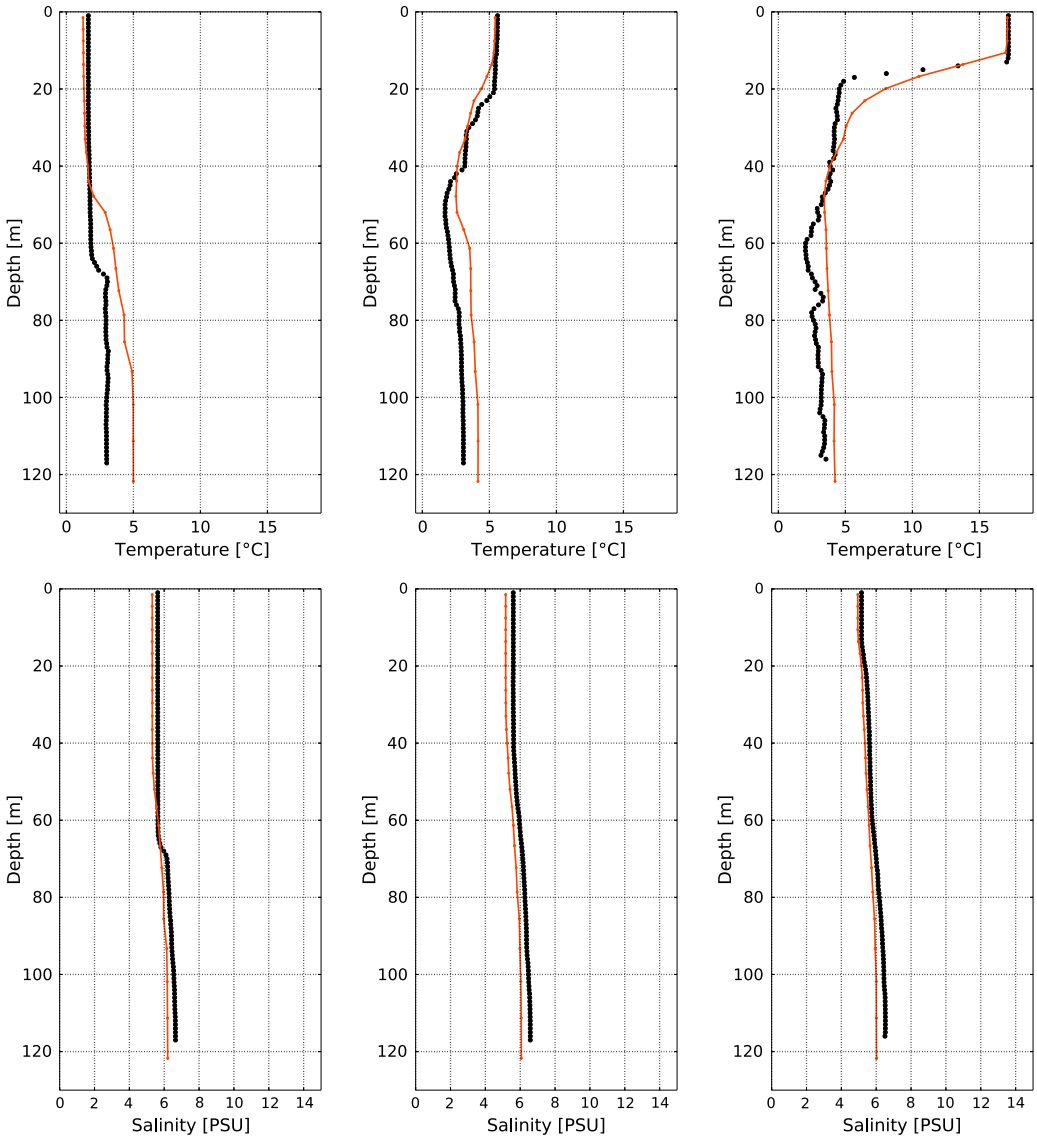


**Fig. 4.** Temperature (upper row) and salinity (lower row) monitoring observations (black dots) from the SR5 station in the Bothnian Sea in 2012 (location shown in Fig. 1). From left to right, the profiles were taken on 11 Feb., 28 May and 21 Aug. 2012. Red lines show NEMO results. (For interpretation of the references to colour in this figure legend, the reader is referred to the web version of this article.)

early summer 2013 might well be to some extent due to the error in atmospheric forcing in June 2013. As for thermocline depths in 2013, we see similar behaviour to the previous year, where the *k*-*ω* scheme underestimated thermocline depth over most of the summer. However, it seems to be the best thermocline depth estimate in late August.

It seems that the slightly better SST estimate of the *k*-*ω* scheme during the warming-up phase was associated with a shallower thermocline than that produced e.g. by the *k*-*ε* scheme. Our findings are similar to Reffray et al. (2015), who studied a 1D NEMO setup both in an idealised experiment and in comparison to the data from the PAPA station (http://www.pmel.noaa.gov/OCS/Papa/index-Papa.shtml). They found that the *k*-*ω* scheme underestimated the mixed layer depth more than the *k*-*ε* scheme. For the PAPA site the *k*-*ω* scheme also produced higher SST values than the *k*-*ε* scheme. Similar behaviour of these two schemes has also been shown by Warner et al. (2005).

Fig. 9 shows temperature profiles from two days in August 2012, when there was a clear deepening of the mixed surface layer visible in the Argo data over roughly two days. Between these two profiles the float drifted 8 km. From these profiles we see that all model runs showed some deepening of the mixed layer and a drop in surface temperature. The drop in modelled daily average surface temperature was approximately 1 °C. The change in sampling location corresponded to a drop of 0.2 °C in the modelled daily averaged profiles. The model results are not as sensitive as they should be, however, as in Argo data

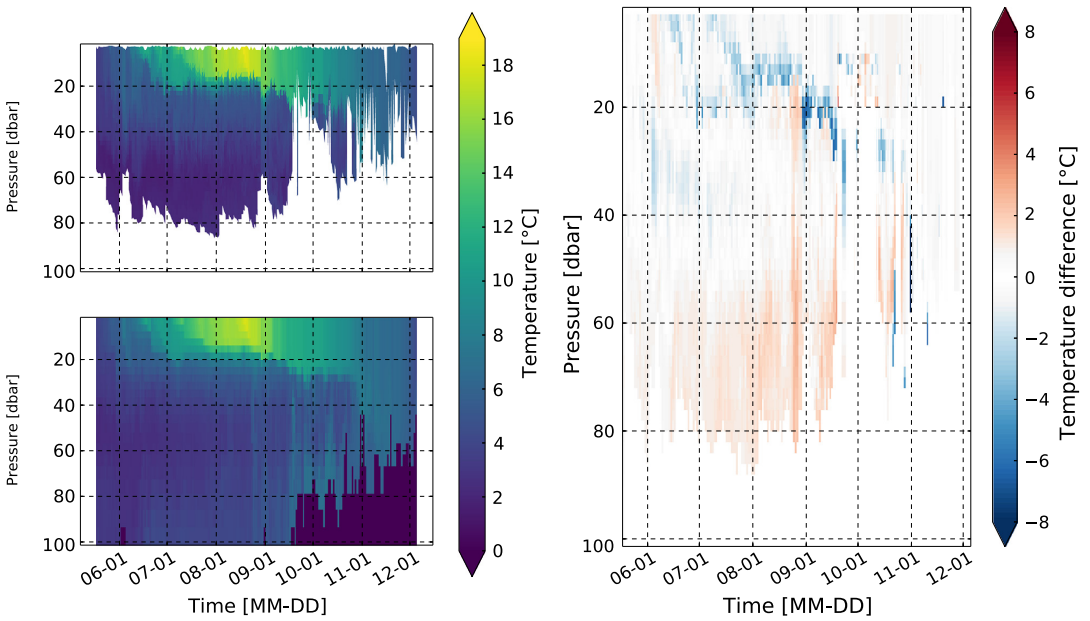


**Fig. 5.** Time series of vertical temperature profiles from an Argo float in the Bothnian Sea in 2012 (upper left panel) and virtual profiles from the NEMO model ($k$-$\varepsilon$ scheme, lower left panel). The difference between the two is shown on the right, with positive values showing where the model was larger than the measurement. Model results have been sampled along the float route.

the temperature drop at 4 m depth was approximately 2.3 °C. A small part of this may be due to the fact that the model profiles were saved as daily averages, which can smooth out some features from the instantaneous data.

## 4. Discussion

The simulation of vertical temperature dynamics is dependent on several factors. In this paper the focus is on vertical turbulence

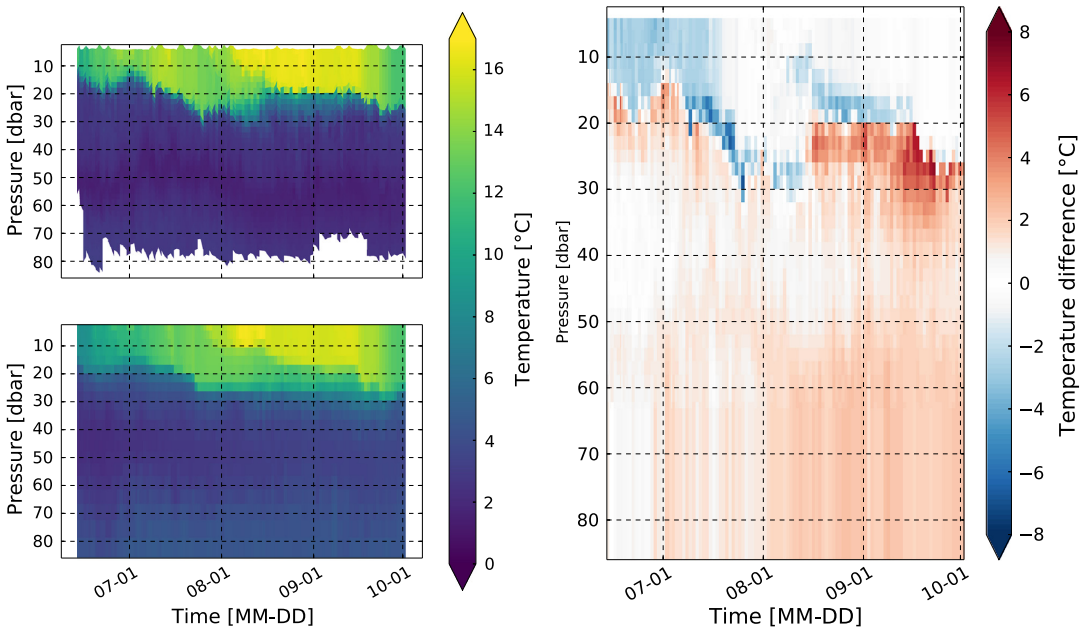


**Fig. 6.** Time series of temperature profiles from an Argo float in the Bothnian Sea in 2013 (upper left panel) and virtual profiles from the NEMO model ($k$-$\varepsilon$ scheme, lower left panel). The difference between the two is shown on the right, with positive values showing where the model was larger than the measurement. Model results have been sampled along the float route.

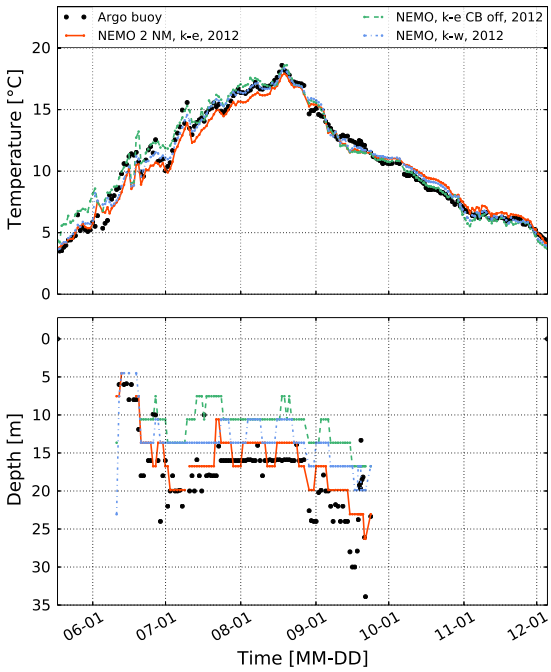


**Fig. 7.** Near-surface temperature in 2012 from the Argo float data and from NEMO with different vertical mixing schemes (upper panel). Thermocline depth estimated as the maximum of vertical temperature gradient (lower panel). Thermocline depths are shown only for the time period when there is a seasonal thermocline present in the water column.

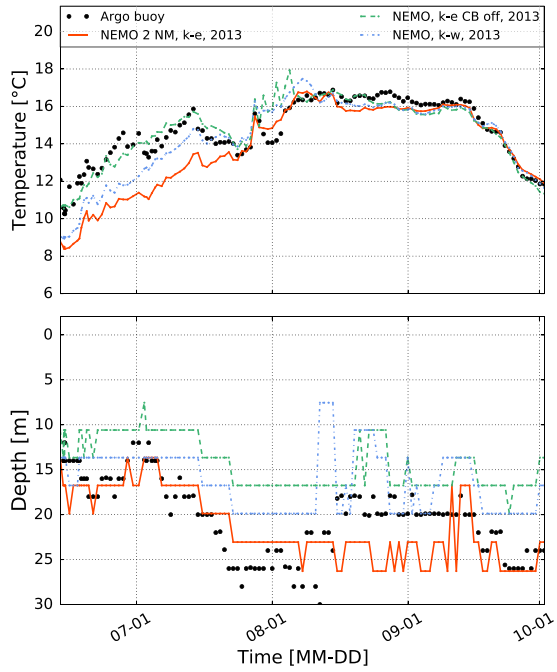


**Fig. 8.** Near-surface temperature in 2013 from the Argo float data and from NEMO with different vertical mixing schemes (upper panel). Thermocline depth estimated as the maximum of vertical temperature gradient (lower panel).

parameterisations, but other factors also play a crucial role. Model performance is affected e.g. by meteorological forcing and boundary conditions, along with parameterisation of radiation and fluxes of heat and momentum. For example, bulk formulae used to estimate the boundary fluxes from the NWP data always introduce an additional source of uncertainty. Also, initial conditions, especially for salinity, are potentially problematic in relatively short model runs such as the ones in this study.

We saw an example of how biases in the meteorological forcing reflect on the accuracy of the surface layer dynamics at the beginning of June 2013 (Fig. 3, right panel), when a technical problem in the FMI-HIRLAM forecasts led to excessively cold air temperatures over the whole Baltic Sea in the NWP data (cf. Fig. 2). In addition to the technical problem in June 2013, there was one other notable issue during the study period with the FMI-HIRLAM temperature forcing over the Baltic Sea. In June and July 2012 there were problems in the Gulf of Finland area with the OSTIA-SST product (Donlon et al., 2012) that is used for data assimilation over sea areas in the FMI-HIRLAM model, which led to errors of approximately 1 °C in daytime 2-metre air temperatures (Sami Niemelä, personal communication). This latter problem could not be directly observed in the results of this article, but it should be kept in mind when investigating the results. It is also noteworthy that any errors induced by the meteorological forcing are visible for longer in the ocean model than in the atmospheric model, since unlike the NWP system we did not use data assimilation in the ocean model.

There are several different criteria available for the thermocline depth (see e.g. de Boyer Montégut et al., 2004). In this article we have chosen to use the maximum of vertical temperature gradient criterion, which has been used in earlier studies in the Baltic Sea (e.g. Tuomi et al., 2012). It should be noted that this method leads to some artefacts in the thermocline depth calculations. For example, in Fig. 8 it can be clearly seen that around 10 August 2013 the criterion led to false interpretation of the modelled thermocline depth, when heating of the uppermost layer and development of secondary thermocline was mistaken for the actual thermocline. In fact, when we investigated the profiles for that day more closely, we saw that the thermocline is simulated relatively well, at least by the $k$-$\varepsilon$ scheme, but the maximum gradient criterion interpreted the secondary thermocline above the main thermocline as the main thermocline for the $k$-$\omega$ scheme.

The wave-breaking parameterisation (CB) seems to have an important role in the deepening of the thermocline and in the heating of the surface layer in spring and early summer. In the Bothnian Sea the use of the CB parameterisation resulted in excessively cold SST values in June. If model performance were to be solely evaluated by its ability to reproduce SST (or near-surface temperature), we would advise against using the wave-breaking parameterisation. However, the impact on the deepening of the thermocline was so evident, that its use in the modelling of the Baltic Sea surface layer dynamics is recommended. But, there is a clear need for improvement on the performance of the turbulence schemes with wave-breaking parameterisation in order to accurately produce SST in spring and early summer. As shown by Mellor and Blumberg (2004), CB formulation is sensitive to the definition of parameters $\alpha_{CB}$ (related to the wave age) and $\beta$ (Charnock's constant). As the wave climate of the relatively small Baltic Sea differs from the oceans, tuning these parameters for the Baltic Sea might improve the model performance.

Furthermore, it was shown that during late summer and early autumn, the wave-breaking parameterisation had little impact on the results, even in situations where wind- and wave-induced mixing was evident. All the turbulence schemes were able to handle the deepening of the mixed surface layer in late August 2012 (Fig. 9). The change in the depth of the thermocline was approximately equal to all the parameterisations, but there was a small difference in how much the temperature of the mixed layer dropped during the event. However, all

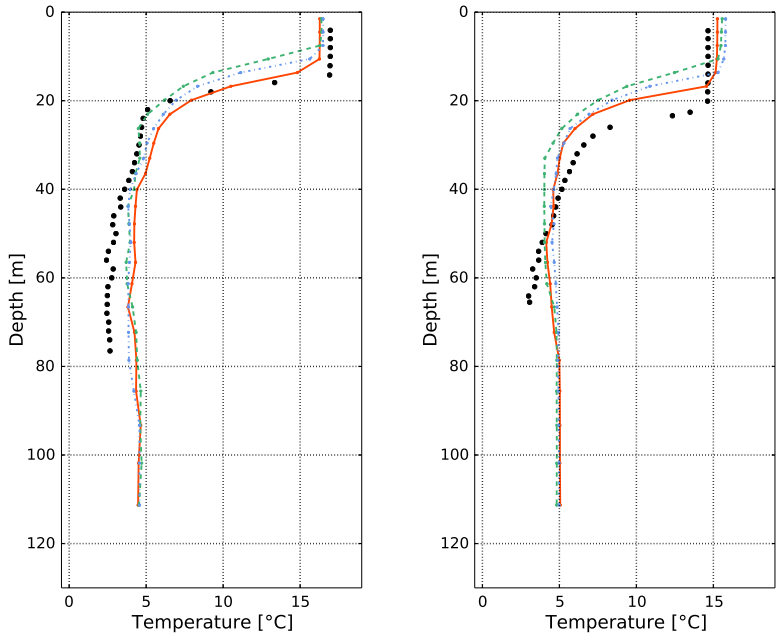


**Fig. 9.** Deepening of mixed surface layer in wind- and wave-induced mixing event. Profiles from 27 and 29 August 2012. Black dots show Argo buoy data, the red line the NEMO "k-e" run, dashed green line the "k-e CB off" run and dotted blue line the "k-w" run. (For interpretation of the references to colour in this figure legend, the reader is referred to the web version of this article.)

the parameterisations underestimated the drop in temperature and the deepening of the thermocline. In order to produce this type of event more accurately in the future, wave effects need to be taken into account better in 3D ocean models. Belcher et al. (2012), for instance, have shown that Langmuir circulation (LC) has an effect on ocean surface-layer mixing. While NEMO has had an implementation of the Axell (2002) parameterisation for LC in the past, it is not available in the GLS package used in the configuration in this study. Therefore, LC is one factor for which an explicit representation is missing from our current NEMO configuration. Recently Breivik et al. (2015) emphasised the role of wave effects in ocean mixing processes. They showed that including wave effects in a global NEMO run results in a reduction of SST biases, as did coupling with a wave model.

We used a two nautical mile (NM) horizontal model resolution in this study. Myrberg and Andrejev (2006) also used two NM for their study in the Gulf of Bothnia. This resolution has been shown to be sufficient to capture essential features of Bothnian Sea dynamics. According to preliminary calculations based on the measured CTD profiles at station SR5 (location shown in Fig. 1), the Rossby radius of deformation in the Bothnian Sea is in the order of 3–5 km (Pekka Alenius, personal communication). It is close to the values presented earlier for the Gulf of Finland, for example, (2–4 km) (Alenius et al., 2003). There Andrejev et al. (2010) found that the performance of the ocean model benefits from higher resolution. Although the dynamics of the Bothnian Sea are very different from those of the Gulf of Finland, it does nevertheless represent a topic for future studies. The reduction of horizontal model resolution might also increase the model performance in the Bothnian Sea.

Finally, it is worth noting the value of the new Argo dataset used in this study. Traditionally, only a few profiles taken during cruises are available from the study area each summer. We can take CTD profiles measured from the *R/V Aranda* in summer 2013 as an example. In July and August 2013 the ship took CTD profiles from the area where the floats operated, on two occasions and from four stations. The first profiles were taken from one station on 12 July as a part of a research cruise. Second, single profiles were taken from three monitoring stations 19–22 August as part of HELCOM-mandated (Baltic Marine Environment Protection Commission) monitoring activity. If we had only these profiles available, we would have no knowledge of several events in the area that are visible in the Argo data. We could not, for example, estimate the ability of different mixing schemes to produce the maximum mixed layer depth in early August. Previously, we have had to rely on rare intensive measurement campaigns, such as the important DIAMIX experiment almost fifteen years ago (Stigebrandt et al., 2002), for fine-resolution observation data from the Baltic Sea.

Naturally, the Argo dataset has some issues, too. We have only limited control of the profile locations. It can sometimes be difficult to separate true changes in vertical structure from changes due to float drift. Argo float usually does not sample the deepest part of the water column to avoid bottom contact. But, even with these challenges, the value of the dataset is evident. We can now validate our models in a much more routine and comprehensive manner, even in an operational setting. As such, the Argo dataset complements the available CTD data in a most useful fashion.

## 5. Conclusions

In this study we used the 3D hydrodynamic model NEMO to simulate vertical temperature dynamics in the Bothnian Sea for the summers 2012 and 2013. We studied different vertical turbulence parameterisations in order to determine their accuracy in reproducing the measured dynamics with new shallow-water Argo floats, operational in the Bothnian Sea since 2012.

The main conclusions are:

- The model was able to reproduce the large-scale seasonal variations in temperature in the area, provided that good quality meteorological forcing was available.
- The $k$-$\varepsilon$ and $k$-$\omega$ schemes showed clear differences in simulating the

surface layer dynamics in the study area, but neither proved superior. While SST was better simulated with the $k$-$\omega$ scheme, the $k$-$\varepsilon$ scheme was clearly better at simulating the thermocline depth.
- As the use of CB parameterisations improved the description of thermocline depth, including the wave effects is clearly important in the Bothnian Sea. However, the use of CB parameterisations led to excessively cool SST at the beginning of the summer. Thus, more sophisticated methods of including surface wave effects in NEMO Nordic are recommended.
- The model was able to produce the seasonal thermocline gradients and depths with sufficient accuracy in order to provide good basis for coupling with a biogeochemical model.
- The new dataset produced by the autonomous shallow-water Argo floats in the Baltic Sea is valuable for model validation and performance evaluation.

## Acknowledgements

This work has been partly financed by the Maj and Tor Nessling Foundation (grant number: 201500179) and the Copernicus MyOcean project (grant number: 283367). Robinson Hordoir and others at SMHI are thanked for their work on the NEMO NORDIC configuration and their support for our efforts. The authors would like to thank the FMI Argo team: Tero Purokoski, Petra Roiha and Simo Siiriä. Hannu Jokinen performed the FMI wave buoy data handling. Tuomo Roine provided information on the FMI Bothnian Sea wave buoy. Sami Niemelä and the FMI-HIRLAM team are acknowledged for providing the FMI-HIRLAM data and useful advice. Continued work on Baltic Sea NEMO has been possible over the years thanks to Jari Haapala, Pekka Alenius and other colleagues at FMI. Finngrundet wave buoy data was obtained from the SMHI open data service (http://opendata-download-ocobs.smhi.se/explore/), licenced under the Creative Commons CC-BY-2.5 licence. Argo data were collected and made freely available by the International Argo Programme and the national programmes that contribute to it (http://www.argo.ucsd.edu, http://argo.jcommops.org). The Argo programme is part of the Global Ocean Observing System. CTD monitoring data was extracted from the ICES Dataset on Ocean Hydrography (The International Council for the Exploration of the Sea, Copenhagen, 2014, http://ices.dk).

## References

Alenius, P., Nekrasov, A., Myrberg, K., 2003. Variability of the baroclinic Rossby radius in the Gulf of Finland. Cont. Shelf Res. 23 (6), 563–573.
Andrejev, O., Sokolov, A., Soomere, T., Värv, R., Viikmäe, B., 2010. The use of high-resolution bathymetry for circulation modelling in the Gulf of Finland. Est. J. Eng. 187–210.
Apel, J.R., 1987. Principles of Ocean Physics. vol. 38. Academic Press.
Axell, L.B., 2002. Wind-driven internal waves and langmuir circulations in a numerical ocean model of the Southern Baltic Sea. J. Geophys. Res. 107 (C11) (25–1).
BACC II Author Team, 2015. Second Assessment of Climate Change for the Baltic Sea Basin. Springer.
Belcher, S.E., Grant, A.L.M., Hanley, K.E., Fox-Kemper, B., Van Roekel, L., Sullivan, P.P., Large, W.G., Brown, A., Hines, A., Calvert, D., Rutgersson, A., Pettersson, H., Bidlot, J.R., Janssen, P.A.E.M., Polton, J.A., 2012. A global perspective on Langmuir turbulence in the ocean surface boundary layer. Geophys. Res. Lett. 39(18), L18605. (URL: http://dx.doi.org/10.1029/2012GL052932).
Berg, P., Poulsen, J.W., 2012. Implementation Details for HBM. Technical Report 12-03 DMI. (URL: http://www.dmi.dk/fileadmin/Rapporter/SR/sr12-03.pdf).
Breivik, Ø., Mogensen, K., Bidlot, J.-R., Balmaseda, M.A., Janssen, P.A., 2015. Surface wave effects in the NEMO ocean model: forced and coupled experiments. J. Geophys. Res. Oceans 120 (4), 2973–2992.
Burchard, H., Bolding, K., Kühn, W., Meister, A., Neumann, T., Umlauf, L., 2006. Description of a flexible and extendable physical–biogeochemical model system for the water column. J. Mar. Syst. 61 (3), 180–211.
Burchard, H., Craig, P.D., Gemmrich, J.R., van Haren, H., Mathieu, P.P., Meier, H.M., Smith, W.A.M.N., Prandke, H., Rippeth, T.P., Skyllingstad, E.D., et al., 2008. Observational and numerical modeling methods for quantifying coastal ocean turbulence and mixing. Prog. Oceanogr. 76 (4), 399–442.
Craig, P.D., Banner, M.L., 1994. Modeling wave-enhanced turbulence in the ocean surface layer. J. Phys. Oceanogr. 24 (12), 2546–2559.
de Boyer Montégut, C., Madec, G., Fischer, A.S., Lazar, A., Iudicone, D., 2004. Mixed layer depth over the global ocean: an examination of profile data and a profile-based climatology. J. Geophys. Res. Oceans (C12), 109.
Donlon, C.J., Martin, M., Stark, J., Roberts-Jones, J., Fiedler, E., Wimmer, W., 2012. The operational sea surface temperature and sea ice analysis (OSTIA) system. Remote Sens. Environ. 116, 140–158.
Eilola, K., Gustafsson, B.G., Kuznetsov, I., Meier, H., Neumann, T., Savchuk, O., 2011. Evaluation of biogeochemical cycles in an ensemble of three state-of-the-art numerical models of the Baltic Sea. J. Mar. Syst. 88 (2), 267–284.
Fleming-Lehtinen, V., Andersen, J.H., Carstensen, J., Łysiak-Pastuszak, E., Murray, C., Pyhälä, M., Laamanen, M., 2015. Recent developments in assessment methodology reveal that the Baltic Sea eutrophication problem is expanding. Ecol. Indic. 48, 380–388.
Fransner, F., Nycander, J., Mörth, C.-M., Humborg, C., Meier, H.E.M., Hordoir, R., Gustafsson, E., Deutsch, B., 2015. Tracing terrestrial DOC in the Baltic Sea — a 3-D model study. Global Biogeochem. Cycles, URL: http://dx.doi.org/10.1002/2014GB005078.
Gröger, M., Dieterich, C., Meier, M., Schimanke, S., 2015. Thermal air–sea coupling in hindcast simulations for the North Sea and Baltic sea on the NW European shelf. Tellus A 67 (0) (URL: http://www.tellusa.net/index.php/tellusa/article/view/26911).
Håkansson, B., Alenius, P., Brydsten, L., 1996. Physical environment in the Gulf of Bothnia. Ambio 5–12.
HELCOM, 2014. Eutrophication status of the Baltic Sea 2007–2011 A concise thematic assessment. Tech. Rep. HELCOM, Baltic Sea Environment Proceedings No. 143 (URL: http://www.helcom.fi/Lists/Publications/BSEP143.pdf).
HIRLAM-B, 2015. System Documentation. Tech. Rep. HIRLAM Consortium (URL: http://www.hirlam.org/).
Hordoir, R., An, B., Haapala, J., Meier, H., 2013a. A 3D ocean modelling configuration for Baltic and North Sea exchange analysis. Technical Report. SMHI (URL: http://www.smhi.se/polopoly_fs/1.28758!RO_48.pdf).
Hordoir, R., Axell, L., Löptien, U., Dietze, H., Kuznetsov, I., 2015. Influence of sea level rise on the dynamics of salt inflows in the Baltic Sea. J. Geophys. Res. 120 (10), 6653–6668. URL: http://dx.doi.org/10.1002/2014JC010642.
Hordoir, R., Dieterich, C., Basu, C., Dietze, H., Meier, H., 2013b. Freshwater outflow of the Baltic Sea and transport in the Norwegian current: a statistical correlation analysis based on a numerical experiment. Cont. Shelf Res. 64 (0), 1–9. http://dx.doi.org/10.1016/j.csr.2013.05.006.
Large, W.G., Yeager, S.G., 2004. Diurnal to decadal global forcing for ocean and sea-ice models: the data sets and flux climatologies. NCAR Technical Note, NCAR/TN-460 + STR. CGD Division of the National Center for Atmospheric Research.
Leclair, M., Madec, G., 2009. A conservative leapfrog time stepping method. Ocean Model. 30 (2), 88–94.
Lehmann, A., Getzlaff, K., Harlaß, J., 2011. Detailed assessment of climate variability of the Baltic Sea area for the period 1958–2009. Clim. Res. 46, 185–196.
Leppäranta, M., Myrberg, K., 2009. Physical Oceanography of the Baltic Sea. Springer Verlag.
Lundberg, C., Jakobsson, B.-M., Bonsdorff, E., 2009. The spreading of eutrophication in the eastern coast of the Gulf of Bothnia, Northern Baltic Sea—an analysis in time and space. Estuar. Coast. Shelf Sci. 82 (1), 152–160.
Madec, G., the NEMO team, 2008. NEMO ocean engine. Institut Pierre-Simon Laplace (IPSL). France. note du Pôle de modélisation, No 27.
Meier, H. E. M., 2001. On the parameterization of mixing in three-dimensional Baltic Sea models. J. Geophys. Res. Oceans 106, (C12) 30997–31016. URL: http://dx.doi.org/10.1029/2000JC000631.
Meier, H.M., Müller-Karulis, B., Andersson, H.C., Dieterich, C., Eilola, K., Gustafsson, B.G., Höglund, A., Hordoir, R., Kuznetsov, I., Neumann, T., et al., 2012. Impact of climate change on ecological quality indicators and biogeochemical fluxes in the Baltic Sea: a multi-model ensemble study. Ambio 41 (6), 558–573.
Mellor, G., Blumberg, A., 2004. Wave breaking and ocean surface layer thermal response. J. Phys. Oceanogr. 34 (3), 693–698.
Myrberg, K., Andrejev, O., 2006. Modelling of the circulation, water exchange and water age properties of the Gulf of Bothnia. Oceanologia 48 (S).
Myrberg, K., Ryabchenko, V., Isaev, A., Vankevich, R., Andrejev, O., Bendtsen, J., Erichsen, A., Funkquist, L., Inkala, A., Neelov, I., Rasmus, K., Medina, M.R., Raudsepp, U., Passenko, J., Söderkvist, J., Sokolov, A., Kuosa, H., Anderson, T., Lehmann, A., Skogen, M., 2010. Validation of three-dimensional hydrodynamic models of the Gulf of Finland. Boreal Environ. Res. 15, 453–479.
Omstedt, A., Axell, L.B., 2003. Modeling the variations of salinity and temperature in the large gulfs of the Baltic Sea. Cont. Shelf Res. 23 (3), 265–294.
Omstedt, A., Elken, J., Lehmann, A., Leppäranta, M., Meier, H., Myrberg, K., Rutgersson, A., 2014. Progress in physical oceanography of the Baltic Sea during the 2003–2014 period. Prog. Oceanogr. 128 (0), 139–171.
Pirinen, P., Simola, H., Aalto, J., Kaukoranta, J.-P., Karlsson, P., Ruuhela, R., 2012. Tilastoja Suomen ilmastosta 1981–2010 — Climatological Statistics of Finland 1981–2010. Reports. Finnish Meteorological Institute (URL: http://hdl.handle.net/10138/35880).
Purokoski, T., Aro, E., Nummelin, A., 2013. First long-term deployment of Argo float in Baltic Sea. Sea Technol. 54 (10), 41–44.
Reffray, G., Bourdalle-Badie, R., Calone, C., 2015. Modelling turbulent vertical mixing sensitivity using a 1-D version of NEMO. Geosci. Model Dev. 8 (1), 69–86.
Reissmann, J.H., Burchard, H., Feistel, R., Hagen, E., Lass, H.U., Mohrholz, V., Nausch, G., Umlauf, L., Wieczorek, G., 2009. Vertical mixing in the Baltic Sea and consequences for eutrophication — a review. Prog. Oceanogr. 82 (1), 47–80.
Rodi, W., 1987. Examples of calculation methods for flow and mixing in stratified fluids. J. Geophys. Res. 92 (C5), 5305–5328 (1978–2012).
Stigebrandt, A., Lass, H.U., Liljebladh, B., Alenius, P., Piechura, J., Hietala, R., Beszczynska, A., 2002. DIAMIX–an experimental study of diapycnal deepwater mixing in the virtually tideless Baltic Sea. Boreal Environ. Res. 7 (4), 363–370.
Svensson, U., 1979. The structure of the turbulent Ekman layer. Tellus 31 (4), 340–350.
Tuomi, L., Myrberg, K., Lehmann, A., 2012. The performance of the parameterisations of vertical turbulence in the 3D modelling of hydrodynamics in the Baltic Sea. Cont. Shelf Res. 50, 64–79.

Umlauf, L., Burchard, H., 2003. A generic length-scale equation for geophysical turbulence models. J. Mar. Res. 61 (2), 235–265.
Umlauf, L., Burchard, H., 2005. Second-order turbulence closure models for geophysical boundary layers. A review of recent work. Cont. Shelf Res. 25 (7), 795–827.
Vancoppenolle, M., Fichefet, T., Goosse, H., Bouillon, S., Madec, G., Maqueda, M.A.M., 2009. Simulating the mass balance and salinity of Arctic and Antarctic Sea ice. 1. Model description and validation. Ocean Model. 27 (1), 33–53.
Warner, J.C., Sherwood, C.R., Arango, H.G., Signell, R.P., 2005. Performance of four turbulence closure models implemented using a generic length scale method. Ocean Model. 8 (1), 81–113.
Wilcox, D.C., 1988. Reassessment of the scale-determining equation for advanced turbulence models. AIAA J. 26 (11), 1299–1310.

II

JOURNAL OF OPERATIONAL OCEANOGRAPHY, 2016
VOL. 9, NO. 2, 115–125
http://dx.doi.org/10.1080/1755876X.2016.1248148

Taylor & Francis
Taylor & Francis Group

# Forecasting upwelling events with monthly ensembles for the eastern coast of the Gulf of Bothnia in the Baltic Sea

Petra Roiha, Antti Westerlund and Noora Haavisto

Finnish Meteorological Institute, Helsinki, Finland

**ABSTRACT**

The upwelling phenomenon is an important player in many physical, chemical and ecological processes in the Baltic Sea. In this study, we demonstrate that it is possible to detect coastal upwelling events well in advance utilising the monthly ensemble ocean forecasts for the northern Baltic Sea. A biogeochemical ocean model, using forcing from the European Centre for Medium-Range Weather Forecasts, was used to produce 27-day forecasts weekly. Upwelling events in the coastal areas of the Gulf of Bothnia in the Baltic Sea were studied and the results showed that the method can predict most major upwelling events with a one-week lead time and a significant number of events with a two-week lead time.

**ARTICLE HISTORY**
Received 25 March 2015
Accepted 10 October 2016

Downloaded by [Finnish Meteorological Institute] at 23:55 10 August 2017

## Introduction

The upwelling phenomenon has a strong impact on the physical and biological marine environment in the Baltic Sea. The upward flowing cool water brings nutrients to the euphotic zone (Vahtera et al. 2005) and cools the environment. It also has an effect on air temperature and potentially on rapid fog formation (Leppäranta & Myrberg 2009), as well as on carbon dioxide cycling between the sea and the atmosphere (Löffler et al. 2012).

In an elongated, stratified basin, such as the Bothnian Sea, the principal response to constant wind along the coast is as follows: Ekman transport emerges in the surface layer in a cross direction. As a result, the sea level rises on the right-hand-side coast from the wind direction and falls on the other side's coast. Consequently, there are coastal jets produced along both coasts, which are compensated for by slow return flows from the central basin (Krauss & Brügge 1991).

For an upwelling to emerge in the Baltic Sea, the wind event must last for at least 60 h, and, besides this, wind direction and water column stratification play important roles (Haapala 1994). In the Baltic Sea, upwelling is a fairly common phenomenon, for example, on the coast of the Gulf of Finland, the Gulf of Bothnia and the east coast of Gotland island (Håkansson et al. 1996) to name but a few. Almost all strong enough wind patterns cause upwelling in some parts of the sea (Lehmann & Myrberg 2008).

The statistical occurrences of the phenomenon have been analysed by numerical modelling, which concludes that the main areas of coastal upwelling events in the Baltic Sea are the Bothnian Sea, the northern coast of the Gulf of Finland, the west coast of the Baltic Proper, the east coast of Gotland, the east coast of the Estonian islands, the east coast of Denmark, including the Straits and areas east of Bornholm island (Myrberg & Andrejev 2003). The statistical occurrences have also been analysed by satellite analysis, which shows similar results as the modelling study but also notes that there are pronounced upwelling events along the Polish coast as well as the Baltic east coast (Lehmann et al. 2012).

Ensemble forecasting has been since beginning of the 1990s, an important tool in many disciplines, especially in meteorology. The first ensemble predictions were produced operationally in US National Meteorological Center (Tracton & Kalnay 1993) and European Centre for Medium-Range Weather Forecasts (ECMWF) (Palmer et al. 1993).

In general, an ensemble forecast can be produced by several methods: by using single model with different forcing (e.g. Molteni et al. 1996), by combining single-model ensembles as multi-model multi-analysis ensembles (e.g. Mylne et al. 2002) or by using several models as a poor-man's ensemble predicted system (EPS) (e.g. Ebert 2001).

In the Baltic Sea, the ensemble forecasts are widely used in climatological studies (e.g. Meier et al. 2011), where the time span reaches up to decades. The ensemble forecasting is also used in operational oceanography, especially with medium-range time scales. The state-of-the-art

**CONTACT** Petra Roiha petra.roiha@fmi.fi Finnish Meteorological Institute, Erik Palménin aukio 1, P.O. Box 503, FI-00101 Helsinki, Finland
© 2016 Institute of Marine Engineering, Science & Technology

Downloaded by [Finnish Meteorological Institute] at 23:55 10 August 2017

operational ensemble forecasting and warning systems in North Sea and Baltic Sea produces medium-range forecasts with lead times of 48, 60 or 72 h (Alfieri et al. 2012; Golbeck et al. 2015).

The deterioration of model forecasts with time is a well-known issue in weather forecasting, where the reliable forecast range today is about a week depending on the parameter and location (Bauer et al. 2015). However, the heat capacity and density of water are much higher than those of air and, because of this, the persistence of some phenomena in the oceans is typically longer than in the atmosphere, which suggests better predictability for these events. The internal weather of the sea, for example, on the oceanic mesoscale, includes mainly phenomena that occur on temporal scales ranging from days to months, and on spatial scales ranging from kilometres to hundreds of kilometres (Lermusiaux 2006).

There are several ways to analyse an ensemble. Variables can be studied by, for example, calculating the ensemble mean, which provides an estimate of the probabilistic expectation forecast. The ensemble can also be divided into smaller sub-ensembles to make alternative forecasts (Brankovic & Palmer 1997) and even individual members can be used for prediction purposes. Ensembles can be used as a quantitative tool for risk assessment. In many applications, their potential economic value can be much higher than the value of a deterministic forecast (Richardson 2000).

In comparison with a single deterministic forecast, ensembles offer the benefit of estimates of the bias, deviation and range of the modelled variables, which may be then compared with real-life situations, and it is also possible to analyse the ensembles and see which forecasts have a low predictive value (Buizza 1997). It is important to know not only the numerical value of the forecast variable but also to get information on the reliability of the prediction (Leutbecher & Palmer 2008). The validity of one ensemble forecast tells very little of the performance of the forecasting system in general (Jolliffe & Stephenson 2003). Therefore, it is necessary to use a statistical approach and to choose the specific methods that best suit the task at hand.

In this study, a probability-based forecast is analysed, including an in-depth look at the monthly ensemble prediction system of sea surface temperature (SST) and its performance. The special conditions of the northern parts of the Baltic Sea are considered, and a case study to show the possibilities and challenges in interpreting ensemble forecasts of upwelling events is examined. A statistical study to deepen the understanding of the system is presented.

In this study, methods of ensemble forecasting are developed and applied to gain information of useful limits of predictability of the upwelling phenomena in the Gulf of Bothnia in the Baltic Sea.

## Materials and methods

### *Model configuration and ensemble production*

We used Baleco, the operational three-dimensional biogeochemical model of the Finnish Meteorological Institute. The model consists of a general circulation model, the MITgcm (Marshall, Adcroft, et al. 1997; Marshall, Hill, et al. 1997), and an ecological module. The model is discretised on a spherical polar grid. The grid size is 0.1° in longitude and 0.2° in latitude: about 11.1 km, or six nautical miles. The model domain consists of 120 grid cells in the latitudinal direction, 108 grid cells in the longitudinal direction and 21 grid cells in the vertical direction. The south-western corner of the model domain is at 53.85°N, 8.7°E. The vertical resolution of the model is concentrated in the euphotic zone, so that the topmost layer is 3 m, reduced to 2 m for the cells touching the coast. The bottom topography is from work of Seifert and Kayser (1995). The spatial discretisation is made with a minimum filter at intervals of six nautical miles. The model appears to have a slight warm bias of approximately 0.5°C (Kiiltomäki 2008). For more information on the modelling system, see Roiha et al. (2010).

The ensembles were created from an unperturbed initial ocean state by running the model several times with perturbed sets of weather forcings. The unperturbed ocean state was taken from the routinely produced deterministic short-term model forecast. The weather ensembles were from the monthly forecasting system of the ECMWF, which is based on the Integrated Forecasting System atmospheric model (from cycle CY32R3V in 2008 to CY35R3 in 2009). They were created with the singular vector method (Molteni et al. 1996). The weather parameters used as external forcing for the ocean model were 6-hourly winds at 10 m, temperature as well as dew point temperature at 2 m, and 12-hourly surface solar radiation and surface thermal radiation. The wind stress is calculated by the model from the ECMWF for 10-m wind forcings. In some cases with stormy winds, the wind stress grows large in certain areas of the model domain, destabilising the system. As model stability and forecast availability are paramount for operational forecasting system, this is compensated for by restricting the stress value growth over a threshold value.

These weather ensembles consist of 50 perturbed ensemble members and an additional deterministic unperturbed control run. For the purposes of this

Downloaded by [Finnish Meteorological Institute] at 23:55 10 August 2017

study, altogether 26 of 27-day forecasts were analysed for the summer seasons of 2008 and 2009. All in all there were 1326 individual model runs. Forecasts were made at one-week intervals, the first ones starting at the beginning of June, and the last ones starting at the end of August.

### Verification methods

Three methods, described below, are used to verify the distribution of the ensemble as a sample from the probability distribution function (Casati et al. 2008) and to evaluate the quality of the ensemble forecasts. These methods exploit the whole ensemble, thus giving more information on the system.

We used a rank histogram to estimate the quality of the formulation of the ensemble forecast system. The rank histogram is a graphical illustration of the spread and the bias of the forecasting system. According to reports, this method has been successfully used for both simple low-order dynamical systems as well as for general circulation models. The first version of this method was introduced by Anderson (1996). In this case, the method is proven to be applicable, but it has to be used carefully with other statistical methods as follows (Hamill 2001; Marzban et al. 2011; Wilks 2011).

In addition, we use the continuous rank probability score (CRPS). With this one can compare observations with the whole ensemble and estimate the absolute error between the system and reality. The CRPS method has several advantages: it is sensitive to the total range of the parameter of interest, it does not need predefined classes, it can be interpreted as an integral over all possible Brier scores and, for a deterministic forecast, it boils down to a mean absolute error (Hersbach 2000).

The third method is to look at results with the residual quartile–quartile (R-Q-Q) (Marzban et al. 2011). In this method, residuals from the model are compared with predicted values. For perfect model, this comparison produces random pattern. Any type of pattern indicates problem with model fitness or variance heterogeneity.

### Observations

To analyse the modelling system and forecasts, three types of measurements were used: (1) SST from Northern Baltic Wave buoy, (2) SST from tide gauges along the shore of the Gulf of Bothnia (Figure 1) and (3) SST from satellite measurements.

The buoy measurements were taken automatically every half an hour and averaged over 24 h. These observations were used to analyse the overall performance of the ensemble forecasting system. Tide gauge measurements along the shore of the Gulf of Bothnia from eight measurement sites were used (Figure 1). The temperature was measured every 10 min and for the upwelling analysis, the data were averaged over 24 h. In addition, satellite SST observations were used to identify the upwelling events. This dataset was based on data from the National Oceanic and Atmospheric Administration (NOAA) Advanced Very High Resolution Radiometer (AVHRR) satellite. Image was processed using a split window method and cloud detection algorithm at SYKE (Finnish Environment Institute) (SYKE 2016).

In this work, upwelling events in the Gulf of Bothnia are considered for the years 2008 and 2009. Tide gauge and satellite observations are used to verify the upwelling events. Only events where the phenomenon was detectable both in tide gauge data and satellite observations are accepted to ensure that the upwelling event is sizeable enough to be able to be seen in the forecasts. For the year 2009, there were no upwelling events which could have been detected by both observation methods, mostly due to the cloudiness in satellite pictures.

The upwelling phenomenon is illustrated with EPS plumes as well as violin plots (Hintze & Nelson 1998), which show the change in SST per day. Violin plots are a developed version of more commonly used boxplots. Their advantage is that the violin plot is more informative showing the full distribution of the data. This enables detection of sub-ensembles, when the ensemble distribution is multi-modal, i.e. has more than one peak.

## Results

### Upwelling events and the accuracy of the forecasts

During an upwelling event, the typical change in surface temperature is from 1 to 5°C/day (Lehmann & Myrberg 2008). Accordingly, 1°C/day was used as a threshold lower limit for an upwelling event.

In forecasting the upwelling events, the interest is mainly on the timing in order to be able to, for example, estimate the possibility of fogginess in a coastal area. This monthly scale prediction could be then refined by shorter-term forecasts. In this work, the forecast was evaluated as successful if the cooling period started during the upwelling period in the tide gauge and satellite observations.

Altogether there were 13 measured upwelling events, which could be detected on one or more from eight tide gauges during the study period. The forecasts were divided into three categories: forecasts of less than 7

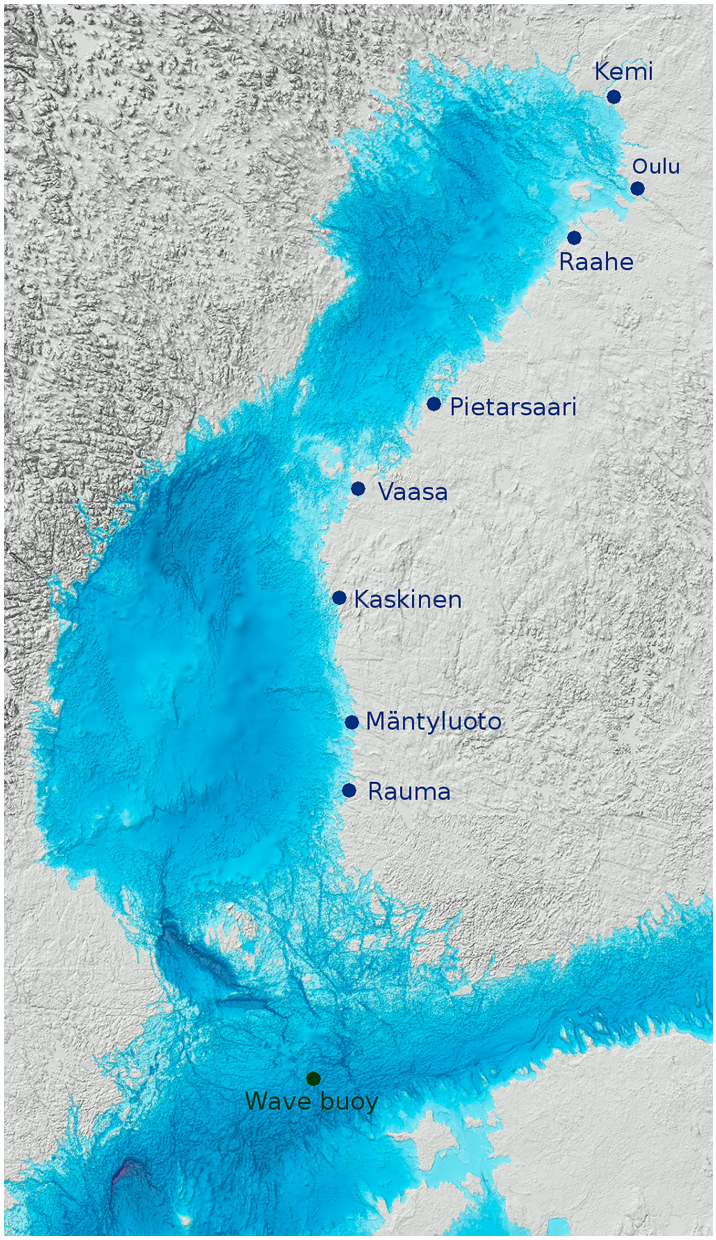


**Figure 1.** Bottom topography (BSHC 2013) for the Gulf of Bothnia.
Note: The tide gauge locations and wave buoy (59.25°N, 21.00°E) are marked with dots.

days, forecasts from 7 to 14 days and forecasts for over 14 days. The shortest forecast period predicted 11 upwelling events, the second 6 and the longest 2. The probability of detection value, which means fraction of observed events that is forecasted correctly, was 84.6% for the shortest forecast, 46.2% for the two-week forecast and 15.4% for the more-than-two-week forecast. The false alarm rate, i.e. fraction of false alarms from all forecasted

Downloaded by [Finnish Meteorological Institute] at 23:55 10 August 2017

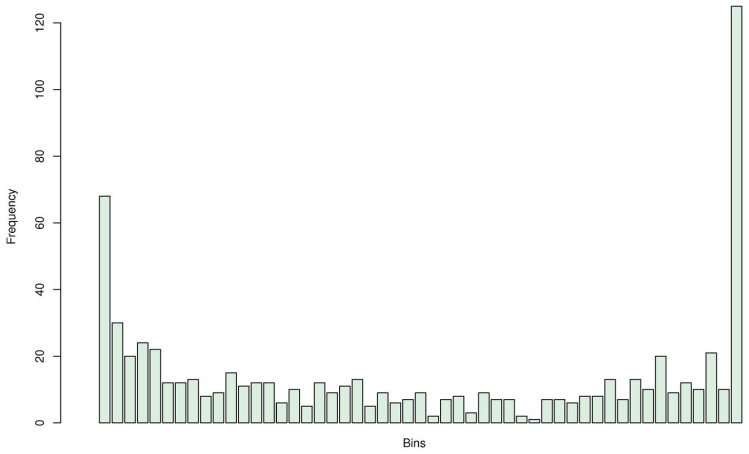


**Figure 2.** Rank histogram for 26 ensemble forecasts for the summers 2008 and 2009, observations from the Northern Baltic buoy.

events, was 15.4% for the less-than-a-week forecast, 68.4% for the two-week forecast and 84.6% for the longest forecast.

### *Verification of the forecasting system*

A rank histogram combined from monthly ensemble forecasts for 2008 and 2009 shows that the observations tend to fall in lower bins than statistically expected (Figure 2). This indicates that the system is slightly biased. The rank histogram also shows that the spread of the ensemble does not cover enough of the future possibilities, and many observations tend to fall outside the forecast plume. In this study, lowest and highest bins of the rank histogram are overrepresented.

The CRPS (Figure 3) shows that the error between the observation and the ensemble grows as the span of the forecast grows. On average, the error between the forecast and the observation tends to grow by around 0.01 degrees per forecast day. The initial error between the model and the observation is 0.66°C, which is in line with earlier verification work on this model. The temperature variation from month to month is quite large, as can be seen from the *in situ* measurements (Figure 4).

The R-Q-Q plot (Figure 5) shows how most of the forecasts produce quantile distributions somewhat S-shaped and at an angle to the horizontal. The S-shape indicates that the distribution of the forecast values is not as wide as that of the observations, that is, the minimum and maximum temperatures are not well produced by the model. This is in good agreement with the rank histogram, which also suggests the same conclusion. From the R-Q-Q plot, one can also see that the curves have a positive slope, which implies that the climatological variance is larger within the ensemble than within the observations. The summers 2008 and 2009 are marked with different colours: the years are not alike.

### *Case study: upwelling on the west coast of Finland from 1 August to 5 August 2008*

We studied more closely the system's ability to forecast an upwelling event that took place on the Finnish coast of the Bothnian Bay from 1 August to 5 August 2008 (Figure 6). This event extended over a 200 km stretch of the Finnish coast, and lasted for five days. In the first forecast, starting on 17 July, 16% of the ensemble members predicted upwelling (Figures 7 and 8, upper panel), while in the second forecast, starting on 24 July, already 20% of the ensemble members predicted upwelling (Figures 7 and 8, middle panel). In the third forecast, starting 31 July, all the ensemble members predicted cooling, and 82% predicted upwelling on 2 August (Figures 7 and 8, lower panel). It can be seen that the distribution of the temperature rate of change is clearly skewed towards negative values, indicating cooling in all the forecasts. This becomes more pronounced as the event gets closer.

## Discussion

Several upwelling events along the coast of the Gulf of Bothnia during the years 2008 and 2009 were studied using the ensemble prediction system. Verified upwelling events were only detected in 2008. The reproduction of

Downloaded by [Finnish Meteorological Institute] at 23:55 10 August 2017

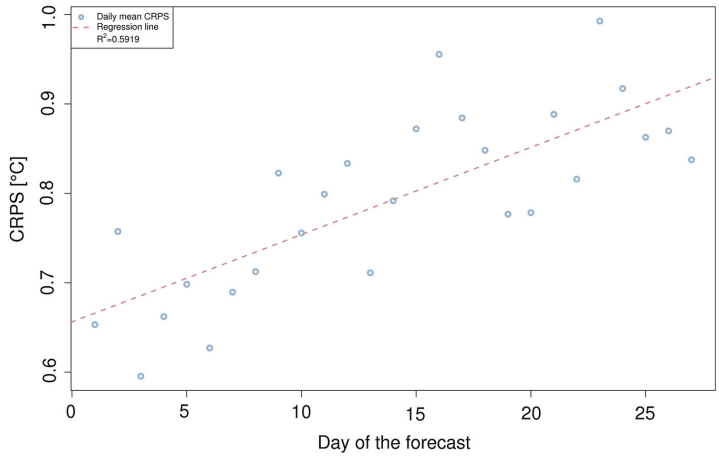


**Figure 3.** Mean daily CRPS.

Note: The equation for the regression line is $y = 0.00976x + 0.65623$. $R^2 = 0.5919$.

the upwelling cases was analysed and the confidence in forecasts in monthly scale was evaluated.

Atmospheric conditions strongly affect the phenomenon, and just a small displacement or change in the strength of the wind pattern can make the difference between an upwelling event happening or not. This is why ensemble prediction is suitable for predicting upwelling – and, moreover, for quantifying its likelihood – since this method produces its forecast from slightly perturbed atmospheric input fields. In the end, upwelling is dependent on wind speed, direction and duration, and the stratification of the water column.

### *Upwelling forecasts*

Upwelling events are triggered by atmospheric phenomena, for example, a low pressure system. It is difficult to predict the timing and location of these systems precisely. Nevertheless, these upwelling events can be seen in different forecasts in slightly different places or at slightly different times, even though their original trigger is in fact the same phenomenon. In the sea, changes are slower, and the inertia of the fluid is greater than in the atmosphere. It is therefore possible to see traces of weather phenomena in the sea after they are no longer


**Figure 4.** Temperature observations from the Northern Baltic buoy (cf. Figure 1), and climatology.

Note: Climatology is from the OCEANSITES project and the national programmes that contribute it.

Downloaded by [Finnish Meteorological Institute] at 23:55 10 August 2017

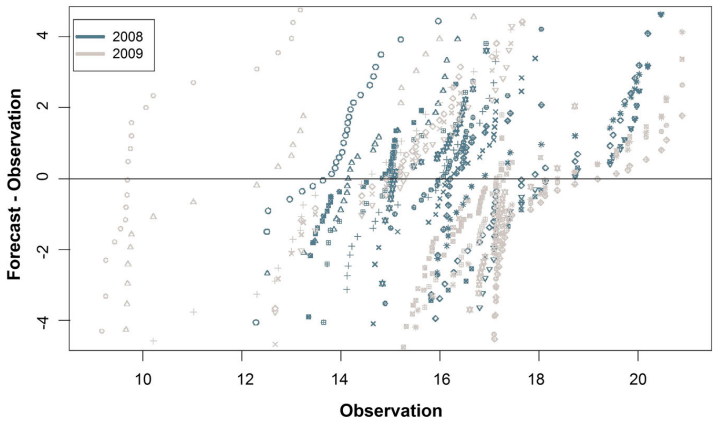


**Figure 5.** Residual quantile–quantile plots for monthly ensemble forecasts for the summers 2008 and 2009.
Note: The values on both axes are degrees in Celsius.

visible in the atmosphere. In upwelling cases, the location plays an important role. Small changes in the wind pattern have a stronger effect on smaller coastal areas than they do on larger coastal areas.

The threshold limit for upwelling was set to be 1°C/day. On one hand, it is unlikely that such a change in temperature would be produced by other phenomena, for example, cold air advection, especially during summer. On the other hand, this limit is still low enough that important events are not missed. In the early summer the ensemble forecast distribution tend to have the greatest number of positive members as the water temperature is rising. In the late summer, the situation is the opposite, when the water is cooling.

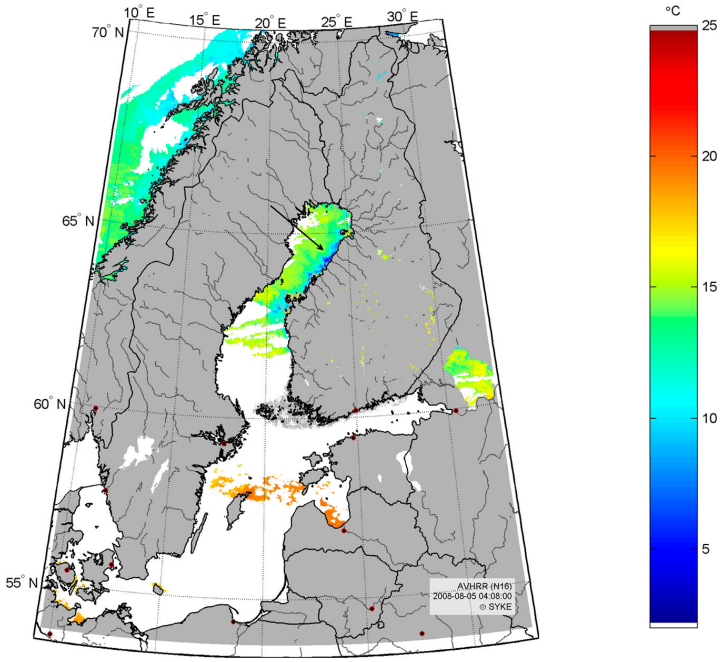


**Figure 6.** Satellite image of sea surface temperature for 5 August 2008. Source: SYKE (2016). Accessed 17 November 2016.
Note: The area of interest is indicated by an arrow.

Downloaded by [Finnish Meteorological Institute] at 23:55 10 August 2017

Downloaded by [Finnish Meteorological Institute] at 23:55 10 August 2017

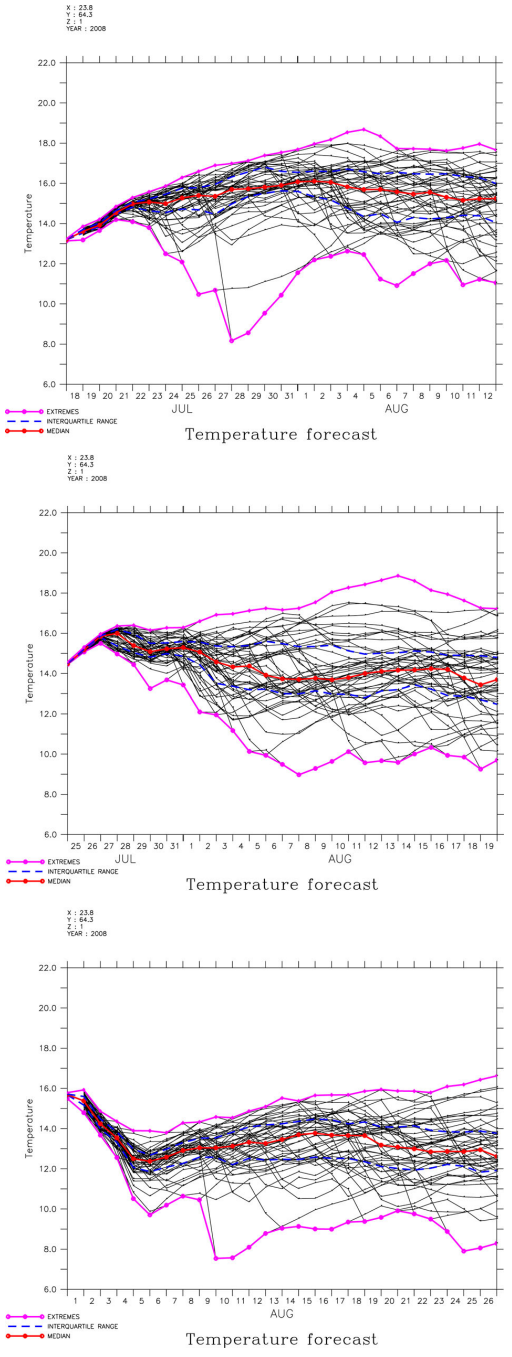


**Figure 7.** Three sequential monthly ensemble SST forecast plumes for the west coast of Finland (Figure 4).

Note: Upwelling was detected 1 August lasting until 5 August.

Forecasts in the study were illustrated with two types of graph: the traditional ensemble plume – which shows the development of the temperature in 50 different, physically realistic scenarios – and the violin plot. These forecasts show the daily change in the temperature; in this study, over a period of 27 days. This is useful when there is a need to estimate the rate of change of SST, for example, during upwelling events when the cooling is relatively fast.

Since upwelling as a mesoscale phenomenon is scaled by the Rossby radius, the grid size should also be of that order or even finer (Lehmann & Myrberg 2008). In this study, the model grid size was 6 NM (around 11.1 km), which is close to the reported upper limit of the baroclinic Rossby radius in the Baltic Proper (Alenius et al. 2003). There is very limited data available on the Rossby radius in the Gulf of Bothnia, but it is generally expected to be of the same order as that of the Baltic Proper.

## The performance of the forecasting system

The verification of the system showed that the forecasts and observations differ somewhat. The three methods used in this study showed similar results.

Rank histograms are a widely used method for the evaluation of meteorological ensemble forecasts. They are well suited for meteorological applications because the availability of observations is relatively good for them. As Hamill (2001) points out, rank histograms do not give meaningful results unless computed on a fairly large sample. Part of the overestimates and underestimates in the rank histogram (Figure 2) might be due to the unperturbed initial conditions of the ocean state and on boundaries, which cause the first day of the forecast to be (in most cases) different from observation. The perturbance of the other variables and boundary conditions should be done so that physical realism is preserved.

The rank histogram showed that the dispersion is too small, which is along the lines of the R-Q-Q plot. Also the systematic error can be seen in the CRPS score as well as in the R-Q-Q plot. In general, it is possible to see the growth rate of the error during the monthly forecast from the CRPS.

Although a detailed analysis of the physical reasons behind this kind of forecast behaviour needs more study, some preliminary reasons for the nonconformities are presented here. One reason behind the lack of dispersion in the model could be the fairly coarse resolution and too large vertical mixing in the model.

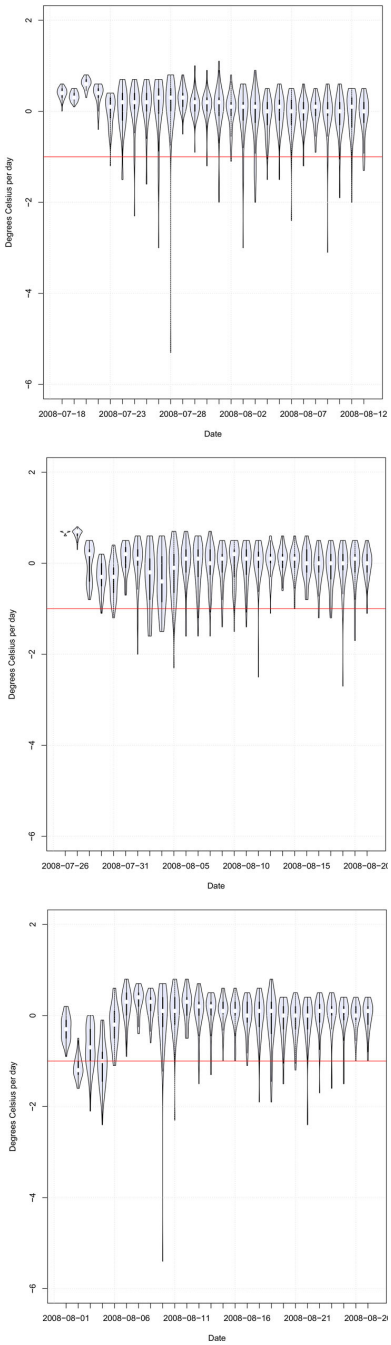


**Figure 8.** Three sequential violin plots of temperature rate of change for the west coast of Finland (Figure 6).

Notes: Upwelling was detected 1 August, and it lasted until 5 August. The defined limit for upwelling, 1°C/day, is marked on the plot by a red line.

The highest temperatures tend to occur on warm days, when the wind is relatively calm. In this situation, a shallow surface layer might warm up a great deal more than the whole mixed layer, thus forming a so-called sub-thermocline near the surface. When the surface layer of a numerical model is used for comparison with the observations, it might be that the observation reflects the temperature of the shallow surface layer at one location, while the modelled temperature reflects the mean temperature of the deeper mixed layer over a larger area, resulting in a relatively large temperature difference.

It is not clear why the coldest temperatures are not well produced in the forecast. This again might be related to an excess of vertical mixing in the model, resulting in too deep a mixed layer with a weaker temperature gradient in the thermocline. In this case, the enhanced mixing would result in higher temperatures than the observations show. The known warm bias also explains part of the model's inability to produce the coldest temperatures.

The performance of the forecast is different in different geographical locations (Marzban et al. 2011). Thus, more observations from different places are needed in order to gain a more comprehensive view of the forecast behaviour.

## Conclusions

Ensemble forecasting on monthly time-scale appears to be a promising tool in operational oceanography. However, the challenges of this approach are somewhat different when applied to oceanography than in some of the more established applications, such as weather forecasting. For example, compared to the atmosphere the characteristics of sea water are different, and the availability of observations is much more sparse. Furthermore, the Baltic Sea has its own particular characteristics, adding to the list of things to take into consideration.

As mentioned in previous sections, sea water has a high density and heat capacity compared with the atmosphere. This means that the scale of phenomena, both spatial and temporal, is different from that of the atmosphere. While this might mean longer predictability for some phenomena, caution is in order and each phenomenon should be considered separately. The start of an upwelling event, for example, might be as difficult to predict as any atmospheric phenomenon. But at the same time, upwelling events, once initiated, can outlast the triggering wind event. It might therefore be plausible to conjecture that the duration of this phenomenon could

Downloaded by [Finnish Meteorological Institute] at 23:55 10 August 2017

be more easily predicted than its start. But this needs further research.

There has been very little research into how oceanic ensemble forecasting differs from other applications. As the Baltic Sea is semi-enclosed, quite small and has a complex coastline, phenomenon such as upwelling is quite common and important. This highlights the need for a sufficiently high resolution in modelling, and improving this aspect is important once more computational capacity makes this practical. As for now, too many aspects of ensemble forecasts are limited by computer capacity.

In spite of these difficulties, the ensemble approach has clear advantages for oceanic applications, even when forecasting relatively poorly known and difficult-to-capture phenomena such as upwelling. In this study, it is shown that on the time range of less than a week, the forecast accuracy is excellent, and even on time ranges from a week to two weeks, forecasts show adequate accuracy. Methods used in other applications were applied here and developed further to suit oceanic uses.

## Acknowledgements

The authors want to thank the organisers and participants of the 4th International Verification Methods Workshop for ideas on ensemble forecasting, and Dr Tapani Stipa, Mr Aleksi Nummelin, Prof. Jari Haapala and Dr Laura Tuomi for their insightful comments. The satellite SST data is available under Creative Commons By 4.0 International license and is processed by Finnish Environment Institute.

## Disclosure statement

No potential conflict of interest was reported by the authors.

## Funding

Development of the FMI ensemble forecasting system has been partly financed by European Union Commission 6th framework project ECOOP European COastal-shelf sea OPerational Observing and forecasting system [contract number 036355] and the Copernicus MyOcean project.

## ORCID

*Petra Roiha* http://orcid.org/0000-0001-9585-206X
*Antti Westerlund* http://orcid.org/0000-0003-2006-3079

## References

Alenius P, Nekrasov A, Myrberg K. 2003. Variability of the baroclinic Rossby radius in the Gulf of Finland. Cont Shelf Res. 23:563–573.

Alfieri L, Salamon P, Pappenberger F, Wetterhall F, Thielen J. 2012. Operational early warning systems for water-related hazards in Europe. Environ Sci Policy. 21:35–49.

Anderson JL. 1996. A method for producing and evaluating probabilistic forecasts from ensemble model integrations. J Clim. 9:1518–1530.

Bauer P, Thorpe A, Brunet G. 2015. The quiet revolution of numerical weather prediction. Nature. 525:47–55.

Brankovic C, Palmer T. 1997. Atmospheric seasonal predictability and estimates of ensemble size. Mon Wea Rev. 125:859–874.

BSHC. 2013. Baltic Sea Bathymetry Database version 0.9.3. [Internet]. [cited 2015 Jan 21]. Available from: http://data.bshc.pro/

Buizza R. 1997. Potential forecast skill of ensemble prediction and spread and skill distributions of the ECMWF Ensemble Prediction System. Mon Wea Rev. 125:99–119.

Casati B, Wilson L, Stephenson D, Nurmi P, Ghelli A, Pocernich M, Damrath U, Ebert E, Brown B, Mason S. 2008. Forecast verification: current status and future directions. Meteorol Appl. 15:3–18.

Ebert EE. 2001. Ability of a poor man's ensemble to predict the probability and distribution of precipitation. Mon Wea Rev. 129:2461–2480.

Golbeck I, Li X, Janssen F, Brüning T, Nielsen J, Huess V, Söderkvist J, Büchmann B, Siiriä S-M, Vähä-Piikkiö O, et al. 2015. Uncertainty estimation for operational ocean forecast products – a multi-model ensemble for the North Sea and the Baltic Sea. Ocean Dyn. 65:1603–1631.

Haapala J. 1994. Upwelling and its influence on nutrient concentration in the coastal area of the Hanko Peninsula, entrance of the Gulf of Finland. Estuar Coast Shelf Sci. 38:507–521.

Håkansson B, Alenius P, Brydsten I. 1996. Physical environment in the Gulf of Bothnia. Ambio Special Report 15.

Hamill TM. 2001. Interpretation of rank histograms for verifying ensemble forecasts. Mon Wea Rev. 129:550–560.

Hersbach H. 2000. Decomposition of the continuous ranked probability score for ensemble prediction systems. Wea Forecast. 15:559–570.

Hintze J, Nelson R. 1998. Violin plots: a box plot-density trace synergism. Am Stat. 52:181–184.

Jolliffe I, Stephenson D, editors. 2003. Forecast verification – a practitioner's guide in atmospheric science. Chichester: John Wiley.

Kiiltomäki A. 2008. Development of the Baltic Sea indicator report by Algaline measurements and BalEco model results [M. Phil. thesis]. Helsinki: University of Helsinki.

Krauss W, Brügge B. 1991. Wind-produced water exchange between the deep basins of the Baltic Sea. J Phys Oceanogr. 21:373–384.

Lehmann A, Myrberg K. 2008. Upwelling in the Baltic Sea – a review. J Mar Syst. 74:S3–S12.

Lehmann A, Myrberg K, Höflich K. 2012. A statistical approach to coastal upwelling in the Baltic Sea based on the analysis of satellite data for 1990–2009. Oceanologia. 54:369–393.

Leppäranta M, Myrberg K. 2009. Physical oceanography of the Baltic Sea. 1st ed. Chichester: Praxis.

Lermusiaux P. 2006. Uncertainty estimation and prediction for interdisciplinary ocean dynamics. J Comput Phys. 217:176–199.

Downloaded by [Finnish Meteorological Institute] at 23:55 10 August 2017

Leutbecher M, Palmer TN. 2008. Ensemble forecasting. J Comput Phys. 227:3515–3539.
Löffler A, Schneider B, Perttilä M, Rehder G. 2012. Air-sea $CO_2$ exchange in the Gulf of Bothnia, Baltic Sea. Cont Shelf Res. 37:46–56.
Marshall J, Adcroft A, Hill C, Perelman L, Heisey C. 1997. A finite-volume, incompressible Navier Stokes model for studies of the ocean on parallel computers. J Geophys Res Oceans. 102:5753–5766.
Marshall J, Hill C, Perelman L, Adcroft A. 1997. Hydrostatic, quasi-hydrostatic, and non-hydrostatic ocean modeling. J Geophys Res Oceans. 102:5733–5752.
Marzban C, Wang R, Kong F, Leyton S. 2011. On the effect of correlations on rank histograms: reliability of temperature and wind speed forecasts from finescale ensemble reforecasts. Mon Weather Rev. 139:295–310.
Meier HEM, Andersson HC, Eilola K, Gustafsson BG, Kuznetsov I, Müller-Karulis B, Neumann T, Savchuk OP. 2011. Hypoxia in future climates: a model ensemble study for the Baltic Sea. Geophys Res Lett. 38. doi:10.1029/2011GL049929
Molteni F, Buizza R, Palmer T, Petroliagis T. 1996. The ECMWF ensemble prediction system: methodology and validation. Q J R Meteorol Soc. 122:73–119.
Mylne KR, Evans RE, Clark RT. 2002. Multi-model multi-analysis ensembles in quasi-operational medium-range forecasting. Q J R Meteorol Soc. 128:361–384.
Myrberg K, Andrejev O. 2003. Main upwelling regions in the Baltic Sea – a statistical analysis based on three-dimensional modelling. Boreal Environ Res. 8:97–112.
Palmer TN, Molteni F, Mureau R, Buizza R, Chapelet P, Tribbia J. 1993. Ensemble prediction. In: Proceedings of the Validation of Models over Europe (Vol. 1); Shinfield Park, Reading, United Kingdom, ECMWF; p. 21–66.
Richardson DS. 2000. Skill and relative economic value of the ECMWF ensemble prediction system. QJR Meteorol Soc. 126:649–667.
Roiha P, Westerlund A, Nummelin A, Stipa T. 2010. Ensemble forecasting of harmful algal blooms in the Baltic Sea. J Mar Syst. 83:210–220.
Seifert T, Kayser B. 1995. A high resolution spherical grid topography of the Baltic Sea. Meereswissenschaftliche Berichte. 9:72–88.
SYKE. 2016. Remote sensing products, Sea Surface Temperature. [Internet]. [cited 2016 Nov 17]. Available from: www.syke.fi/earthobservation
Tracton MS, Kalnay E. 1993. Ensemble forecasting at NMC: operational implementation. Wea Forecast. 8:379–398.
Vahtera E, Laanemets J, Pavelson J, Huttunen M, Kononen K. 2005. Effect of upwelling on the pelagic environment and bloom-forming cyanobacteria in the western Gulf of Finland, Baltic Sea. J Mar Syst. 58:67–82.
Wilks DS. 2011. Statistical methods in the atmospheric sciences. Amsterdam: Elsevier.

Downloaded by [Finnish Meteorological Institute] at 23:55 10 August 2017

III

Oceanologia (2018) 60, 16—31

Available online at www.sciencedirect.com

ScienceDirect

journal homepage: www.journals.elsevier.com/oceanologia/

ORIGINAL RESEARCH ARTICLE

# Attributing mean circulation patterns to physical phenomena in the Gulf of Finland

**Antti Westerlund** [a,*], **Laura Tuomi** [a], **Pekka Alenius** [a], **Elina Miettunen** [b], **Roman E. Vankevich** [c]

[a] *Finnish Meteorological Institute, Marine Research, Helsinki, Finland*
[b] *Finnish Environment Institute/Marine Research Centre, Helsinki, Finland*
[c] *Russian State Hydrometeorological University, Saint Petersburg, Russia*

Received 15 September 2016; accepted 19 May 2017
Available online 12 June 2017

**KEYWORDS**
Circulation;
Upwelling;
Modelling;
Baltic Sea;
Gulf of Finland

**Summary** We studied circulation patterns in the Gulf of Finland, an estuary-like sub-basin of the Baltic Sea. According to previous observations and model results, the long-term mean circulation in the gulf is cyclonic and mainly density driven, whereas short-term circulation patterns are wind driven. We used the high-resolution 3D hydrodynamic model NEMO to simulate the years 2012—2014. Our aim was to investigate the role of some key features, like river runoff and occasional events, in the formation of the circulation patterns. Our results show that many of the differences visible in the annual mean circulation patterns from one year to another are caused by a relatively small number of high current speed events. These events seem to be upwelling-related coastal jets. Although the Gulf of Finland receives large amounts of fresh water in river runoffs, the inter-annual variations in runoff did not explain the variations in the mean circulation patterns.
© 2017 Institute of Oceanology of the Polish Academy of Sciences. Production and hosting by Elsevier Sp. z o.o. This is an open access article under the CC BY-NC-ND license (http://creativecommons.org/licenses/by-nc-nd/4.0/).

* Corresponding author at: Finnish Meteorological Institute, Erik Palménin aukio 1, P.O.Box 503, FI-00101 Helsinki, Finland. Tel.: +358 29 539 1000
*E-mail address:* antti.westerlund@fmi.fi (A. Westerlund).
Peer review under the responsibility of Institute of Oceanology of the Polish Academy of Sciences.

ELSEVIER Production and hosting by Elsevier

## 1. Introduction

The Gulf of Finland (GoF) in the Baltic Sea is a long, estuary-like sea area that is a direct continuation of the Baltic Proper. Short-term surface circulation in the gulf is mainly wind driven. The stability of currents varies from season to season. The relatively large freshwater input from the eastern end and the more saline deep water flow from the main basin at the western end maintain horizontal density gradients. The

http://dx.doi.org/10.1016/j.oceano.2017.05.003
0078-3234/© 2017 Institute of Oceanology of the Polish Academy of Sciences. Production and hosting by Elsevier Sp. z o.o. This is an open access article under the CC BY-NC-ND license (http://creativecommons.org/licenses/by-nc-nd/4.0/).

dominating south-westerly winds, freshwater input locations and the rotation of the Earth lead one to expect that the long-term mean circulation pattern would be cyclonic. Such residual circulation in the gulf was already described by Witting (1912) and later by Palmén (1930) in his classical study of circulation in the sea areas around Finland. For in-depth descriptions of the gulf, see e.g. Alenius et al. (1998), Soomere et al. (2008, 2009), Leppäranta and Myrberg (2009), and Myrberg and Soomere (2013).

In recent years, the circulation patterns in the gulf have been studied in many numerical model studies. While the model results have generally agreed with the features described by Witting, the results of the model studies vary somewhat from each other. For example, Maljutenko et al. (2010), Elken et al. (2011), Soomere et al. (2011) and Lagemaa (2012) show stronger mean currents west of Narva Bay on the southern coast than what was reported earlier by Andrejev et al. (2004). Also, the intensity of the outflow from the gulf seems to differ from one study to another and from one year to another. Where Andrejev et al. (2004) and Elken et al. (2011) observed a clear outflow in the subsurface layer, Maljutenko et al. (2010) did not. Lagemaa (2012) found the outflow to differ significantly from one year to another.

There are some obvious reasons for the differences between model results. Different studies have simulated different years, and model setups have been different. Also, there is significant inter-annual variability in the mean circulation. But these differences in results may also indicate that the reasons why such a statistical mean circulation pattern emerges are still not fully understood. By studying the physical mechanisms underlying the mean circulation pattern, we can also better understand the relative strengths and weaknesses of different hydrodynamic models and model configurations. For example, if we find that models overestimate or underestimate the effect of certain forcing inputs to the mean circulation, we know those processes need further attention in the model.

Suhhova et al. (2015) speculated that the role of upwelling-related coastal jets may be significant for the mean circulation in the gulf. Coastal upwelling is prevalent in the Gulf of Finland (Lehmann and Myrberg, 2008). Because the dominating wind direction in the GoF is from the south-west, upwelling events are expected to be more common in the northern (Finnish) side of the gulf than in the southern (Estonian) side. A coastal jet is developed simultaneously with the upwelling event. In the GoF, these jets have been both directly observed (e.g. Suursaar and Aps, 2007) and modelled (Zhurbas et al., 2008).

The effects of the residual circulation pattern can be indirectly seen, for example, in the intensity and whereabouts of the salinity gradients across the gulf. The salinity field in the gulf varies significantly both in space and in time. The four largest rivers in the area flow to the eastern gulf. The GoF receives the largest single freshwater input of the whole Baltic Sea from the river Neva at its eastern end. One way to view the gulf is to think of it as a transition zone between the fresh waters of the Neva and the brackish waters of the Baltic Proper (Myrberg and Soomere, 2013). The surface salinity decreases from 5 to 6.5 in the western part of the GoF to about 0 to 3 in the easternmost part of the gulf (Alenius et al., 1998).[1] In the western part of the GoF, a quasi-permanent halocline is located at the depth of 60–80 m and the bottom salinity can reach values up to 8–10 when more saline water masses advect from the Baltic Proper. In the eastern part of the GoF, there is no permanent halocline and the salinity typically increases linearly with depth. Changes in circulation patterns are relatively quickly reflected in the mean salinities, especially in the volatile upper layers. This means that it is possible to indirectly validate the mean circulation field of the gulf by investigating the patterns of salinity in the gulf. This method has been previously employed by e.g. Myrberg et al. (2010) and Leppäranta and Myrberg (2009).

The residual mean circulation must be distinguished from the instantaneous or short-term circulation patterns. It lies more behind the scenes but is nevertheless important for many applications, such as estimating the transport, distribution and residence times of substances discharged to the sea. These substances can be, for instance, nutrients from the land or oil and chemicals from accident sites. Improving substance transport estimates is a high priority task in the area as the coastline is densely populated and ship fairways are highly trafficked. When high-resolution numerical models are used in these tasks, they must be able to faithfully reproduce the mean circulation patterns. Correctly working numerical models can bring significant added value to decision support systems that are built to evaluate the effects of environmental protection measures on marine systems. Unfortunately, evaluating model performance is not straightforward. Where current measurements exist, they lack coverage, both spatial and temporal. Thus, questions remain about the accuracy of modelled circulation patterns.

Our objective is to study how physical processes are attributed to features that are observed in mean circulation patterns. We use the numerical 3D model NEMO (Madec and the NEMO team, 2008), an increasingly popular model in the investigations of the Baltic Sea, to calculate the mean circulation pattern in the Gulf of Finland for the years 2012–2014. We use two setups of the model, one fine resolution and one of coarser resolution, which are validated against observations and benchmarked against other model data. We analyse some of the key circulation features and especially the contribution that high current speed events make to the longer term averages. Finally, we investigate how these details relate to specific phenomena such as upwelling.

## 2. Material and methods

### 2.1. Modelling

#### 2.1.1. NEMO

We used two setups of the NEMO 3D ocean model (V3.6), a coarse resolution setup with a two nautical mile (NM) horizontal resolution covering the Baltic Sea and the North Sea area, and a fine resolution setup for the Gulf of Finland with 0.25 NM horizontal resolution. We ran the model from the

[1] All salinities in this paper are on the practical salinity scale.

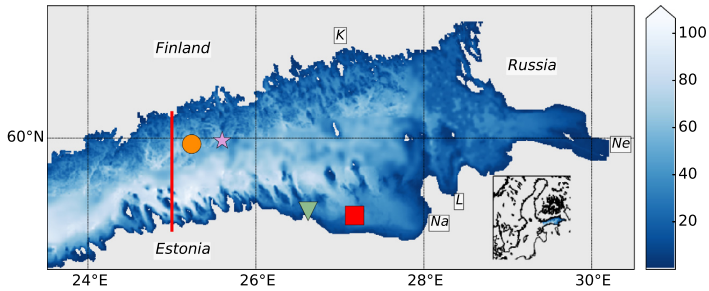


**Figure 1** The model domain and bathymetry (in metres) from the fine resolution 0.25 NM NEMO setup. Stations and sites referenced in the article (from the west): H (orange circle), Kalbådagrund (magenta star), G (green triangle) and 15 (red square). The thin red line shows the location of the 25°E transect. Also indicated on the map are the approximate locations of the Neva (Ne), Narva (Na), Luga (L) and Kymi (K) river mouths. Inset is the location of the model domain on a map of the Baltic Sea. (For interpretation of the references to color in this figure legend, the reader is referred to the web version of the article.)

beginning of 2011 to the end of 2014. We considered the results from 2011 as the stabilisation of the model and chose the years 2012–2014 for closer analysis. The model saved daily mean values of temperature, salinity and current fields.

The horizontal resolution of the fine resolution setup, approximately 500 m, is well below the typical range of internal Rossby radius (2–4 km) in the GoF (Alenius et al., 2003). This configuration is based on the setup by Vankevich et al. (2016) with some modifications related to atmospheric forcing and boundary conditions. The model domain covers the GoF east from longitude 23.5°E, where an open boundary to the Baltic Proper is located (see Fig. 1). Model bathymetry is based on Andrejev et al. (2010). This setup has 94 z-coordinate (with partial step) vertical layers. The topmost vertical layers are 1 m thick, and the layer thickness slightly increases with depth, being about 1.08 m at the lower bound of the z-axis. The time step of the model was 100 s. The ice model LIM3 was included in the setup (Vancoppenolle et al., 2009). Due to the high computational requirements of the configuration, and since the focus of this study is on the ice-free period, the ice model was only run with a thermodynamical formulation. Like Vankevich et al. (2016), we used initial conditions for the beginning of 2011 from the operational version of HIROMB (High Resolution Operational Model for the Baltic). The lateral boundary condition on the open boundary was taken from the coarser setup. Flather boundary conditions were used for barotropic velocities and sea surface height; flow relaxation was used for temperature and salinity.

The coarser 2 NM NEMO setup for the Baltic Sea and the North Sea was also used for analyses. This setup was documented and validated in Westerlund and Tuomi (2016) and is based on the NEMO Nordic configuration by Hordoir et al. (2013a, 2013b, 2015). The layer thickness of this setup starts from 3 m in the surface layer, growing with depth. Unlike in Westerlund and Tuomi (2016), the boundary condition of the coarse setup was updated to use Copernicus Marine Environment Monitoring Service (CMEMS) Global Ocean Reanalysis product (Ferry et al., 2016) to improve the representation of sea levels in the model. Furthermore, the additional strong isopycnal diffusion that was previously applied in the Neva estuary, described in Hordoir et al. (2015), was turned off in order to make the description of currents in the eastern part of the GoF more realistic. The bathymetry of the setup was updated to the latest version of the NEMO Nordic bathymetry and the ice model of the coarser setup was turned off to improve run times.

### 2.1.2. Meteorological forcing

We used forecasts from the HIRLAM (High Resolution Limited Area Model) numerical weather prediction system (HIRLAM-B, 2015) of the Finnish Meteorological Institute (FMI) for atmospheric forcing. Its domain covers the European region with a horizontal resolution of 0.15° (V73 and earlier; before 6 March 2012) or 0.068° (V74; after 6 March 2012). Vertically the domain is divided into 60 (V73) or 65 (V74) terrain-following hybrid levels, the lowest level being about 12 m above the sea surface. The forecasts are run four times a day (00, 06, 12, and 18 UTC) using boundary conditions from the Boundary Condition Optional Project of the ECMWF (European Centre for Medium-Range Weather Forecasts). Each day of forcing was extracted from the 00 forecast cycles with the highest available temporal resolution in the model archive, varying from 1 to 6 h.

Forcing taken from HIRLAM includes the two-metre air temperature, total cloud cover, mean sea-level pressure and 10-m winds, and either the two-metre dew point temperature or relative humidity, depending on the availability in the model archive. Forcing was read into the NEMO run with CORE bulk formulae (Large and Yeager, 2004).

### 2.1.3. River runoff and precipitation data

River runoff forcing for the four main rivers running into the GoF was based on data obtained from two sources. For the river Kymi, we used the same climatological runoff data from Stålnacke et al. (1999) as was used in Vankevich et al. (2016). The discharges for the Neva, Narva and Luga rivers were from HydroMet, received as a part of the Gulf of Finland Year 2014 (GoF2014) project.

The sensitivity of the model configuration to changes in the river runoff forcing was evaluated by running experiments for the years 2013–2014 with modified runoffs. The first experiment had no river runoffs and the second experiment had runoff volume multiplied by two.

Precipitation fields were climatological and based on downscaling of the ERA40 reanalysis for the period 1961—2007 (cf. Hordoir et al., 2015).

#### 2.1.4. CMEMS reanalysis product

In addition to NEMO, we used CMEMS Baltic Sea Reanalysis (Axell, 2016) to further analyse the circulation in the gulf. This product is based on the HIROMB model with the horizontal resolution of approximately 3 NM, with 51 vertical levels. The top layer in this model is 4 m thick and layer thickness increases with depth. This product implements a data assimilation algorithm for salinity, temperature, and ice concentration and thickness.

### 2.2. Measurements

#### 2.2.1. CTD

Usually model development and evaluation are limited by the availability of measured datasets with sufficient temporal and spatial resolutions. We hoped to be a little bit better off with the GoF2014 dataset. The official GoF2014 data covers the whole gulf with data from 1996 to 2014 from Estonia, Finland and Russia. This dataset consists of almost 38,500 depth observations with several parameters from 53 different observation stations covering the whole gulf. The number of visits to stations varies and only some of them can be considered to be like a time series.

Additionally, the FMI did three one-week CTD surveys with over 80 stations each in the western gulf, in Finnish and Estonian waters. One of these was done in 2013 and two were done in 2014. These surveys were planned to collect data on temperature, salinity and density fields for model development. The horizontal spacing of the stations was around 4 NM across the gulf and around 9 NM along the gulf. The observation grid was a compromise between the needed resolution (the Rossby radius of deformation is of the order of 2—4 km), the available ship time and the area that we wanted to cover. CTD casts were done at every station with SeaBird SBE911 ctd.

The 2013 observations were made 3—7 June 2013, from east to west. In 2014 there were two cruises, the first 15—19 June, from west to east, and the second 8—12 September, from west to east. The duration of each cruise was five days. Thus, the whole grid may not be considered synoptic. The time of each section across the gulf was of the order of 6 h and those sections may be considered rather synoptic, though the transversal Seiche period of the gulf is of the same order. For analysis, the cruise data was then interpolated to a 3D grid using the DIVA (Data-Interpolating Variational Analysis) interpolation method (Troupin et al., 2012).

#### 2.2.2. Weather stations

We used wind measurements from the FMI's coastal weather station Kalbådagrund (location shown in Fig. 1) in order to evaluate the accuracy of the meteorological forcing. This weather station is considered to be representative for open sea weather conditions in the Gulf of Finland and it has been used in many earlier studies (e.g. Lips et al., 2011; Tuomi et al., 2012). At Kalbådagrund, wind measurements are made at 32 m height. From this station, we have data for the main meteorological parameters at 10-min intervals.

## 3. Results

### 3.1. The mean circulation field in the Gulf of Finland in the NEMO model

In the Gulf of Finland, the persistency of the circulation field (defined as the ratio of the vector velocity to scalar speed) is known to be rather low. Alenius et al. (1998), among others, cite Palmén's estimates, which ranged from 6% to 26% for long-term persistency. This means that the current field is very variable in time (and space). Therefore it is to be expected that the residual circulation pattern is different from year to year too. We present here the mean circulation patterns from the two NEMO model setups, averaged over time and depth. Depth averaging was done from the surface to 7.5 m depth. These limits for averaging were chosen to make sure that averaging does not include the thermocline, which can at times be shallower than 10 m.

The annual mean circulation, modelled with 2 NM NEMO, was quite different for the years 2012—2014 (Fig. 2). Of these years, 2012 resembles most the traditional mean circulation patterns, while the years 2013 and 2014 showed quite different mean circulation fields. In 2012, there was a westward residual current on the northern coast (also called the Finnish Coastal Current, Stipa, 2004) with speeds of a few centimetres per second and a relatively strong jet with top speeds over 10 cm $s^{-1}$ along the south-eastern coast, west of Narva Bay. In 2013, the residual in the northern coast is eastward and the jet on the southern coast is even stronger than in 2012. In 2014, the residual in the northern gulf is weak, only a few centimetres per second, but the jet on the southern coast exists still.

The annual mean circulation from the fine resolution 0.25 NM setup showed similar results to the 2 NM setup, as shown in Fig. 3. However, as this setup also resolves the submesoscale, the overall picture is much more detailed. While the circulation direction is similar to that in the coarser NEMO setup, the 0.25 NM NEMO setup generally simulated higher mean current speeds. Contrary to the 2 NM NEMO setup, there was no clear outflow on the northern coast in 2012, albeit the general flow direction was the same. In 2013 and 2014, the residual circulation patterns were mostly similar to those in the coarser run.

The mean circulation for the whole period 2012—2014 shows four circulation loops in the gulf (Fig. 4). The centre of the first loop is located at approximately 23.5°E (loop A, in the nomenclature of Lagemaa, 2012). As this loop is very close to our 0.25 NM setup domain boundary, we only capture it fully in the coarser model. The second loop (B) is roughly at 25°E. The third loop (C), at 27°E, includes the coastal current west of Narva Bay. The fourth loop (D), at 28.5°E, is located in the Neva estuary.

The wind measurements at the Kalbådagrund weather station were used, along with corresponding HIRLAM model data, to evaluate whether the differences in the annual mean circulation patterns could be linked to differences in the wind conditions in 2012—2014. All the years have a dominating wind component from the south-southwest (Fig. 5). There are, however some differences in the frequency and magnitude of the easterly winds between the years. In 2012, the

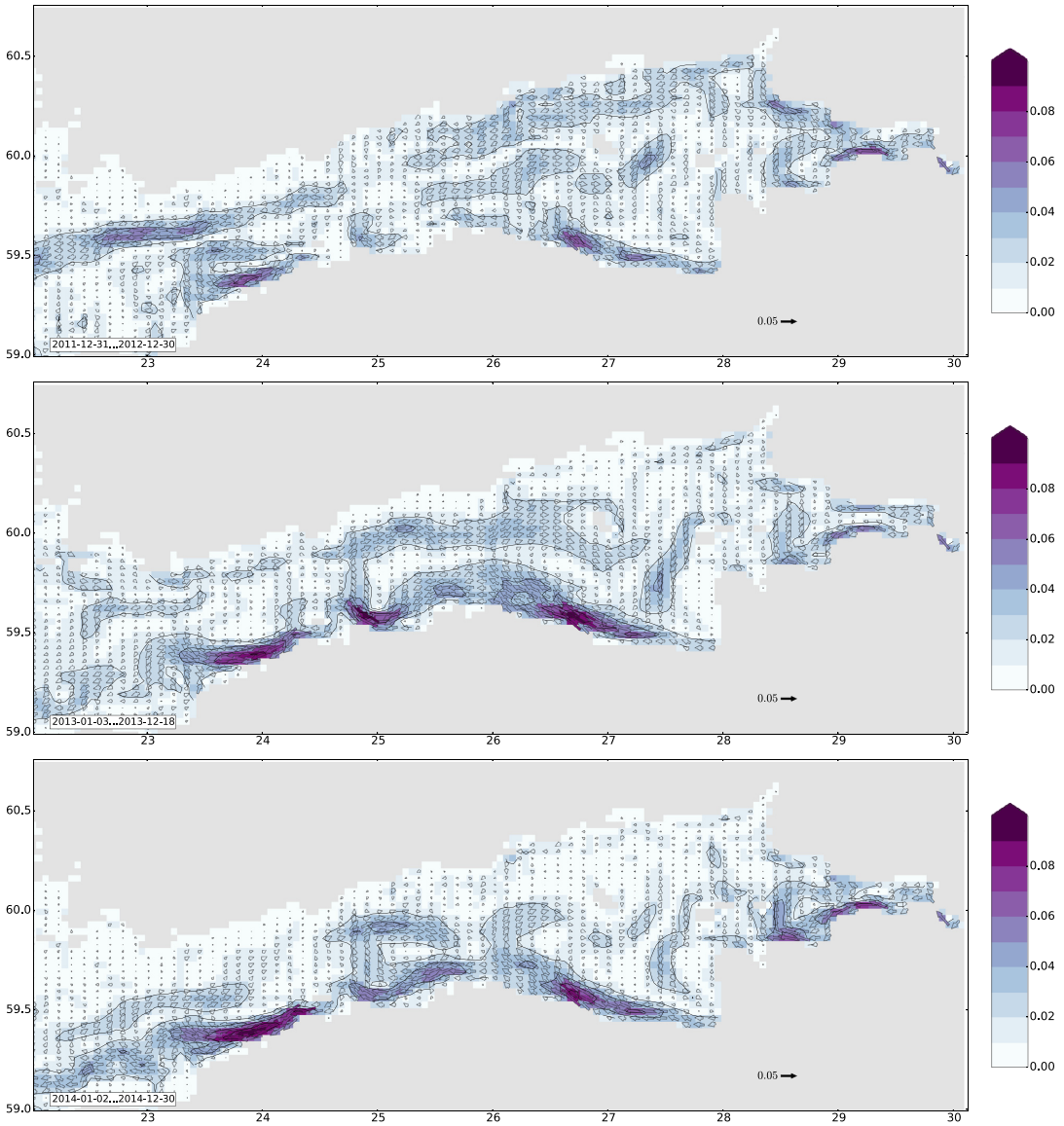


**Figure 2** Annual mean circulation in the 2 NM setup averaged from 0 m to 7.5 m depth for the years 2012 (top), 2013 (middle) and 2014 (bottom). Velocities are in m $s^{-1}$. Vector arrows are drawn for every other grid point in the longitudinal direction and for every grid point in the latitudinal direction.

quantity of easterly winds is smallest and in 2014 it is largest. In 2013, there is also a significant component of high wind speeds from the west, contrary to the other years. We also compared the forcing wind field to the measured values at Kalbådagrund and found that HIRLAM forecast the wind speed and direction fairly well. In 2012, there were relatively few differences, although the forcing data shows weaker south-eastern winds than the measurements. In 2013, the forcing data has a stronger component of northerly winds than the measurements. In 2014, easterly winds are not as well represented in the forcing data.

## 3.2. Benchmarking the circulation field

As validation of the whole circulation field is difficult and spatial coverage of measurements is sparse, we instead

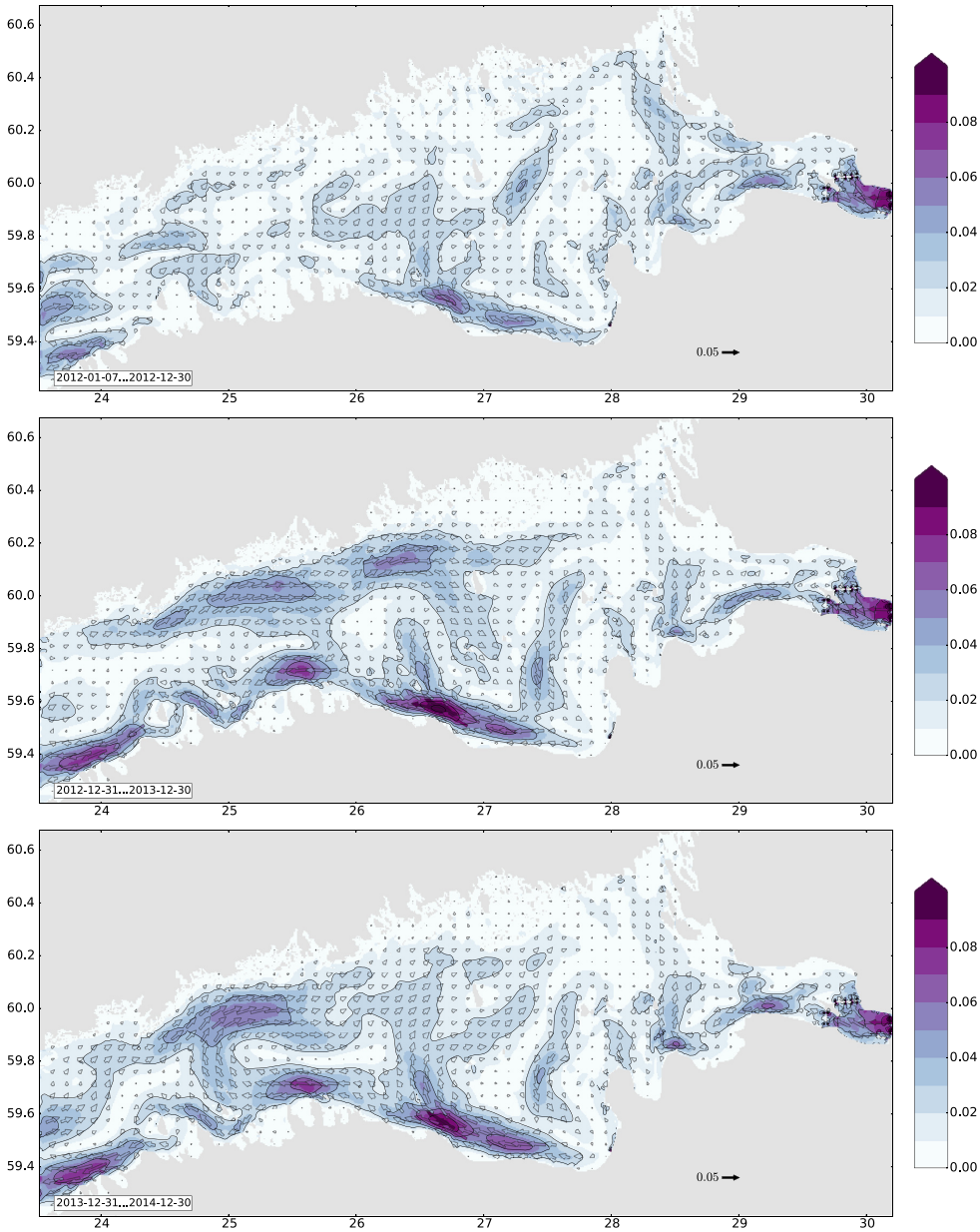


**Figure 3** Annual mean circulation in the 0.25 NM setup averaged from 0 m to 7.5 m depth for the years 2012 (top), 2013 (middle) and 2014 (bottom). Velocities are in m $s^{-1}$. Vector arrows are drawn for every 13th grid point in the longitudinal direction and in every 11th grid point in the latitudinal direction.

benchmark the two NEMO setups against the HIROMB-based CMEMS product. We consider this model indicative of the general performance of hydrodynamic models in the area (cf. Myrberg et al., 2010). In the HIROMB results, the outflow in the northern gulf is clearly visible in 2012, almost non-existent in 2013 and reversed in 2014 (Fig. 6). The direction of flow is more uniform and the field is smoother than in NEMO. Furthermore, HIROMB does not show a clear coastal current on the southern coast in 2012. The years before 2012 had a similar mean circulation pattern as the

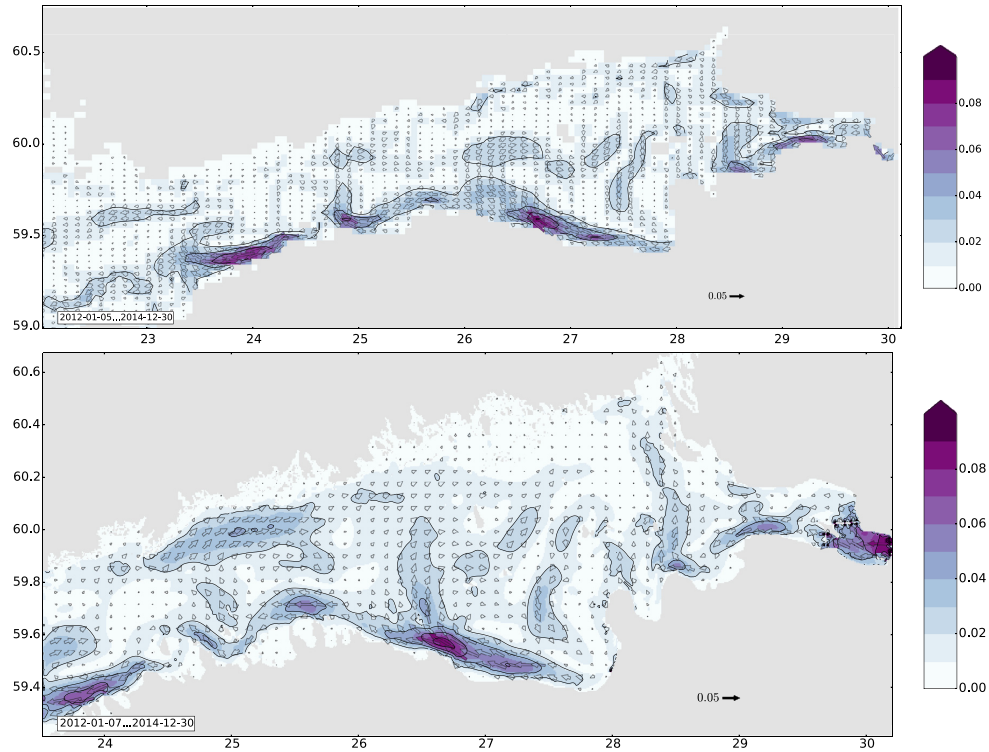


**Figure 4** Mean circulation for 2012–2014 averaged from 0 m to 7.5 m depth in the 2 NM (top) and the 0.25 NM (bottom) setup. Velocities are in m $s^{-1}$. For the upper figure, vector arrows are drawn for every other grid point in the longitudinal direction and for every grid point in the latitudinal direction. For the lower figure, vector arrows are drawn for every 13th grid point in the longitudinal direction and in every 11th grid point in the latitudinal direction.

year 2012 (not shown here). In the 2013 results there is a marked difference: in NEMO the residual current in the Finnish coast is mainly to the east, while in HIROMB it is to the west. In other areas the speeds in NEMO are stronger but the directions are similar to those of HIROMB. The reversal of the outflow in 2014 from that of 2012 is more or less similar in the coarser NEMO model and in HIROMB. All the models show a clear alongshore current on the southern coast in 2014 too.

## 3.3. Salinity validation

We compared the model salinity with observations, as the mean salinity field can be used as a proxy for the mean circulation field. In these comparisons we used the CTD survey data from 2013 to 2014. Model data has been averaged over the span of the cruises (cf. Section 2.2.1). North–south salinity cross-sections show that the 0.25 NM NEMO model is able to describe the vertical structure of the water column rather well (Fig. 7). In the near-surface layers, however, the freshest water is somewhat incorrectly placed in each case in both NEMO and HIROMB. In 2013, the surface layer in NEMO was less saline than in the observations. In 2014, the observations show less saline water on the northern coast. The model shows the opposite.

## 3.4. Attributing the features of the mean circulation field with physical phenomena

### 3.4.1. River runoff

As the Gulf of Finland is in many ways like a large estuary, the density gradients are significant for the mean currents in the gulf. Therefore, correctly prescribing river runoff forcing is even more important than in the other sub-basins of the Baltic Sea. Runoff data with high enough temporal resolution is still inaccessible or sometimes non-existent for many rivers. Therefore it is common to use data from hydrological models, such as E-HYPE (Donnelly et al., 2016) or climatological runoff data (e.g. Bergström and Carlsson, 1994).

The datasets gathered during the GoF2014 include monthly mean runoffs from the Neva, Narva and Luga rivers from recent years. This allowed us to compare them to respective values from E-HYPE. The comparison showed that the modelled runoffs often differ significantly from the observed ones. For example, for the GoF2014 study period

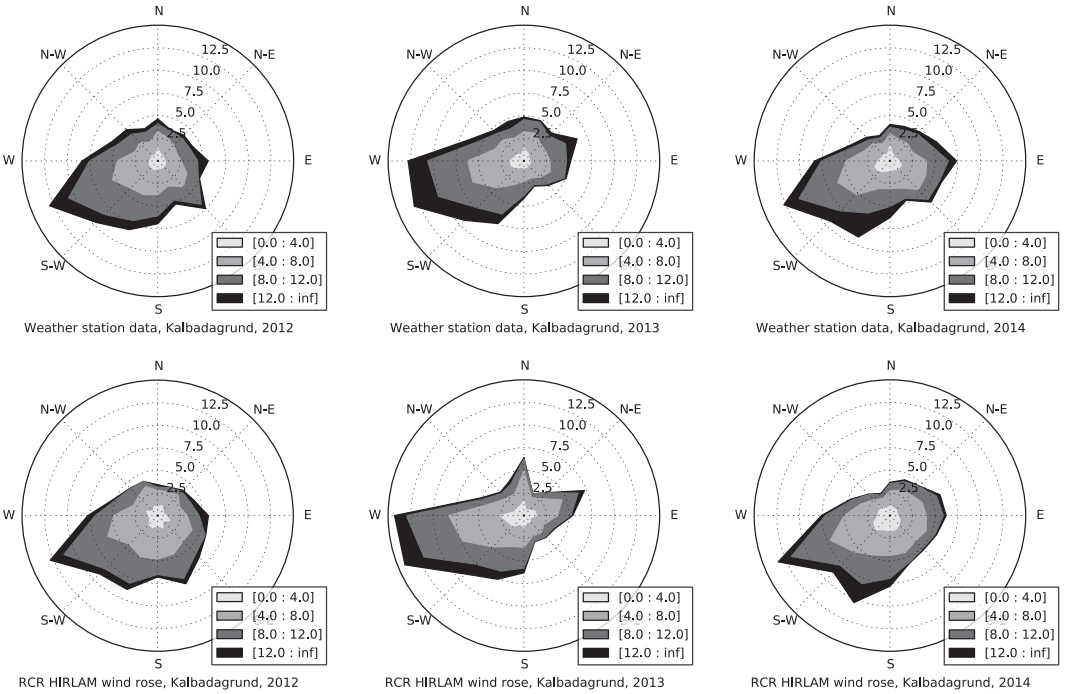


**Figure 5** Annual wind roses at Kalbådagrund meteorological station in 2012, 2013 and 2014. Top: observation; bottom: HIRLAM model 10 m winds. Wind speeds are in m $s^{-1}$, frequencies are in percent.

1996–2014, the mean observed runoff from the Neva was 2345 $m^3$ $s^{-1}$ (about 73 $km^3$ $a^{-1}$, which is in one year almost 7% of the volume of GoF: 1090 $km^3$). The mean runoff from E-HYPE was 1881 $m^3$ $s^{-1}$, which means almost a 28% difference from the observed value. More detailed information about GoF2014 and the dataset can be found in Raateoja and Setälä (2016).

To investigate how incorrectly estimated river runoffs could affect the modelled circulation patterns, we performed two simulations with the 0.25 NM NEMO setup using modified runoff forcing, namely (1) no runoff from the four major rivers into the gulf and (2) doubled runoff from the four major rivers into the gulf. Although, this approach is somewhat artificial, it shows how sensitive the modelled near-surface current fields are to river runoff forcing. The changes in the river runoff mainly affected the magnitude of the near-surface currents, as shown in Fig. 8. There were hardly any changes in the direction of the mean currents. When the runoffs are doubled, the Neva river plume became very easily identifiable. Compared to the reference run (Fig. 4), the highest mean current speeds increased by roughly half.

### 3.4.2. High flow speed events

The averaging of variable currents over time periods of years can hide different kinds of physical situations. Rare high energy events can show up and even dominate averages in certain areas. A relatively small number of days with high current speeds can contribute to the mean circulation field in a significant way. We demonstrate this using the coastal flow near the northern coast of the gulf as an example.

To quantify the contribution of days with high current speeds, we divided the model dataset into two parts based on the modelled current speed at a point near the Finnish coast. This point is indicated in Fig. 1 as site H. It was chosen because it is in an area where strong coastal currents were seen in the NEMO results (Fig. 4).

We found that strong current episodes contributed significantly to the formation of the jet in the residual pattern of currents on the Finnish coast (Fig. 9). Even though days with high current speeds are only 18% of all days in 2012–2014 (when the criterion for high current speed is 10 cm $s^{-1}$ daily mean speed), they still are a major contribution to the overall mean circulation field. If we removed the days with strong currents from the analysis, the magnitude of the eastward current in the Finnish coast was smaller, but the direction was still towards the east. For example, mean current speed was approximately 3.3 cm $s^{-1}$ at site H in 2012–2014. If we include only days with strong currents in the calculation, the magnitude of the current was 1.3 cm $s^{-1}$, which is around 41% of the total. The direction of the current in both cases was nearly the same. On the southern coast, a similar analysis revealed the same, with high current speed days contributing significantly to the coastal current visible in the annual mean circulation field (not shown).

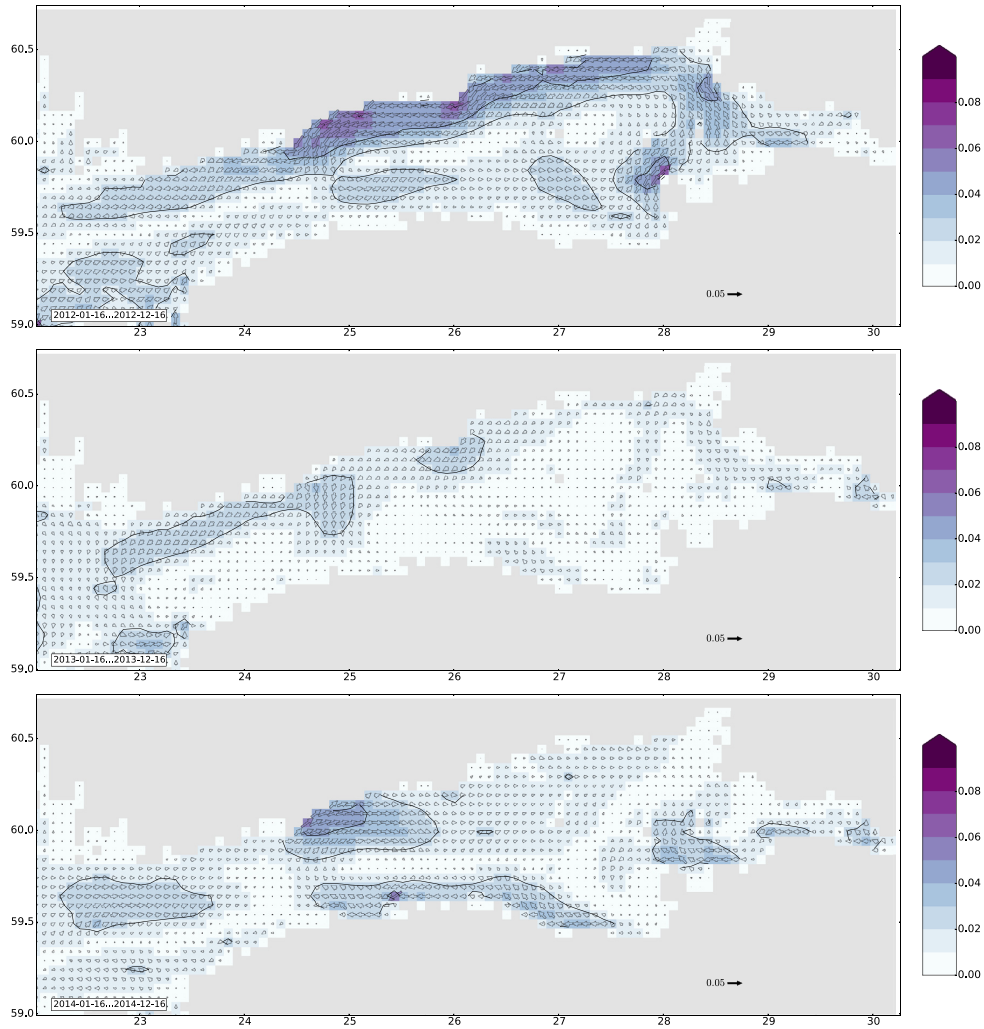


**Figure 6** Annual mean circulation in the CMEMS product averaged from 0 m to 7.5 m depth for the years 2012 (top), 2013 (middle) and 2014 (bottom). Velocities are in m $s^{-1}$. Vector arrows are drawn for every grid point.

### 3.4.3. Upwelling-related jets

To further understand what sort of events contribute to the strong coastal currents in the annual mean current fields in different years, we investigated how these high-speed events relate to coastal upwelling. We selected an area in the south-eastern GoF, west of Narva Bay, for closer inspection. In this area the annual mean current fields of the 0.25 NM NEMO run showed high-speed westward currents, especially in the years 2013 and 2014 (Fig. 3). We chose the nearshore station 15 (location shown in Fig. 1) from which there were several temperature measurements available during 2012–2014. On a number of occasions, the modelled temperature decreased rapidly within a short time period during the summer stratified season, indicating a possible upwelling event (Fig. 10, upper panel). Many of the temperature drops, including the two events with the highest current speed at this station, can be associated with high-speed alongshore currents, visible in the modelled current speeds at the nearby station 15 (Fig. 10, lower panel). Similar analysis for two stations near the northern coast gave concurring results (not shown).

The model reproduced the seasonal temperature cycle in the surface layer fairly well (Fig. 10). During two of the possible upwelling events, the measured temperature also shows lower values. However, the temporal resolution of the measurements is not sufficient enough to differentiate between upwelling and cooling of surface water due to other processes.

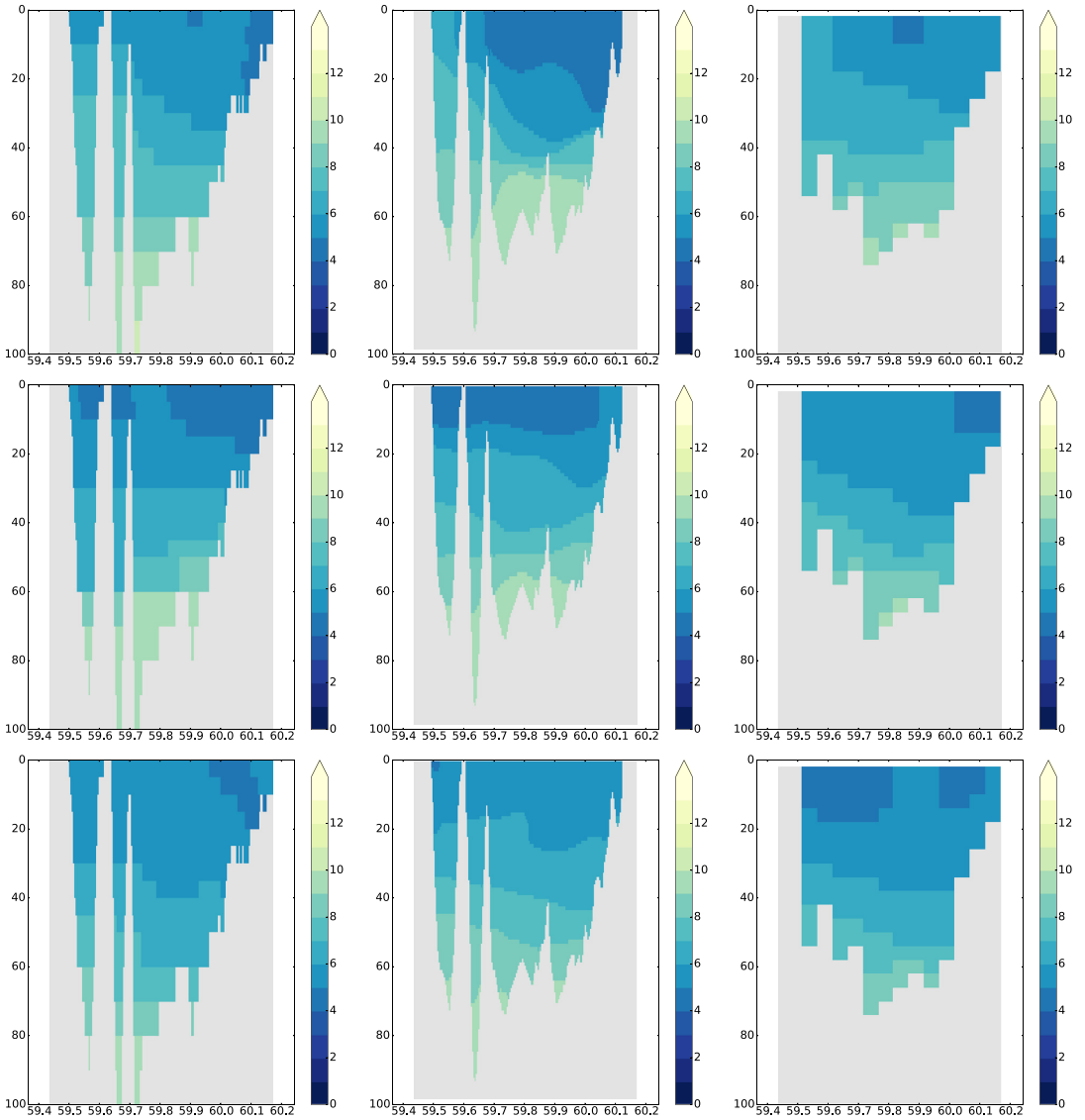


**Figure 7** A south–north salinity cross-section at 25°E from gridded observations (left) and the 0.25 NM NEMO model averaged over the time span of the cruise (middle). For reference, the monthly mean from the 3 NM HIROMB-based CMEMS product is also provided (right). The June 2013 cruise (top), the June 2014 cruise (middle) and the September 2014 cruise (bottom) are shown. The south coast is on the left-hand side.

For a rough quantitative estimate of the effect that these possible upwelling events have on the annual mean current speed in this area, we focused on one specific event at station 15 in September 2013. Like in the previous section, we take the average speed of 10 cm $s^{-1}$ as the lower limit of a high current speed day, since during these possible upwelling events the current speed peaks are clearly higher than 10 cm $s^{-1}$ and in most of the other higher current speed events the peaks are around or smaller than 10 cm $s^{-1}$. This event had 15 high-speed days (from 11 to 25 Sep 2013) with a mean velocity of 18 cm $s^{-1}$. Averaged over the year, if we assume that the flow direction stays the same during this event, this single event contributes approximately 0.7 cm $s^{-1}$ to the yearly mean. As the yearly mean velocity for this station was 6 cm $s^{-1}$ in 2013, it means that this single event contributed over 10% of that figure. As there were five events in

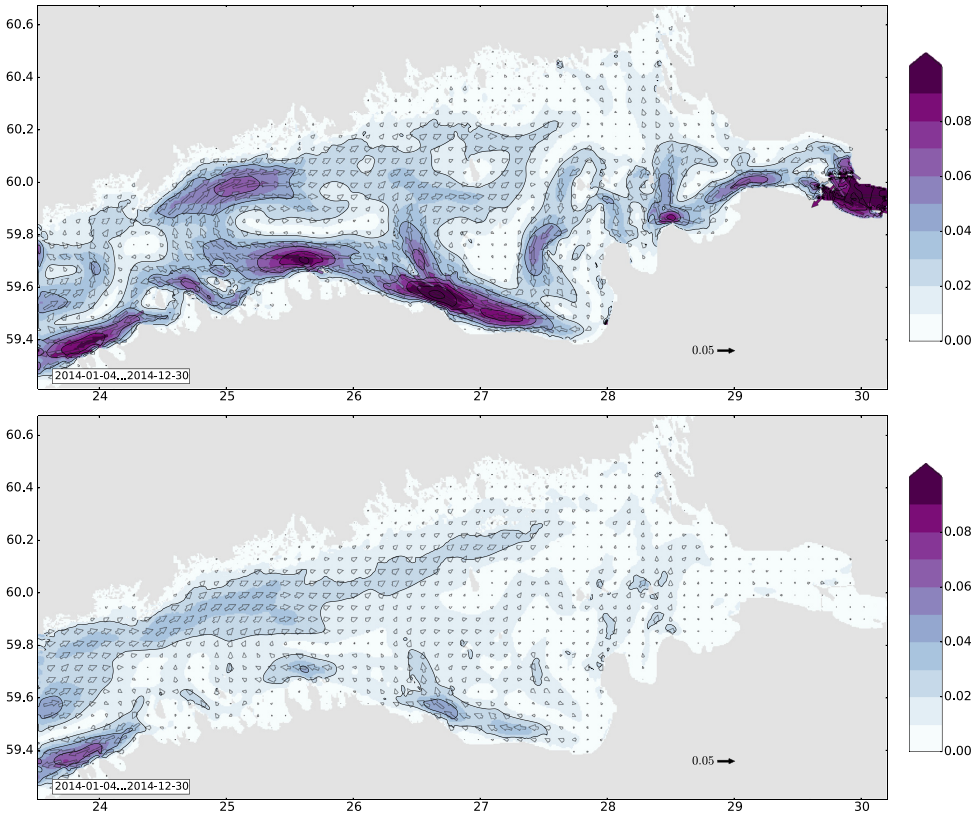


**Figure 8** Mean circulation in 2014 averaged from 0 m to 7.5 m depth in two runs of the NEMO 0.25 NM setup. The top figure shows the run with double volume runoffs, the bottom run is the one without river runoff. Velocities are in m $s^{-1}$. Vector arrows are drawn for every 13th grid point in the longitudinal direction and in every 11th grid point in the latitudinal direction.

2013 where the current speed exceeded this threshold of 10 cm $s^{-1}$, these high-speed events were reflected in a significant way in the annual mean current field at this point.

The modelled surface temperature field shows that this event displays the characteristics of an upwelling event along the southern coast of the Gulf of Finland (Fig. 11). The modelled mean surface salinity field from the same day confirmed that this cooler water originated from deeper layers with more saline water. The salinity field also shows how the freshwater plume from the Neva estuary is directed towards the south-west, towards the southern coast. The extent of this event in September 2013 suggests that coastal jets might emerge further west on the southern coast, thus contributing highly to the annual mean values, as in the case of station 15.

## 4. Discussion

The horizontal resolution of the 3D hydrodynamic model, as well as that of the meteorological forcing, have a large effect on the modelled surface and near-surface current fields. Andrejev et al. (2010) have shown that the trajectories of Lagrangian tracers in the Gulf of Finland are much affected by the horizontal resolution of the circulation model. Of the two NEMO setups we used, the fine resolution setup (0.25 NM) has sufficient scale to solve the Rossby radius of deformation in the gulf. Compared to the 2 NM NEMO setup or the HIROMB model, the 0.25 NM setup gave more detailed mean circulation fields, as expected, but also produced somewhat different circulation in the middle part of the GoF than the coarse resolution setups. Unfortunately, the good quality datasets that are presently available are not sufficient to validate the accuracy of the simulated circulation patterns in detail.

Meteorological forcing is one of the key factors in the ability of a 3D hydrodynamic model to simulate the surface and near-surface current fields. In relatively small basins these currents are mainly driven by wind stress. In the GoF, long-term runs tend to produce a cyclonic mean surface circulation pattern as a result of the prevailing south-westerly winds, density-driven circulation, Coriolis force and topographic steering. But, the variable wind conditions have a large effect on the annual circulation patterns, as can be seen from the previous studies of Andrejev et al. (2004), Maljutenko et al. (2010), Elken et al. (2011), Soomere et al. (2011), and Lagemaa (2012).

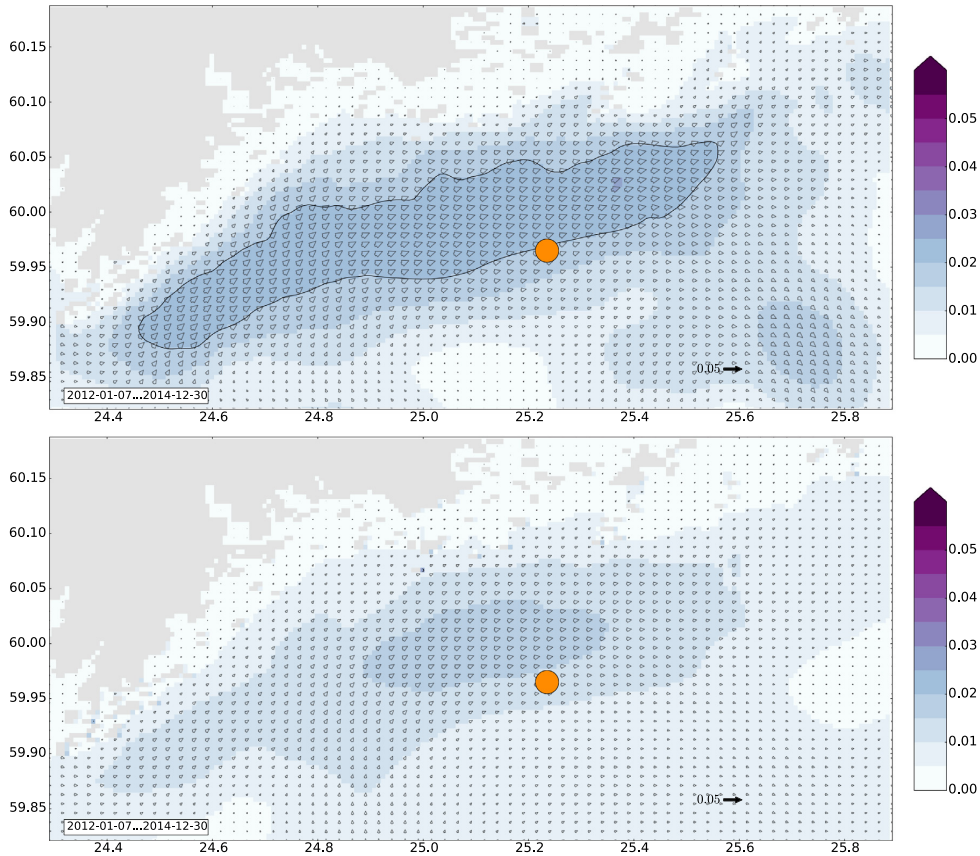


**Figure 9** Mean circulation 2012–2014 off Helsinki, split into the contribution of low and high current speed days. The modelled circulation field from the 0.25 NM NEMO setup has been averaged from 0 m to 7.5 m depth. The upper panel shows the contribution of days with low modelled current speed at a chosen location (site H, indicated with an orange circle, cf. Fig. 1). The lower panel shows the contribution of days with the high current speed at the same site. The mean circulation field is the vector sum of the two figures. The limit for high-speed days was 0.1 m $s^{-1}$, which means that the upper figure has approximately 82% of days and the lower figure 18%. Velocities are in m $s^{-1}$. Vector arrows are drawn for every third grid point in the longitudinal direction and in every second grid point in the latitudinal direction. Note the colour scale, which is different from the other figures. (For interpretation of the references to color in this figure legend, the reader is referred to the web version of the article.)

The wind roses from Kalbådagrund station show some variability in the directionality of the wind field over the years. Especially the proportion and magnitude of easterly winds varied. This could have a large effect on the frequency and location of the upwelling events in the gulf and influence the annual mean surface and near-surface current fields significantly. For instance, in 2013 and 2014, when the easterly winds were stronger compared to those of 2012, there were much higher current speeds on the southern coast of the GoF which we associated with coastal currents.

The meteorological forcing used in this study had a resolution of c. 7.5 km, except for the two first months of 2012 when it was coarser. This resolution is high enough to produce a wind field and other meteorological parameters in the GoF with sufficient accuracy for marine modelling. The peak of the high-wind situations is predicted more accurately than in some of the earlier modelling studies that have utilised the SMHI (Swedish Meteorological and Hydrological Institute) gridded meteorological dataset with one-degree resolution (Andrejev et al., 2004; Tuomi et al., 2012). However, a comparison of the wind roses at Kalbådagrund showed that HIRLAM was not able to describe the directional properties of the wind field in full detail. Furthermore, HIRLAM slightly underestimates higher wind speeds (of over 12 m $s^{-1}$). This affects the ability of NEMO to simulate the intensity of the upwelling events and the resulting coastal jets.

The upwelling-related alongshore coastal jets west of Narva Bay have been earlier presented by Suursaar and Aps (2007), who analysed RDCP (Recording Doppler Current Profiler) measurements from summer 2006 west of Narva Bay during an upwelling event. Also, Suhhova et al. (2015) have

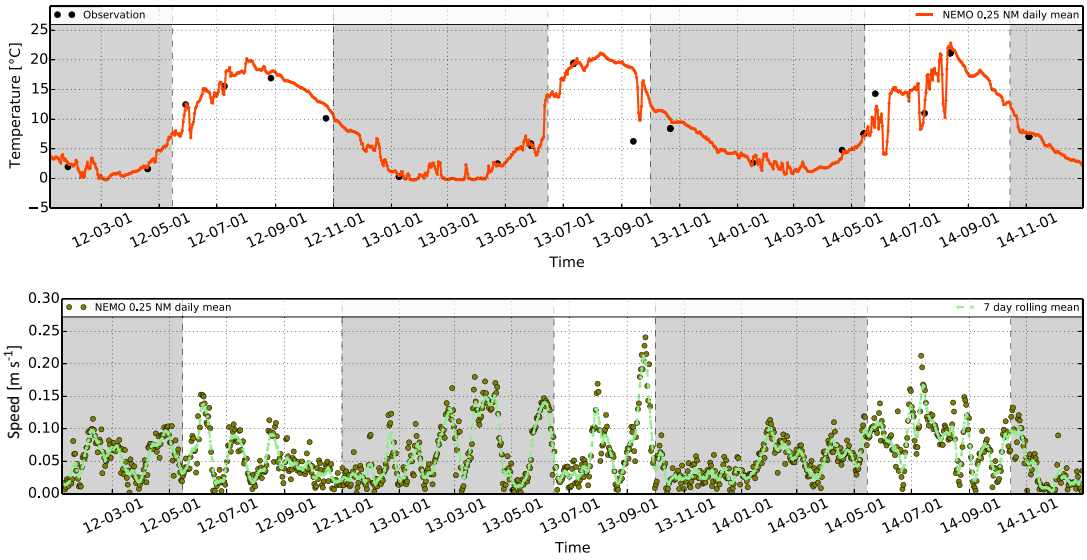


**Figure 10** Top: a time series of water temperature at 5 m depth (station G). The red line is from the 0.25 NM NEMO setup and black dots are observations. Bottom: a time series of horizontal current speed at 10 m depth (station 15). Dark green dots are from the 0.25 NM setup and light green dashed line is the seven-day moving average. A shaded background indicates the approximate time intervals when there was no seasonal thermocline in the water column. The results cover 2012—2014, the date is given in the YY-MM-DD format. (For interpretation of the references to color in this figure legend, the reader is referred to the web version of the article.)

investigated the westward surface currents off the Estonian coast near the Pakri Peninsula, based on approximately four months of ADCP (Acoustic Doppler Current Profiler) measurements made in 2009 and HIROMB simulations. They found that upwelling-related jets were mainly responsible for the westward current in this area.

The ability of the model to simulate coastal upwelling events and their extent and magnitude greatly affects how the model simulates the alongshore coastal jets. For example, Lagemaa (2012) has shown that HIROMB model generally overestimates currents in the Estonian coast compared to ADCP measurements. He discussed that incorrectly described upwelling and downwelling jets may be one of the reasons for the overestimation. Vankevich et al. (2016) have shown that a fine resolution NEMO setup, which is similar to our setup, simulates the spatial patterns of an upwelling event well. However, further investigation of the link between the scale of the upwelling events and the magnitude of the coastal jet simulated by NEMO would be beneficial.

There are also measurements that indirectly allow us to gain some understanding about the circulation field. The profiles measured during the Gulf of Finland year 2014 gave a possibility to analyse the horizontal and vertical extent of the salinity stratification in the gulf. As our results showed, there was diversity in the ability of the models to simulate this. A situation in which less saline water is found in the southern coast of the gulf suggests that circulation has been more or less anti-cyclonic around that time. Although that situation might be rare, it has been observed several times in ferrybox measurements on the Helsinki—Tallinn route (Kikas and Lips, 2016).

Several questions remain. For example, the intensity and direction of the outflow at the northern side of the gulf differs between the models and should be investigated further. In our model runs the direction and intensity of the outflow at the Finnish coast is greatly influenced by the high current speed situations. To determine if this response is correctly estimated, the results need to be verified against current measurements. The FMI has made ADCP measurements in 2009—2014 on the Finnish coast but those datasets need further processing before they can be used for analyses. Also, more observations are needed from the Narva estuary and its vicinity. Further study is also required to quantify the impact of upwelling-related jets in the longer term. It is clear that our three-year runs do not as such represent the same thing as, say, a 30-year climatological run. If such high-resolution runs were feasible at this point in time, they would surely prove informative.

Further effort and observations are also required to understand if parameterisations in hydrodynamic models that are currently used allow the frequency and intensity of these events to be modelled correctly. For example, a more detailed investigation of the sensitivity of model results to river runoff variance might help us understand how to better capture the Neva river plume correctly after it enters the gulf. Another subject area worthy of attention is current-induced substance transport and its relation to the mean circulation field. From our results, it is clear that single high-energy events can strongly affect the mean circulation. But what this means for simulations of substances leaked into the sea is an open question still.

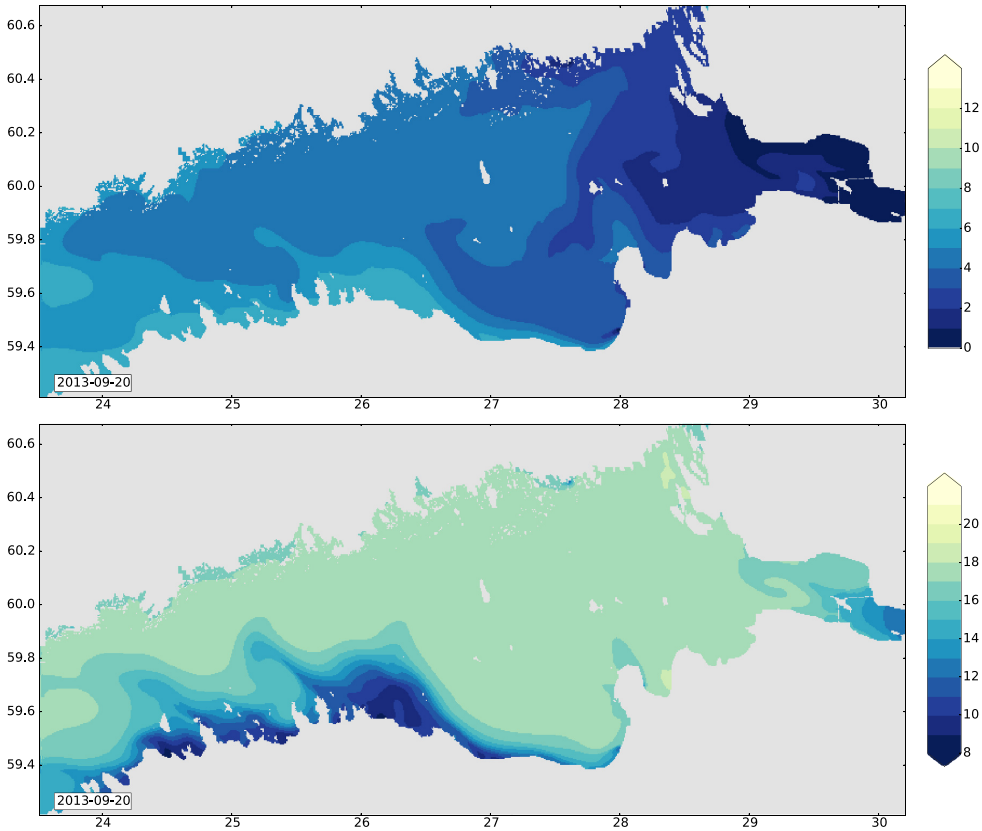


**Figure 11** The surface salinity (top) and temperature (°C, bottom) fields from the 0.25 NM NEMO model run on the 20 September 2013 during an upwelling event on the southern coast of the Gulf of Finland.

## 5. Conclusions

In this study we analysed circulation patterns in the Gulf of Finland with two setups of the NEMO 3D hydrodynamic model.

We found that our model produces notable differences in the residual circulation patterns from year to year and from one model setup to another. Benchmarking the results to the HIROMB-based CMEMS product showed that the overall pattern was similar in both models. Comparison to salinity observations from the area revealed that vertical salinity structure was well represented. There were differences in the surface salinities, however, as is often the case for hydrodynamic models of this area. The models seem to need further development before they are able to capture the location of the surface salinity gradients in the Gulf of Finland.

We found that days with strong currents contribute significantly to the mean flow west of Narva Bay and off the Finnish coast, causing relatively strong coastal currents. We also found that most notable high-speed events were associated with upwelling.

Further, we found that the variations in runoff mainly affected the magnitude of near-surface currents. The directions of the currents seemed less sensitive to the changes. It is unlikely that runoff changes have a major effect on the year-to-year variations in the mean circulation patterns.

The experiments with the NEMO model have been beneficial to understanding the model behaviour in the area. The dynamics of the Gulf of Finland will continue to be a worthwhile topic of study as the gulf is vulnerable to accidents, and marine traffic is heavy both along and across the gulf. Also, further studies will advance the development of the high-resolution NEMO configurations for the gulf as an operational tool for everyday predictions and an aide when compiling environmental assessments of the possible changes in the gulf.

## Acknowledgements

This work has been partly financed by the Maj and Tor Nessling Foundation [grant numbers 201500179, 201600161, 201700056]; the EXOSYSTEM RUSPLUS_S&T_FULL-240 project; and the Finnish Ministry of Environment. Roman Vankevich was supported by the Russian Foundation for Basic Research

[grant N 16-55-76021]. The authors would like to thank Robinson Hordoir and others at SMHI for their work on the NEMO Nordic configuration and their support for our efforts. Sami Niemelä and the FMI-HIRLAM team are acknowledged for providing the FMI-HIRLAM data and useful advice. Continued work on Baltic Sea NEMO has been possible over the years thanks to Jari Haapala and other colleagues at FMI. This study has been conducted using E.U. Copernicus Marine Service Information. The Gulf of Finland Year 2014 data providers include Estonian Marine Institute (EMI); Marine Systems Institute (MSI); Finnish Environment Institute (SYKE); Uusimaa and South-East Finland Centres for Economic Development, Transport and the Environment (UUDELY and KASELY); City of Helsinki Environment Centre (HELSINKI); and North-West Interregional Territorial Administration for Hydrometeorology and Environmental Monitoring (HYDROMET).

## References

Alenius, P., Myrberg, K., Nekrasov, A., 1998. The physical oceanography of the Gulf of Finland: a review. Boreal Environ. Res. 3, 97—125.

Alenius, P., Nekrasov, A., Myrberg, K., 2003. Variability of the baroclinic Rossby radius in the Gulf of Finland. Cont. Shelf Res. 23, 563—573.

Andrejev, O., Myrberg, K., Alenius, P., Lundberg, P.A., 2004. Mean circulation and water exchange in the Gulf of Finland — a study based on three-dimensional modelling. Boreal Environ. Res. 9, 1—16.

Andrejev, O., Sokolov, A., Soomere, T., Värv, R., Viikmäe, B., 2010. The use of high-resolution bathymetry for circulation modelling in the Gulf of Finland. Est. J. Eng. 19, 187—210, http://dx.doi.org/10.3176/eng.2010.3.01.

Axell, L., 2016. Baltic Sea Physics Reanalysis from SMHI. [WWW Document], http://marine.copernicus.eu/documents/PUM/CMEMS-BAL-PUM-003-008.pdf.

Bergström, S., Carlsson, B., 1994. River run-off to the Baltic Sea: 1950—1990. Ambio 23, 280—287.

Donnelly, C., Andersson, J.C.M., Arheimer, B., 2016. Using flow signatures and catchment similarities to evaluate the E-HYPE multi-basin model across Europe. Hydrol. Sci. J. 61, 255—273.

Elken, J., Nomm, M., Lagemaa, P., 2011. Circulation patterns in the Gulf of Finland derived from the EOF analysis of model results. Boreal Environ. Res. 16, 84—102.

Ferry, N., Parent, L., Masina, S., Storto, A., Zuo, H., Balmaseda, M., 2016. Global Ocean Physics Reanalysis Glorys2V3. [WWW Document], http://marine.copernicus.eu/documents/PUM/CMEMS-GLO-PUM-001-009-011-017.pdf.

HIRLAM-B, 2015. System Documentation. [WWW Document], http://www.hirlam.org/.

Hordoir, R., An, B.W., Haapala, J., Meier, H.E.M., 2013a. A 3D Ocean Modelling Configuration for Baltic and North Sea Exchange Analysis. [WWW Document], http://www.smhi.se/polopoly_fs/1.28758!RO_48.pdf.

Hordoir, R., Dieterich, C., Basu, C., Dietze, H., Meier, H.E.M., 2013b. Freshwater outflow of the Baltic Sea and transport in the Norwegian current: a statistical correlation analysis based on a numerical experiment. Cont. Shelf Res. 64, 1—9, http://dx.doi.org/10.1016/j.csr.2013.05.006.

Hordoir, R., Axell, L., Löptien, U., Dietze, H., Kuznetsov, I., 2015. Influence of sea level rise on the dynamics of salt inflows in the Baltic Sea. J. Geophys. Res. Ocean. 120, 6653—6668, http://dx.doi.org/10.1002/2014JC010642.

Kikas, V., Lips, U., 2016. Upwelling characteristics in the Gulf of Finland (Baltic Sea) as revealed by Ferrybox measurements in 2007—2013. Ocean Sci. 12, 843—859, http://dx.doi.org/10.5194/os-12-843-2016.

Lagemaa, P., 2012. Operational Forecasting in Estonian Marine Waters. TUT Press, Tallinn, http://digi.lib.ttu.ee/i/?714.

Large, W.G., Yeager, S.G., 2004. Diurnal to decadal global forcing for ocean and sea-ice models: the data sets and flux climatologies. In: NCAR Technical Note, NCAR/TN-460+STR, CGD Division of the National Center for Atmospheric Research. , http://dx.doi.org/10.5065/D6KK98Q6 PDF 112 pp.

Lehmann, A., Myrberg, K., 2008. Upwelling in the Baltic Sea — a review. J. Mar. Syst. 74, S3—S12, http://dx.doi.org/10.1016/j.jmarsys.2008.02.010.

Leppäranta, M., Myrberg, K., 2009. Physical Oceanography of the Baltic Sea. Springer-Verlag, 378 pp.

Lips, U., Lips, I., Liblik, T., Kikas, V., Altoja, K., Buhhalko, N., Rünk, N., 2011. Vertical dynamics of summer phytoplankton in a stratified estuary (Gulf of Finland, Baltic Sea). Ocean Dyn. 61, 903—915, http://dx.doi.org/10.1007/s10236-011-0421-8.

Madec, G., the NEMO team, 2008. NEMO Ocean Engine, Institut Pierre-Simon Laplace (IPSL), France, note du Pôle de modélisation, No 27, 386 pp., https://www.nemo-ocean.eu/bibliography/documentation/.

Maljutenko, I., Laanemets, J., Raudsepp, U., 2010. Long-term high-resolution hydrodynamical model simulation in the Gulf of Finland. In: Baltic International Symposium (BALTIC), 2010 IEEE/OES US/EU. 1—7, http://dx.doi.org/10.1109/BALTIC.2010.5621641.

Myrberg, K., Soomere, T., 2013. The Gulf of Finland, its hydrography and circulation dynamics. In: Preventive Methods for Coastal Protection, Springer, 181—222.

Myrberg, K., Ryabchenko, V., Isaev, A., Vankevich, R., Andrejev, O., Bendtsen, J., Erichsen, A., Funkquist, L., Inkala, A., Neelov, I., Rasmus, K., Medina, M.R., Raudsepp, U., Passenko, J., Söderkvist, J., Sokolov, A., Kuosa, H., Anderson, T.R., Lehmann, A., Skogen, M.D., 2010. Validation of three-dimensional hydrodynamic models of the Gulf of Finland. Boreal Environ. Res. 15, 453—479.

Palmén, E., 1930. Untersuchungen über die Strömungen in den Finnland umgebenden Meeren. Soc. Scient. Fenn., Comm. Phys.-Math. 12, 1—94, (in German).

Raateoja, M., Setälä, O. (Eds.), 2016. The Gulf of Finland Assessment. Rep. Finnish Environ. Insti., Helsinki PDF 368 pp., http://hdl.handle.net/10138/166296.

Soomere, T., Myrberg, K., Leppäranta, M., Nekrasov, A., 2008. The progress in knowledge of physical oceanography of the Gulf of Finland: a review for 1997—2007. Oceanologia 50 (3), 287—362.

Soomere, T., Leppäranta, M., Myrberg, K., 2009. Highlights of the physical oceanography of the Gulf of Finland reflecting potential climate changes. Boreal Environ. Res. 14, 152—165.

Soomere, T., Delpeche, N., Viikmäe, B., Quak, E., Meier, H.E.M., Doos, K., 2011. Patterns of current-induced transport in the surface layer of the Gulf of Finland. Boreal Environ. Res. 16, 49—63.

Stålnacke, P., Grimvall, A., Sundblad, K., Tonderski, A., 1999. Estimation of riverine loads of nitrogen and phosphorus to the Baltic Sea, 1970—1993. Environ. Monit. Assess. 58, 173—200.

Stipa, T., 2004. Baroclinic adjustment in the Finnish Coastal Current. Tellus A 56, 79—87.

Suhhova, I., Pavelson, J., Lagemaa, P., 2015. Variability of currents over the southern slope of the Gulf of Finland. Oceanologia 57 (2), 132—143, http://dx.doi.org/10.1016/j.oceano.2015.01.001.

Suursaar, Ü., Aps, R., 2007. Spatio-temporal variations in hydrophysical and-chemical parameters during a major upwelling event off the southern coast of the Gulf of Finland in summer 2006. Oceanologia 49 (2), 209—228.

Troupin, C., Barth, A., Sirjacobs, D., Ouberdous, M., Brankart, J.-M., Brasseur, P., Rixen, M., Alvera-Azcárate, A., Belounis, M., Capet, A., Lenartz, F., Toussaint, M.-E., Beckers, J.-M., 2012. Generation

of analysis and consistent error fields using the Data Interpolating Variational Analysis (Diva). Ocean Model. 52—53, 90—101, http://dx.doi.org/10.1016/j.ocemod.2012.05.002.

Tuomi, L., Myrberg, K., Lehmann, A., 2012. The performance of the parameterisations of vertical turbulence in the 3D modelling of hydrodynamics in the Baltic Sea. Cont. Shelf Res. 50, 64—79.

Vancoppenolle, M., Fichefet, T., Goosse, H., Bouillon, S., Madec, G., Maqueda, M.A.M., 2009. Simulating the mass balance and salinity of Arctic and Antarctic sea ice. 1. Model description and validation. Ocean Model. 27, 33—53.

Vankevich, R.E., Sofina, E.V., Eremina, T.E., Ryabchenko, V.A., Molchanov, M.S., Isaev, A.V., 2016. Effects of lateral processes on the seasonal water stratification of the Gulf of Finland: 3-D NEMO-based model study. Ocean Sci. 12, 987—1001, http://dx.doi.org/10.5194/os-12-987-2016.

Westerlund, A., Tuomi, L., 2016. Vertical temperature dynamics in the Northern Baltic Sea based on 3D modelling and data from shallow-water Argo floats. J. Mar. Syst. 158, 34—44, http://dx.doi.org/10.1016/j.jmarsys.2016.01.006.

Witting, R., 1912. Zusammenfassende Uebersicht der Hydrographie des Bottnischen und Finnischen Meerbusens und der Nördlichen Ostsee nach den Untersuchungen bis Ende 1910. Soc. Sci. Fenn. Finländische Hydr.-Biol. Untersuchungen, No. 7.

Zhurbas, V., Laanemets, J., Vahtera, E., 2008. Modeling of the mesoscale structure of coupled upwelling/downwelling events and the related input of nutrients to the upper mixed layer in the Gulf of Finland, Baltic Sea. J. Geophys. Res. Ocean. 113 (C5), C05004, http://dx.doi.org/10.1029/2007JC004280.

IV

# Circulation patterns in the Gulf of Finland from daily to seasonal timescales

Antti Westerlund[a], Laura Tuomi[a], Pekka Alenius[a], Kai Myrberg[b,c], Elina Miettunen[b], Roman E. Vankevich[c], Robinson Hordoir[d]

[a]Finnish Meteorological Institute, Marine Research, Helsinki, Finland; [b]Finnish Environment Insitute SYKE, Helsinki, Finland; [c]Department of Natural Sciences of Faculty of Marine Technology and Natural Sciences, University of Klaipeda, Klaipeda, Lithuania [d]Shirshov Institute of Oceanology, Russian Academy of Sciences, Saint Petersburg, Russia; [e]Swedish Meteorological and Hydrological Institute, Norrköping, Sweden

**ARTICLE HISTORY**
Compiled October 29, 2018

**ABSTRACT**
We studied circulation patterns in the Gulf of Finland, an estuary-like sub-basin of the Baltic Sea. Circulation patterns in the Gulf of Finland are complex and vary from season to season and year to year. Estuarine circulation in the gulf is heavily modified by many factors, such as wind forcing, topography and geostrophic effects. Based on a 7-year run of the NEMO 3D hydrodynamic model with a 500 m horizontal resolution, we analysed seasonal changes of mean circulation patterns. We found that there were clear seasonal differences in the circulation patterns in the Gulf of Finland. Features that moved or changed direction from season to season were damped or hidden in the averages. To further study these differences, we also carried out a self-organizing map (SOM) analysis of currents for several latitudinal sections. The results of the SOM analysis emphasised the estuary-like nature of the Gulf of Finland. Circulation changed rapidly from normal estuarine circulation to reverse estuarine circulation. The dominant southwesterly winds supported the reversal of the estuarine circulation. Both normal and reversed estuarine circulation were roughly as common in our data. The SOM analysis also demonstrated how the long-term cyclonic mean circulation field and the average salinity field emerged from the interaction of normal and reversed estuarine circulation.

**KEYWORDS**
circulation; modelling; Baltic Sea; Gulf of Finland; SOM

## 1. Introduction

Northern marginal seas experience many seasonal variations, which can be expected to modify their circulation field significantly, as many forcing factors vary from season to season. For example, in the Baltic Sea wind forcing is stronger in autumn and winter than in summer and spring. Seasonal ice cover modifies the response to wind forcing in the winter. In the spring, melting sea ice affects surface salinity. River runoffs also

CONTACT A. Westerlund. Email: antti.westerlund@fmi.fi. Postal Address: P.O. BOX 503, FI-00101 Helsinki, Finland. ORCID id: https://orcid.org/0000-0003-2006-3079

Received: January 18, 2018. Received in revised form: May 4, 2018.

increase with melting waters. Precipitation is lowest in the spring and then increases towards autumn. In the summer, increasing temperatures lead to the formation of thermal stratification, which then collapses in the autumn. The interplay of these factors results in seasonal circulation changes that are not always intuitive.

The Gulf of Finland (GoF) is the easternmost sub-basin of the Baltic Sea (Fig. 1). It is a direct continuation of the Baltic Proper with no separating sills between the two. It is estuary-like, with the Neva River — the largest single freshwater input to the Baltic Sea — at the eastern end, and a more saline deep water wedge extending from the Baltic Proper at the western end. These opposite inputs maintain a permanent horizontal density gradient. The GoF is an elongated basin approximately 400 km long. At the eastern end of the basin, there is the shallow and narrow Neva estuary and its transition zone. Next, there is a wider part of the basin between 26 °E and 28 °E (maximum width c. 135 km) and then a narrower part between 23 °E and 26 °E (minimum width 48 km). For in-depth descriptions of the physical oceanography of the GoF, see e.g. Alenius et al. (1998), Soomere et al. (2008), Soomere et al. (2009), Leppäranta and Myrberg (2009), and Myrberg and Soomere (2013).

Perhaps the simplest way to consider the circulation patterns of the GoF is to begin from standard estuarine circulation, which is established by freshwater forcing and density-driven currents (for a general discussion of estuaries, see e.g. Talley et al., 2011). In the case of the Gulf of Finland this would mean that the fresh river waters from the head of the estuary in the east flow on the surface outwards, towards the mouth of the estuary in the west. A compensating flow of saltier, denser water is transported deeper in the water column to the opposite direction. (See Hela (1952) for an early English-language description of this for the GoF.)

The estuarine circulation is, however, heavily modified by factors such as wind forcing, topography and geostrophic effects. The current direction can change quickly for several reasons. On a timescale of hours to days, periodic processes such as inertial oscillations and seiches can be important. On a timescale of days to weeks, variable winds are the main driver of currents in the GoF. Sometimes surface currents are almost unidirectional nearly everywhere in the whole gulf, if the wind forcing is uniform enough. At other times, there is more spatial variability. Overall, on any given day, the circulation patterns in the GoF can be expected to be very complicated and variable.

The dominating wind direction in the GoF is southwesterly. If there are strong enough winds from this direction, the transport of water near the surface is roughly towards south-east or east, as per the Ekman motion theory (e.g. Cushman-Roisin and Beckers, 2011). This drives water towards the head of the estuary and can lead to full reversal of the normal estuarine circulation, with outward compensating flows deeper in the water column (e.g. Elken et al., 2003; Liblik et al., 2013). This reversal can then lead to a collapse of water column stratification in winter (Elken et al., 2014).

Circulation patterns look different at different timescales. Averaging currents over longer time periods smoothens the signal and damps features visible in the shorter term. In a large estuary like the GoF, where rotational effects are also important, a cyclonic circulation pattern emerges when the currents are averaged over a sufficiently long period of time. Witting (1912) and Palmén (1930) were the first to note this in the GoF, based on light vessel observations. However, these early estimates were based on only a few data points. Nevertheless, later works by e.g. Hela (1952), Mikhailov and Chernyshova (1997), Andrejev et al. (2004), Maljutenko et al. (2010), Elken et al. (2011), Soomere et al. (2011), Lagemaa (2012) and Westerlund et al. (2018) have mostly confirmed the main outcomes of these early studies. There is some variation in the results of these studies, mostly explained by inter-annual variability and differences in

methodology. In general, long-term average currents are on the order of 1–2 cm/s and have low stability.

As there is seasonal variation in the forcing, so there is seasonal variation in the circulation patterns. Already in the 20th century, it was known that the stability of currents during seasons was higher than annually. Still, seasonal circulation variations in the GoF have been studied relatively little. Witting (1912) published seasonal circulation maps for the GoF (reproduced by Alenius et al. (1998)). Later, Hela (1952) computed monthly currents from lightship observations for two stations between Tallinn and Helsinki. More recently, Soomere et al. (2011) divided the year into four periods (calm and windy periods, and transitional periods between them) for their analysis of current-induced surface transport in the GoF.

With changes in climate, changes to seasonal variation of forcing are also expected (BACC II Author Team, 2015). Investigation of seasonal circulation patterns can deepen our understanding of the dynamics of the basin and how circulation conditions in the GoF will change in the coming decades. Furthermore, as the marine traffic in the gulf is very intensive and the shores of the gulf are heavily populated, a better understanding of circulation dynamics is needed for applications such as estimating the transport of oil, chemicals and nutrients.

In recent years, fully automated measurement platforms, satellites and high-resolution modelling have transformed oceanography. Traditionally, oceanographers had to routinely draw their conclusions from a limited number of observations. While this is still commonly the case for many types of observations, at the same time the amount of data that needs to be processed and analysed is growing rapidly. It is not often possible for a scientist to manually investigate all the data. In these cases, new methods such as machine learning can assist. Machine learning algorithms can be used as exploratory tools to find structure in the data. This data can be both observational and modelling datasets. The use of machine learning methods began in the environmental sciences in the 1990s, and they are nowadays used extensively (for an overview, see e.g. Hsieh, 2009). An important example of a machine learning method in the field of oceanography is the Self-Organizing Map (SOM), which is a neural-network-based method that can be used for feature extraction (Kohonen, 1982, 2001; Liu and Weisberg, 2011; Thomson and Emery, 2014).

In this study, we examine circulation patterns in the Gulf of Finland on a timescale of days to years. The aim is to identify frequent patterns in a hydrodynamic model simulation along with factors affecting their emergence. We analyse connections between different timescales and investigate relations between model forcing and circulation patterns. The data from the high-resolution Gulf of Finland configuration of the numerical 3D model NEMO (Madec and the NEMO team, 2008) are analysed for the years 2007-2013. Circulation conditions are studied more in-depth for chosen north-south sections with the SOM analysis.

## 2. Materials and Methods

### *2.1. Modelling*

We used the NEMO 3D ocean model (V3.6) for the GoF with a 0.25 NM (nautical mile), or roughly 500 m, horizontal resolution. This setup is similar to the one presented by Westerlund et al. (2018), which wasoriginally based on the setup by Vankevich et al. (2016). The main differences in the configuration in the present study are in the

atmospheric forcing, boundary conditions, and the bathymetry. We ran the model from the beginning of 2006 to the end of 2013. We considered the results from 2006 as the initialisation of the model and chose the years 2007-2013 for a closer analysis. The daily mean values of temperature, salinity and current fields were saved for the analysis.

The horizontal resolution of the configuration (500 m) is well below the typical range of the internal Rossby radius (2–4 km) in the GoF (Alenius et al., 2003). The model domain covers the GoF east from the Vormsi–Kimitoön line roughly at 23 °E, where an open boundary towards the Baltic Proper is located (see Fig. 1). Model bathymetry is based on the data from the VELMU (Finnish Inventory Programme for the Marine Environment) depth model from SYKE (Finnish Environment Institute) and the Baltic Sea Bathymetry Database (Baltic Sea Hydrographic Commission). This setup has 94 z-coordinate (with partial step) vertical layers. The topmost vertical layers are 1 m thick, and the layer thickness slightly increases with depth, being about 1.08 m at the lower bound of the z-axis. The time step of the model is 100 s. The ice model LIM3 was included in the setup (Vancoppenolle et al., 2009). Due to the high computational requirements of the configuration, the ice model was only run with a thermodynamic formulation. The lateral boundary condition on the open boundary was taken from the NEMO Nordic 2 NM configuration for the Baltic Sea and North Sea (Hordoir et al., 2013, 2015, 2018). We used initial conditions for the beginning of 2006 from this same model run. Flather boundary conditions were used for barotropic velocities and sea surface height; flow relaxation was used for temperature and salinity.

#### *2.1.1. Model forcing*

The EURO4M regional reanalysis product (Dahlgren et al., 2016; Landelius et al., 2016) was used as atmospheric forcing, both in the 0.25 NM GoF configuration and in the coarser configuration that provided the boundary condition. This product has the approximate horizontal resolution of 22 km, and its domain is centred in Europe. We used 10-metre wind, longwave and shortwave radiation, humidity, 2-metre air temperature, and precipitation fields at 3-hour intervals. The reanalysis was produced with the HIRLAM NWP (Numerical Weather Prediction) model version 7.3. It was constrained with the ERA-Interim product (Dee et al., 2011) on lateral boundaries and also via data assimilation.

Previously, forecasts from the operational HIRLAM NWP system have been used as forcing for the high-resolution GoF configuration (Westerlund et al., 2018). While the reanalysis product used as forcing in this study is also based on the HIRLAM model core, there are differences between this forcing dataset and the one that was used by Westerlund et al. (2018). In the reanalysis product, the forcing is more homogeneous for the whole period, since it is produced with the same resolution and version of the system over the whole time period. This is not always the case when forecasts are used. Also, reanalyses use a larger amount of data for the data assimilation, as usually all observational data are not yet available in real-time for the forecast runs.

By using the reanalysis dataset for this study, we have the same forcing dataset for both this model configuration and the coarser model used for boundary conditions. Furthermore, it enables us to have a longer modelling period than by using forecasts alone, where the aforementioned issues with data homogeneity and technical problems make compilation of a long-term forcing dataset challenging or practically impossible.

On the other hand, it should be noted that the resolution of the reanalysis is coarser than that of the NWP system, which might be an issue in some circumstances. For example, in the Finnish archipelago area on the northern coast of our modelling domain

the shape of the shoreline is complex and requires sufficient resolution in the atmospheric model. Furthermore, a Europe-wide reanalysis product might not be as well-tuned to the local conditions of the Nordic countries as is an NWP product that is mainly focused on forecasting the weather in that area.

River runoffs included data for the four main rivers in the GoF area and was based on two sources. The river Kymi discharges were taken from the open data of the Finnish Environment Institute (SYKE). For the Neva, Narva and Luga rivers, data were provided by HydroMet as a part of the Gulf of Finland Year 2014 (GoF2014) activities (`http://www.gulfoffinland.fi`).

### *2.2. Measurements*

We used CTD data from three monitoring stations near the northern coast of the GoF for model validation: Haapasaari (depth 66 m), Länsi-Tonttu (depth 53 m) and Längden (depth 60 m, locations shown in Fig. 1). Temperature and salinity were available at 1, 5, 10, 20 and 40 m depths and the bottom layer, measured 1–3 times a month during the ice-free season.

We used wind measurements from the FMI's coastal weather station Kalbådagrund (location shown in Fig. 1) to evaluate the accuracy of the meteorological forcing. This weather station is considered to be representative of open sea weather conditions in the Gulf of Finland, and it has been used in many earlier studies (e.g. Lips et al., 2011; Tuomi et al., 2012). At Kalbådagrund, wind measurements are made at a 32 m height. From this station, we have data for the main meteorological parameters at 10-minute intervals.

### *2.3. Self-organizing map (SOM)*

The Self-Organizing Map (SOM), also known as the Kohonen Map, is an unsupervised learning algorithm based on artificial neural networks (Kohonen, 1982, 2001). It can be used as a way to reduce the dimensionality and extract features of a large dataset in a way similar to the classical EOF (Empirical Orthogonal Function) analysis or PCA (Principal Component Analysis). This will facilitate visualisation and analysis of the high-dimensional data, which is projected non-linearly, for example, in one- or two-dimensional space. The algorithm finds weight vectors from the original data, which are used to form a map or a codebook. The weights or nodes in this map can be reshaped back to characteristic data patterns. The best matching node is assigned for each point of the original time series (best matching unit, BMU). This way all data points in the time series are clustered into a predefined number of groups represented by nodes of the map. One of the benefits of this method for Earth sciences is that topological properties of the input space are preserved, i.e., similar states are near each other on the map.

SOM has previously been used for a number of applications in physical oceanography (Liu and Weisberg, 2011; Thomson and Emery, 2014) from analysing ADCP to satellite data to model results. Applications include identification of characteristic current patterns (e.g. Liu and Weisberg, 2005) and hydrodynamics of coastal and estuarine environments (Williams et al., 2014). There are also other recent examples, for instance from the Mediterranean Sea (Falcieri et al., 2014; Fraysse et al., 2014) and the Pacific Ocean (Hisaki, 2013).

SOM offers some benefits with respect to EOF/PCA analysis. For example, the temporal mean does not have to be removed prior to applying the algorithm, which makes

the output easier to visualise (Liu and Weisberg, 2005; Liu et al., 2006a). The outputs of the algorithm are not anomalies, as with EOF/PCA. Also, unlike EOF/PCA analysis, SOM is a non-linear method, which makes it better-suited for asymmetric patterns. Furthermore, missing data values are easier to handle in SOM analysis. A basic example of how SOM and EOF methods differ for feature extraction was provided by (Liu et al., 2006b). They combined several waveforms into a time series and then tried to recover them with both analysis methods. The EOF analysis was unable to recover the sine, step, sawtooth and cosine functions present in the data. A SOM map, however, recovered the waveforms successfully.

An inherent problem with the SOM algorithm is that the user predefines map dimensions. This always involves striking a balance between the easy interpretability of the output and the accuracy of mapping. This deficiency could be addressed with Growing Hierarchical Self Organised Maps (GHSOM) (Thomson and Emery, 2014), but those also add complexity to the analysis. It is also worth noting that statistical clustering algorithms such as SOM do not consider physical conditions, and any placement of a particular data point in any cluster is not definitive but depends on the chosen analysis parameters.

We used the SOMpy implementation of the algorithm (`https://github.com/sevamoo/SOMPY`). There are a number of parameters that can be adjusted for the SOM. We mostly followed suggestions by Liu et al. (2006b) for small map sizes: we used rectangular neural lattice, planar map shape and batch training. Unlike Liu et al. (2006b), we used random initialisation, as for our application the number of iterations before stabilisation was manageable. We used the Gaussian neighbourhood function, which according to Liu et al. (2006b) gives the smoothest patterns with the lowest noise levels.

## 3. Results

### *3.1. Model validation*

Westerlund et al. (2018) validated a model configuration similar to the one in this paper. They compared salinity fields to gridded CTD salinity observations for three cruises in June 2013, June 2014 and September 2014. These 5-day cruises covered over 80 stations each in the western GoF, resulting in a grid with about 4 NM horizontal resolution across the gulf and 9 NM resolution along the gulf. It was found that the vertical structure of the salinity field was overall well-reproduced. In some cases the freshest water on the surface was incorrectly located and distributed wider than in the observations. This is often the case for model configurations of this area (Myrberg et al., 2010). Benchmarking the circulation patterns visually against a HIROMB-based reanalysis product showed that, overall, the patterns were similar in both models. The NEMO configuration in Westerlund et al. (2018) was mostly the same as the one in this study, but it used different atmospheric forcing, boundary conditions, and bathymetry. The atmospheric forcing in Westerlund et al. (2018) was based on FMI-HIRLAM forecasts for the years 2012-2014, and it used a 2 NM Baltic Sea–North Sea configuration on the boundary forced with the same forcing dataset. The domain of that configuration was slightly smaller with the western edge located at 23.5 °E.

Here we present additional validation to the version of the configuration at hand. Statistical comparison to CTD observations from three frequently sampled stations (Haapasaari, Länsi-Tonttu and Längden, see Table 1) revealed that the ability of the model to reproduce temperature and salinity values in the area during the time period

of investigation is in line with other GoF models. The model performed best in the western GoF, although the differences between stations were relatively small, especially for temperature. The model consistently seems to overestimate temperatures at these stations. Salinity biases are also in most cases negative, indicating modelled salinities at these stations were too high. Errors near the surface are in general smaller than lower in the water column.

The differences between meteorological forcing used in this study and the one used by Westerlund et al. (2018) were discussed in Section 2.1.1. To assess the differences between the forcing datasets, we calculated the statistics for wind forcing at the Kalbådagrund meteorological station for 2013, which was a common year for both of these datasets. Table 2 shows that FMI-HIRLAM has a lower wind speed RMS error and bias at this station. A comparison of wind speed time series (not shown) reveals that while both forcing datasets appear to be similar, the reanalysis-forcing in general has less extreme wind speeds than the forecast-forcing. There are fewer differences in the wind direction.

### *3.2. Seasonal mean currents*

Fig. 2 shows near-surface currents averaged over a 7-year period 2007-2013. In Fig. 3, mean currents are shown separately for spring (March–May), summer (June–August), autumn (September–November) and winter (December–February) periods. We see that those features that become most clearly visible in the mean over the whole run are those that also consistently appear in the seasonal means. However, those features that change place or direction from one season to another are not clearly visible in the full mean.

The average over the whole period shows moderate (less than 2 cm/s) mean current speeds near the northern coast directed mostly towards west, and stronger (mostly from 2 to 6 cm/s) currents near the centre-line of the gulf. Several loops appear. There is a clear loop between 23 °E and 24 °E in the west, and a second one around 26 °E. There are clear alongshore currents outwards from Neva along the northern coast. Another along-shore current is located west of Narva Bay along the southern coast. See Westerlund et al. (2018) for a discussion of this feature.

Seasonal averages reveal distinctly different structures of the circulation field from one season to another, and from the average over the whole run. We see that stronger currents generally appear in the autumn and the winter. This is expected, as wind speeds are also higher in those seasons than in summer and spring. An outflowing surface current near the northern coast is visible in the summer, winter, and to some extent in the spring. The location of the current pattern has some north-south variability. There is an inflow near the central part of the GoF in summer, autumn and winter seasons, but not in the spring.

In the summer, it is easy to distinguish an inflow near the centre of the gulf and an outflow near the northern coast. The same kind of pattern is visible also in the winter, although in general the field is less structured.

In the spring there is no clear inflow in the western gulf, but rather an outflow both near the southern coast and the centre line of the GoF. Average currents near the northern coast are small. In the autumn there is a strong loop in the westernmost part of the domain and inflowing currents near the centre of the gulf.

### *3.3. Inter-annual variability*

As noted in Section 1, there is inter-annual variability in the circulation field, which explains many of the differences between different studies. Also in our results, circulation maps differ from one year to another. We can demonstrate this by investigating more closely the mean surface circulation maps for 2007-2008 and for 2010-2011 (not shown). These periods were chosen to facilitate the comparison to circulation maps presented by Elken et al. (2011) and Lagemaa (2012) for 2006-2008 and 2010-2011, calculated from the HIROMB model at 1 NM resolution (see Section 4).

When compared to the map of the full simulation period in Fig. 2, the map for 2007-2008 shows somewhat stronger currents overall in the domain. There is a stronger westward current on the northern coast of the GoF extending from the east to approximately 25 °E, with current speeds of mostly 2 to 4 cm/s. On the other hand, the map for 2010-2011 shows much weaker currents in this area on the northern coast. The current towards the east, visible near the centre line in the wider part of the GoF, is shifted towards the northern coast. Overall, the current speeds are lower than in 2007-2008.

### *3.4. SOM analysis of daily mean currents*

Averages of the circulation fields revealed interesting differences between the seasons. We used a one-dimensional SOM analysis to further understand how circulation varied during the modelling period on different timescales. We performed the analysis for daily mean velocity fields for the years 2007-2013. This averaging period is longer than the period of inertial oscillations in the Baltic Sea (about 14 hours) and shorter than the longest seiche periods in the basin (around 31 hours). Due to the nature of the algorithm, we estimated that occasional seiches would not affect the output of the clustering in a significant way. We tested this with a sensitivity study that showed filtering the input with a rolling mean filter (window from 1 to 10 days) caused only small changes in the output of the SOM algorithm. Cf. e.g. Leppäranta and Myrberg (2009) or Suhhova et al. (2018) for a discussion of periodic oscillations in the Baltic Sea.

Modelled currents were analysed by extracting 7 north-south sections along the domain from 24 °E to 28 °E (cf. Fig. 1). Locations of these sections were chosen so they would represent topographically and dynamically different domains of the GoF. The easternmost was located in the transitional area between the Neva estuary and the wider gulf, then two in the wider part of the basin between 26 °E and 27 °E. The rest were in the western gulf. Each of these sections were separately analysed. Vertical velocity was omitted from the analysis; only horizontal velocity components were considered. The number of nodes was set to five, which provided an acceptable compromise between the generality of the information, easy interpretability, and the level of detail.

The resulting maps for four of these sections are presented in Figs. 4, 5, 6 and 7. As we chose to use five map nodes, we see five current patterns in each map. Each of these characteristic patterns represents a number of daily current fields that the algorithm has determined to belong to the same cluster. The patterns are topologically ordered on a 1D line so that patterns next to each other represent clusters that the algorithm considers similar. Conversely, patterns furthest away from each other at both ends of the map are considered by the algorithm to represent clusters that differ most from each other. Each pattern or node, numbered here from 0 to 4, also shows the percentage of daily fields that fall into this cluster. For example, in Fig. 4 we see that node 0 shows inflowing currents in the deepest parts of the section, and outflowing currents near the surface. Node 4 shows the opposite. Between these two outermost cases, there

are patterns depicting what seem to be transitional states between the two.

The BMU time series corresponding to the map in Fig. 4 is shown in Fig. 8. For each day in the model run, it shows which cluster that day belongs to. From the BMU time series, we see that there is inter-annual variability and frequent changes of the best matching node. BMU plots for the other sections (not shown) are similar overall, and the BMU is often the same at all the sections. There are some differences, however, and sections further to the east show more frequent and rapid changes of the BMU.

For all inspected sections, the results consistently showed a node in one end (node 4), where the zonal component of the surface current is towards east, either across the whole gulf or almost across the gulf. This depicts reverse estuarine circulation. The thickness of the surface layer varies, but it is most commonly less than 20 m. It is slightly thicker in the western sections than in the east. In the other end, there is a node that shows zonal currents that are mostly directed towards west on the surface (node 0). This depicts normal estuarine circulation.

Overall, nodes representing normal estuarine circulation display a more heterogeneous structure than nodes depicting reversed estuarine circulation. In many of the nodes representing normal estuarine circulation, there are maxima and minima present near the surface. If we compare these nodes to the mean circulation maps presented in Section 3.2, we see that those complex circulation patterns with numerous eddies and loops visible in those maps cannot emerge alone from averages of the relatively homogeneous and overall more barotropic circulation patterns that were observed in the model for reverse estuarine circulation. The nodes representing normal estuarine circulation are a significant contribution to the horizontal structures visible in the seasonal means.

In general, when moving from west to east, the sections display a gradually less regular structure. The shallower, wider part of the gulf in the east has a more complex bottom bathymetry, which also seems to affect the modelled patterns. The relative frequency of the two outermost nodes is quite close to each other for most sections, with both being the BMU for a little more than 1/5 of all days in the dataset. The transitional nodes are the BMU slightly less frequently. The transitional states depict situations where there is a significant amount of variability in the surface circulation, with non-permanent structures like loops or eddies near the surface.

The two outermost nodes shown in the SOM analysis can be more concretely understood by taking two example days when they were the best matching unit and then visualising the circulation in the GoF (Fig. 9). The case when node 4 was the BMU (2013-12-16) shows a uniform surface layer moving to the east and a compensating flow below it. This resembles reversed estuarine circulation. A comparison of this case from December 2013 to published observations from around this time (Lips et al., 2017, their Fig. 2) shows concurring results, with outbound currents in most of the water column, but also inbound currents near the surface. In the case when node 0 was the BMU (2013-01-21), the areas of strong westward surface flows are near the coasts, and strong flows are in general more jet-like. This more closely resembles normal estuarine circulation. In this case, current speeds seem to be overall slightly higher near the northern coast.

### *3.5. Wind forcing and currents*

Next, we compared the BMU at 24.04 °E to model wind forcing at the Kalbådagrund weather station to evaluate the connection between circulation patterns and wind forcing. The years 2011 and 2013 are shown in Figs. 10 and 11. In general, it seems that

there is a relation between wind and the BMU. We see that when southwesterly winds dominate, nodes indicating eastward flows near the surface are more frequent at 24.04 °E. An example of this can be seen in late 2011. This event from December 2011 to January 2012 was documented by Liblik et al. (2013), based on two ADCPs and CTD data. On the other hand, we see that in summer 2011, southwesterly and easterly winds alternate, and current nodes alternate as well. There is also an interesting period in late 2013, when southwesterly winds dominate for approximately three months. This is associated with reversed estuarine circulation in the model. This event is significantly longer in the model than the reversal event in 2011, which according to Liblik et al. (2013) was unusually large. Lips et al. (2011) reported observations for the latter part of the 2013 event, which show a qualitative agreement with the model. An outflowing compensating current is clearly visible in the current observations. Vertical CTD sections show a retreating salt wedge near the bottom during the event, also suggesting outflowing currents. (Modelled surface salinity in the GoF during the 2013 event is discussed further in Section 3.7.)

When we look at a histogram of wind direction for different nodes in Fig. 12, we see that reversal of estuarine circulation is clearly associated with southwesterlies and westerlies. There is another but smaller peak in the distribution for normal estuarine circulation for easterlies. Transitional nodes have a more even distribution. If we look at the corresponding histogram for wind speed (not shown), such clear differences are not observed. Reversed estuarine circulation is associated with slightly higher wind speeds, which is expected, as southwesterly winds tend to be stronger than easterlies in the GoF.

### *3.6. Seasonality of circulation, based on the SOM analysis*

The SOM analysis also allows a more fine-grained understanding of seasonal frequencies of different circulation types, for example by investigating the BMU hit count for each node for each day of the year over the whole modelling period (not shown). This means, that for each day of the year and for each SOM node, we calculate how many times that particular node is the BMU, summed over the modelled time period. This analysis revealed that the relative frequency of the nodes as the BMU changes from one season to another. No clear way to divide the year to different kinds of circulation regimes emerges from this analysis. Overall, we see that in our dataset fully developed reversed estuarine circulation is more common early and late in the year, while the transitional nodes are the best matching unit more frequently in the middle of the year. There is also a period in the autumn when normal estuarine circulation is more common. Another way of looking at the same situation is that from September to March transitional nodes are relatively rare, but from March to September they become more common. These results can also be compared to the division used by Soomere et al. (2011), where May–August is considered the calm period and October–March is considered the windy period. These time spans do not clearly stand out in our analysis.

### *3.7. Salinity gradients in the GoF*

One of the main features of the salinity field in the GoF is that surface salinity gradients across the gulf are slanted and the field is not homogeneous on sections across the gulf. Surface salinity is, on average, lower on the northern coast than on the southern coast. For example, Kikas and Lips (2016) reported an average salinity difference of roughly

0.5 g/kg on the Tallinn-Helsinki Ferrybox line for the years 2007-2013 (their Fig. 3). This salinity difference is one of the most important indirect observations suggesting that a cyclonic long-term mean circulation pattern exists in the GoF. The SOM analysis gives an intuitive way to understand how this horizontal salinity structure emerges from the daily circulation patterns.

As noted, the reverse circulation field is quite homogeneous near the surface, as are the transitional states closest to it. Therefore the asymmetry in the long-term salinity structure can only come about from the circulation nodes depicting normal estuarine circulation, where flow is more heterogeneous across the GoF. Typically during normal estuarine circulation, there are outflowing currents present in the model, often on both coasts. Currents near the northern coast are often stronger than near the southern coast, as was the case in Fig. 9.

The surface salinity fields in Fig. 13, taken from the model around the same time as the circulation maps in Fig. 9, demonstrate this process. In January 2013, after normal estuarine circulation had been the dominant unit in the SOM analysis for some time, the surface salinity field shows clearly slanted salinity gradients, with higher salinity on the southern coast than on the northern coast. In December, after reversed estuarine circulation had been dominant for most of autumn, the surface salinity field shows a more complex structure. This point is further elaborated when we compare the difference in the model salinity on the northern and southern coast of the model to the BMU from the SOM analysis (Fig. 14). We see that, on average, salinity is higher on the southern coast when normal estuarine circulation is the BMU. On the other hand, the salinity difference is smaller, or salinity can even be higher, on the northern coast when the SOM analysis suggests there was reversed estuarine circulation in the GoF. This comparison does not take into account the time it takes for the salinity field to react to changed circulation patterns. But it still shows that the BMU and salinity differences are connected to each other and that normal estuarine circulation is required to establish the long-term average salinity field.

## 4. Discussion

Seasonal averaging of the circulation fields revealed interesting differences between the seasons. In the spring, for example, there is often ice cover in the area early in the season and thermocline begins to develop closer to summer. We also know that in the spring, winds are generally weaker than on average, but runoffs are larger (as noted by e.g. Hela, 1952). These differences seem to show up in our results as weaker surface currents in the seasonal average and a stronger outflow from the GoF towards the Baltic Proper.

It is also worth considering the many features visible in the seasonal averages that were not visible in the mean of the whole simulation period. For example, there is at least some outflow visible near the northern coast in three of the four seasonal plots. But this feature is practically non-existent in the full mean, as inflowing currents in the same area late in the year overshadow it in the averages.

This same phenomenon was illustrated on a different scale in the BMU figures from the SOM analysis, where we can see several time periods when circulation quickly alternates from one outermost node to another (for example, in summer 2011). When an average field is calculated over a period of quick changes between different circulation patterns, this results in a pattern that in practice was not present during that period. Long-term patterns represent different processes from short-term patterns.

The modelled mean over the whole 7-year high-resolution model run of the GoF did

not reveal the classical cyclonic circulation pattern first described by Witting (1912) and later by Palmén (1930). However, our analysis suggests several reasons why this was so.

Variation from one year to another is an important factor. As our analysis showed, for some periods the mean circulation field resembles more the classical cyclonic pattern than for other periods. The choice of averaging interval is always subjective. A full analysis of inter-annual variability of circulation patterns in the GoF would require a multi-decadal high-resolution model run, which currently does not exist and would be computationally extremely demanding. This is therefore left for future studies.

In addition to inter-annual variability, our study underlines the importance of wind forcing for the long-term mean circulation field in the Gulf of Finland. From our analysis, it is possible to see how different patterns contribute to the long-term means. Differences in forcing can lead to differences in the frequencies of the BMU nodes. If model forcing over- or under-represents some particular wind circumstances, these errors accumulate in the long-term averages. For example, from our analysis it seems that common-enough standard estuarine circulation is required for the cyclonic mean circulation pattern to emerge. Therefore, differences in wind direction distribution affecting the frequency of standard estuarine circulation may be one factor why some authors have obtained the classical cyclonic mean circulation pattern while some have not. For instance, if the wind direction distribution in the model forcing data has too frequent southwesterlies, the cyclonic mean circulation pattern would be weaker in the model than in reality.

Westerlund et al. (2018) also presented maps of the long-term mean circulation in the Gulf of Finland. There were some differences between the results, most of which are likely normal variability between the years and due to differences in methodology. For example, the overall values of mean currents were slightly greater in Westerlund et al. (2018), but as that paper had a shorter averaging interval than this study, it was expected. Westerlund et al. (2018) used data gathered from the operational FMI-HIRLAM model as atmospheric forcing. This paper used the EURO4M atmospheric reanalysis. By comparing the forcing datasets for the overlapping period of these studies, we saw that the FMI-HIRLAM forecasts represented extreme wind events better than the reanalysis product. This may also contribute to the differences in results.

The forcing is also an important difference between the model runs in this study and the ones presented in earlier studies, such as Andrejev et al. (2004). The meteorological dataset in Andrejev et al. (2004) had geostrophic wind forcing with one-degree resolution which was extrapolated to the sea surface and corrected with a constant multiplier. It is possible that with a higher resolution forcing with higher, more variable and less smooth wind speed and direction, the circulation features are less persistent than in the study by Andrejev et al. (2004). Further study is needed to investigate this more closely.

Andrejev et al. (2004) discussed the two-layer structure of the circulation in the GoF visible in their results. Circulation in the very top layer seemed to be mainly wind-driven, whereas in the layers below that a more permanent structure could be observed in their longer-term averages, with outflowing current near the northern coast. Our SOM analysis revealed that many of the nodes had a similar circulation structure to the one presented by Andrejev et al. (2004), even though it does not show up as clearly in the mean values over the whole period. It seems that the averaged current fields presented by Andrejev et al. (2004) correspond more closely to the transient nodes in our SOM analysis. It is possible to find points from the SOM analysis where the currents seem to be quite stable at certain depths.

Elken et al. (2011) and Lagemaa (2012) presented mean circulation maps for two periods partially covered by our analysis period, calculated from the HIROMB model

at 1 NM resolution. The map for 2006-2008 showed more features consistent with the cyclonic circulation pattern, with a relatively strong (around 5 cm/s) current along the northern coast of the GoF, and a number of loops in the southern side of the GoF. The map for 2010-2011 did not show such a strong current along the northern coast. Lagemaa (2012) also presented a map of the 2010-2011 circulation field run with a higher 0.5 NM resolution of the model. When we compare these maps to our results (see Section 3.3), we note that we saw similar differences in the mean circulation maps for 2007-2008 and 2010-2011 near the northern coast, although the magnitude of the currents was somewhat lower in our results. The map for 2007-2008 overall resembled more the traditional cyclonic pattern than the one for 2010-2011. We also note from their results that improved resolution intensified currents in many parts of the domain, for example in the southern coast west of Narva Bay, where their results show a relatively strong outward along-shore flow. This feature is similar to the one observed in our results, and it was discussed in length by Westerlund et al. (2018).

Lagemaa (2012) also presented an analysis of wind stress for the two periods discussed and noted that 2010-2011 saw much lower wind stresses along the dominating wind direction than 2006-2008. Our analysis shows that in addition to the wind stress, the wind direction distribution also needs to be considered. There were considerable differences in the wind direction distribution from one year to another, for example in the frequency of southwesterlies.

The results of the EOF/PCA analysis of GoF currents carried out by Elken et al. (2011) provide an interesting point of comparison for our results. They analysed the HIROMB model results for sections in the GoF. Decomposition of zonal currents into EOF modes revealed first what they called a 'barotropic mode' (42% of explained variance at a north-south section located at 24.38 °E), showing unidirectional currents in the water column. The second mode they called the 'Ekman mode' (18% of variance), which showed uniform currents in the upper part of the water column, but then a compensating current of opposite direction in the deeper part. The third mode (7% of variance) and the fourth mode (6% of variance) showed a clearly non-uniform structure in the meridional direction, unlike the two first modes. They identified the third mode as the 'Bennett-Csanady' mode, representing a situation in long channels where along-wind coastal jets are compensated by an opposite direction flow in the middle of the channel. As the SOM analysis identifies prototypical flow patterns and the EOF/PCA analysis is a linear decomposition of the flow field anomalies into modes, these two results are not directly comparable. But nevertheless, we can see how the structure of the nodes representing standard estuarine circulation and reverse estuarine circulation, and especially the most notable heterogeneous structures discussed in this article, can arise as a linear combination of these EOF/PCA modes.

Elken et al. (2011) divided the GoF into two regions based on circulation variability. The western region behaves like a wide channel, while the eastern region has a more complex circulation structure due to the topographical features and the vicinity of the Neva estuary. This was seen also in our investigation when sections from east and west were compared. Our analysis suggests that the transition between these two states usually takes place somewhere near 26 °E where the gulf widens. This is also consistent with the persistency maps by Andrejev et al. (2004), which showed lower values of persistency in the eastern parts of the GoF. The exact location of this transition zone can of course vary in time.

The SOM analysis revealed that in general the circulation patterns in the GoF can be classified with a one-dimensional presentation, with standard estuarine circulation in one end and reversed estuarine circulation in the other. The response of the circulation

field to changing forcing can be fairly rapid, although it may take a day or two due to the inertia of the system. Reversal of estuarine circulation has been studied in the Gulf of Finland by e.g. Elken et al. (2003), Liblik et al. (2013), Elken et al. (2014) and Lilover et al. (2017). This means events where southwesterly winds push the surface waters towards the head of the estuary and deeper waters are flowing outwards. Southwesterly winds dominate in the area, and the long axis of the gulf is oriented roughly in the west-east direction. These two factors together support reversal of the estuarine circulation. Our study suggests that in our data, standard and reversed estuarine circulation are roughly as common, although further study is required to build confidence in what the exact percentages of the two modes are in the GoF overall.

Some indication of the relative frequencies can be inferred from the analysis of flow variability by Lilover et al. (2017), based on data from 10 ADCP installations between 2009 and 2014, measuring usually 4–5 months each. They analysed data from four installations near the thalweg and categorised the flow into four regimes: estuarine circulation (EC), reversed estuarine circulation (REC), unidirectional inflow (UIN) and unidirectional outflow (UOUT). They found that REC was the most common flow type in their data (EC 26%, REC 30%, UIN 25 %, UOUT 19 %). EC was more common in the summer (34 %) than in the winter (17 %). UIN was more common than UOUT in the winter but not in the summer. Overall their results show relatively common reversals of estuarine circulation, both in summer and in winter, as did our data. Due to differences in methodology, such as the definition of categories, the relative frequencies of the regimes presented by Lilover et al. (2017) are not directly comparable to our results. Further study would be required for comprehensive comparison and to pinpoint the reasons for the differences. For example, it is possible that some cases categorised as UOUT in their analysis might be reversed estuarine circulation in ours if the layer with eastwards flow in the surface is thin and that is not reliably captured by the ADCP measurement. (They report that uppermost reliable measurements were 5 m or 10 m below the surface, depending on the location.) The same is possible for UIN and standard estuarine circulation. Furthermore, our transitional nodes could be categorised in any of the categories in their analysis, depending on the exact location of the contours.

The analysis of surface salinity in the model revealed that the traditional surface salinity pattern with slanted salinity gradients and lower salinities on the northern coast than on the southern coast emerges from the highly variable currents in the GoF visible on the timescale of days. The heterogeneous structures in surface circulation during normal estuarine circulation supports this pattern, even though a cyclonic circulation pattern does not typically appear in daily averages. Furthermore, as the reversal of estuarine circulation was seen to disrupt the traditional salinity pattern, and as this reversal is associated with southwesterly winds, it is understandable that any changes in the wind direction distribution will also affect the salinity pattern. If reversals become more common, we can expect on average saltier water on the northern coast of the GoF and fresher water on the southern coast than now.

The results of this article rely mainly on model calculations, which is natural given that models enable the study of current patterns in a way that is not possible from spatially or temporally sparse observations. But it is important to keep in mind the value of observations. For example, existing long-term ADCP measurements (e.g. Rasmus et al., 2015; Lilover et al., 2017; Lips et al., 2017; Suhhova et al., 2018) and Ferrybox measurements (e.g. Kikas and Lips, 2016) could be used far more to build confidence in model results. These kinds of comparisons will be in a key role in the work to determine if in fact the long-term circulation patterns in the GoF are changing, as some of the recent modelling studies suggest. Also, new measurements could be helpful. For example,

a series of ADCP installations on ideally several latitudinal sections would enable a more detailed investigation of how well models are able to capture true circulation features.

Self-organising maps proved to be a powerful tool for the analysis of the circulation in the area. While they have been successfully used for numerous oceanographic applications around the world, to our knowledge this is the first application to the hydrodynamic modelling of the Baltic Sea. This analysis can be considered complementary to many more traditional techniques such as the EOF/PCA analysis.

As other techniques, SOM also has pros and cons. In addition to the general issues mentioned in Section 2.3, in our case the selection of input to the algorithm was non-trivial. We had to choose by hand which sections were analysed, as it was impossible to analyse the full model output at once due to computational limits. Although we tested several different locations for the sections, it is still possible that some other choice of sections would have resulted in differing results. The brute force way of addressing this problem would be to run the analysis again for larger parts of the output data at once, when available computing power allows it. Another issue that required consideration was how the input data to the algorithm should have been filtered to remove periodic motions. In the end, we opted to use daily averages, as the use of additional filtering did not seem to greatly affect the output of the algorithm. But for other applications and/or algorithms, it may be necessary to use a longer time-averaging window, for instance. Nevertheless, even with these limitations and when applied with care, these algorithms can provide significant insight into huge datasets.

Further applications of the SOM technique could be illuminating. For example, here we chose to use a relatively small, but robust 1D map to make the results more easily accessible. More detailed information might be extracted by using a more refined approach. One might, for example, try to use a larger 2D map to chart transitions from one circulation state to another. This method, along with other machine learning methods, could be applied more extensively, both to modelling and observational data sets in the future. It could be used, for example, as a tool for exploratory analysis of huge modelling or observational datasets.

## 5. Conclusions

We applied the NEMO 3D hydrodynamic model to the analysis of circulation patterns in the Gulf of Finland. Based on a high-resolution 7-year run of the model, we studied how circulation patterns in the GoF change from season to season.

The main conclusions are:

- There is clear seasonal variation in the circulation patterns in the GoF.
- In many cases, averages hide or dampen circulation patterns that move or change direction from season to season.
- SOM analysis of the modelled currents emphasised the estuarine character of the GoF. It showed how circulation in the gulf changes rapidly between normal estuarine circulation and reverse estuarine circulation, along with transitional states between the two. The dominant wind direction supports this reversal.
- The SOM analysis demonstrated that in our model results, both normal and reverse estuarine circulation are roughly as common in the GoF.
- The emergence of the cyclonic mean circulation pattern seems to require that standard estuarine circulation is common enough during the averaging period, as during standard estuarine circulation there are more heterogeneous structures in

the surface currents. A multi-decadal high-resolution model run would be required for a full analysis of inter-annual variability of circulation patterns in the GoF.

- The long-term surface salinity field structure in the GoF, where surface salinities are higher on the southern coast and across-gulf salinity gradients are slanted, is also supported by the heterogeneous structure of the surface currents during normal estuarine circulation. Surface currents during reversed estuarine circulation are quite homogeneous and do not support this structure.

## 6. Acknowledgements

We thank Kimmo Tikka for compiling the bathymetry for the Gulf of Finland and Simo Siiriä for assistance with the forcing data. Continued work on Baltic Sea NEMO has been possible over the years thanks to Jari Haapala and other colleagues at FMI. The bathymetric data was obtained from the VELMU depth model (Finnish Environment Institute, `http://www.syke.fi/en-US/Open_information/Spatial_datasets`) and the Baltic Sea Bathymetry Database (Baltic Sea Hydrographic Commission, 2013) version 0.9.3, downloaded from `http://data.bshc.pro` on 25 Aug 2014. VELMU data is licensed under the Creative Commons BY 4.0 and BSBD data under the Creative Commons BY 3.0 licences (`http://creativecommons.org/licenses`). The Gulf of Finland Year 2014 data providers include Estonian Marine Institute (EMI); Marine Systems Institute (MSI); Finnish Environment Institute (SYKE); Uusimaa and South-East Finland Centres for Economic Development, Transport and the Environment (UUDELY and KASELY); City of Helsinki Environment Centre (HELSINKI); and North-West Interregional Territorial Administration for Hydrometeorology and Environmental Monitoring (HYDROMET).

## Disclosure statement

No potential conflict of interest was reported by the authors.

## Funding

This work has been partly financed by the Maj and Tor Nessling Foundation [grant numbers 201500179, 201600161, 201700056]; the EXOSYSTEM RUSPLUS_S&T_FULL-240 project; and the Finnish Ministry of Environment RaKi Nutrient Cycling project [project number 7020P-00696YMP01].

## References

Alenius, P., Myrberg, K., Nekrasov, A., 1998. The physical oceanography of the Gulf of Finland: a review. Boreal Environment Research 3 (2), 97–125.

Alenius, P., Nekrasov, A., Myrberg, K., 2003. Variability of the baroclinic Rossby radius in the Gulf of Finland. Continental Shelf Research 23 (6), 563–573.

Andrejev, O., Myrberg, K., Alenius, P., Lundberg, P. A., 2004. Mean circulation and water exchange in the Gulf of Finland – a study based on three-dimensional modelling. Boreal Environment Research 9 (1), 1–16.

BACC II Author Team, 2015. Second assessment of climate change for the Baltic Sea basin. Springer.

Cushman-Roisin, B., Beckers, J.-M., 2011. The Ekman layer. In: Cushman-Roisin, B., Beckers, J.-M. (Eds.), Introduction to Geophysical Fluid Dynamics, Physical and Numerical Aspects. Vol. 101 of International Geophysics Series. Academic Press, pp. 239 – 270.

Dahlgren, P., Landelius, T., Kållberg, P., Gollvik, S., 2016. A high-resolution regional reanalysis for Europe. Part 1: Three-dimensional reanalysis with the regional HIgh-Resolution Limited-Area Model (HIRLAM). Quarterly Journal of the Royal Meteorological Society 142 (698), 2119–2131.
URL http://dx.doi.org/10.1002/qj.2807

Dee, D. P., Uppala, S. M., Simmons, A. J., Berrisford, P., Poli, P., Kobayashi, S., Andrae, U., Balmaseda, M. A., Balsamo, G., Bauer, P., Bechtold, P., Beljaars, A. C. M., van de Berg, L., Bidlot, J., Bormann, N., Delsol, C., Dragani, R., Fuentes, M., Geer, A. J., Haimberger, L., Healy, S. B., Hersbach, H., Hólm, E. V., Isaksen, L., Kållberg, P., Köhler, M., Matricardi, M., McNally, A. P., Monge-Sanz, B. M., Morcrette, J.-J., Park, B.-K., Peubey, C., de Rosnay, P., Tavolato, C., Thépaut, J.-N., Vitart, F., 2011. The ERA-Interim reanalysis: configuration and performance of the data assimilation system. Quarterly Journal of the Royal Meteorological Society 137 (656), 553–597.
URL http://dx.doi.org/10.1002/qj.828

Elken, J., Nõmm, M., Lagemaa, P., 2011. Circulation patterns in the Gulf of Finland derived from the EOF analysis of model results. Boreal environment research 16, 84–102.

Elken, J., Raudsepp, U., Laanemets, J., Passenko, J., Maljutenko, I., Pärn, O., Keevallik, S., 2014. Increased frequency of wintertime stratification collapse events in the Gulf of Finland since the 1990s. Journal of Marine Systems 129 (Supplement C), 47 – 55.
URL https://doi.org/10.1016/j.jmarsys.2013.04.015

Elken, J., Raudsepp, U., Lips, U., 2003. On the estuarine transport reversal in deep layers of the Gulf of Finland. Journal of Sea Research 49 (4), 267 – 274, proceedings of the 22nd Conference of the Baltic Oceanographers (CBO), Stockholm 2001.
URL https://doi.org/10.1016/S1385-1101(03)00018-2

Falcieri, F. M., Benetazzo, A., Sclavo, M., Russo, A., Carniel, S., 2014. Po river plume pattern variability investigated from model data. Continental Shelf Research 87 (Supplement C), 84 – 95, oceanography at coastal scales.

Fraysse, M., Pairaud, I., Ross, O. N., Faure, V. M., Pinazo, C., 2014. Intrusion of Rhone River diluted water into the Bay of Marseille: Generation processes and impacts on ecosystem functioning. Journal of Geophysical Research: Oceans 119 (10), 6535–6556.

Hela, I., 1952. Drift currents and permanent flow. Soc. Scient. Fenn., Comm. Phys.-Math. XVI (14).

Hisaki, Y., 2013. Classification of surface current maps. Deep Sea Research Part I: Oceanographic Research Papers 73 (Supplement C), 117 – 126.

Hordoir, R., Axell, L., Höglund, A., Dieterich, C., Fransner, F., Gröger, M., Liu, Y., Pemberton, P., Schimanke, S., Andersson, H., Ljungemyr, P., Nygren, P., Falahat, S., Nord, A., Jönsson, A., Lake, I., Döös, K., Hieronymus, M., Dietze, H., Löptien, U., Kuznetsov, I., Westerlund, A., Tuomi, L., Haapala, J., 2018. Nemo-Nordic: A NEMO based ocean model for Baltic & North Seas, research and operational applications. Geoscientific Model Development Discussions 2018, 1–29.
URL https://dx.doi.org/10.5194/gmd-2018-2

Hordoir, R., Axell, L., Löptien, U., Dietze, H., Kuznetsov, I., 2015. Influence of sea level rise on the dynamics of salt inflows in the Baltic Sea. Journal of Geophysical Research: Oceans 120 (10), 6653–6668.
URL http://dx.doi.org/10.1002/2014JC010642

Hordoir, R., Dieterich, C., Basu, C., Dietze, H., Meier, H., 2013. Freshwater outflow of the Baltic Sea and transport in the Norwegian current: A statistical correlation analysis based on a numerical experiment. Continental Shelf Research 64 (0), 1 – 9.

Hsieh, W. W., 2009. Machine Learning Methods in the Environmental Sciences: Neural Net-

works and Kernels, 1st Edition. Cambridge University Press, New York, NY, USA.
Kikas, V., Lips, U., 2016. Upwelling characteristics in the Gulf of Finland (Baltic Sea) as revealed by ferrybox measurements in 2007–2013. Ocean Science 12 (3), 843–859.
URL http://dx.doi.org/10.5194/os-12-843-2016
Kohonen, T., 1982. Self-organized formation of topologically correct feature maps. Biological cybernetics 43 (1), 59–69.
Kohonen, T., 2001. Self-Organizing Maps. Physics and astronomy online library. Springer Berlin Heidelberg.
Lagemaa, P., 2012. Operational forecasting in Estonian marine waters. TUT Press, Marine Systems Institute at Tallinn University of Technology, Tallinn.
URL http://digi.lib.ttu.ee/i/?714
Landelius, T., Dahlgren, P., Gollvik, S., Jansson, A., Olsson, E., 2016. A high-resolution regional reanalysis for Europe. Part 2: 2D analysis of surface temperature, precipitation and wind. Quarterly Journal of the Royal Meteorological Society 142 (698), 2132–2142.
URL http://dx.doi.org/10.1002/qj.2813
Leppäranta, M., Myrberg, K., 2009. Physical oceanography of the Baltic Sea. Springer Verlag.
Liblik, T., Laanemets, J., Raudsepp, U., Elken, J., Suhhova, I., 2013. Estuarine circulation reversals and related rapid changes in winter near-bottom oxygen conditions in the Gulf of Finland, Baltic Sea. Ocean Science 9 (5), 917–930.
URL https://doi.org/10.5194/os-9-917-2013
Lilover, M.-J., Elken, J., Suhhova, I., Liblik, T., 2017. Observed flow variability along the thalweg, and on the coastal slopes of the Gulf of Finland, Baltic Sea. Estuarine, Coastal and Shelf Science 195, 23–33.
URL https://doi.org/10.1016/j.ecss.2016.11.002
Lips, U., Laanemets, J., Lips, I., Liblik, T., Suhhova, I., Ülo Suursaar, 2017. Wind-driven residual circulation and related oxygen and nutrient dynamics in the Gulf of Finland (Baltic Sea) in winter. Estuarine, Coastal and Shelf Science 195, 4–15.
URL https://doi.org/10.1016/j.ecss.2016.10.006
Lips, U., Lips, I., Liblik, T., Kikas, V., Altoja, K., Buhhalko, N., Rünk, N., 2011. Vertical dynamics of summer phytoplankton in a stratified estuary (Gulf of Finland, Baltic Sea). Ocean Dynamics 61 (7), 903–915.
URL http://dx.doi.org/10.1007/s10236-011-0421-8
Liu, Y., Weisberg, R. H., 2005. Patterns of ocean current variability on the West Florida Shelf using the self-organizing map. Journal of Geophysical Research: Oceans 110 (C6), c06003.
URL http://dx.doi.org/10.1029/2004JC002786
Liu, Y., Weisberg, R. H., 2011. A review of self-organizing map applications in meteorology and oceanography. In: Self Organizing Maps-Applications and Novel Algorithm Design. InTech.
Liu, Y., Weisberg, R. H., He, R., 2006a. Sea surface temperature patterns on the West Florida Shelf using growing hierarchical self-organizing maps. Journal of Atmospheric and Oceanic Technology 23 (2), 325–338.
URL https://doi.org/10.1175/JTECH1848.1
Liu, Y., Weisberg, R. H., Mooers, C. N. K., 2006b. Performance evaluation of the self-organizing map for feature extraction. Journal of Geophysical Research: Oceans 111 (C5), c05018.
URL http://dx.doi.org/10.1029/2005JC003117
Madec, G., the NEMO team, 2008. NEMO ocean engine. Institut Pierre-Simon Laplace (IPSL), France, note du Pôle de modélisation, No 27.
Maljutenko, I., Laanemets, J., Raudsepp, U., 2010. Long-term high-resolution hydrodynamical model simulation in the Gulf of Finland. In: Baltic International Symposium (BALTIC), 2010 IEEE/OES US/EU. IEEE, pp. 1–7.
Mikhailov, A. E., Chernyshova, E., 1997. General water circulation. In: "Baltica" Project, issue 5, part 2. Ecosystem models. Assessment of the modern state of the Gulf of Finland. Hydrometeoizdat, St. Peterburg, Russia, pp. 245–260, in Russian.
Myrberg, K., Ryabchenko, V., Isaev, A., Vankevich, R., Andrejev, O., Bendtsen, J., Erichsen, A., Funkquist, L., Inkala, A., Neelov, I., Rasmus, K., Medina, M. R., Raudsepp, U.,

Passenko, J., Söderkvist, J., Sokolov, A., Kuosa, H., Anderson, T., Lehmann, A., Skogen, M., 2010. Validation of three-dimensional hydrodynamic models of the Gulf of Finland. Boreal Environmental Research 15, 453–479.

Myrberg, K., Soomere, T., 2013. The Gulf of Finland, its hydrography and circulation dynamics. In: Preventive Methods for Coastal Protection. Springer, pp. 181–222.

Palmén, E., 1930. Untersuchungen über die Strömungen in den Finnland umgebenden Meeren. Soc. Scient. Fenn., Comm. Phys.-Math. V (12), in German.

Rasmus, K., Kiirikki, M., Lindfors, A., 2015. Long-term field measurements of turbidity and current speed in the Gulf of Finland leading to an estimate of natural resuspension of bottom sediment. Boreal Environmental Research 20, 735–747.
URL https://helda.helsinki.fi/handle/10138/228308

Soomere, T., Delpeche, N., Viikmäe, B., Quak, E., Meier, H. E. M., Doos, K., 2011. Patterns of current-induced transport in the surface layer of the Gulf of Finland. Boreal environment research 16, 49–63.

Soomere, T., Leppäranta, M., Myrberg, K., 2009. Highlights of the physical oceanography of the Gulf of Finland reflecting potential climate changes. Boreal environment research 14 (1), 152–165.

Soomere, T., Myrberg, K., Leppäranta, M., Nekrasov, A., 2008. The progress in knowledge of physical oceanography of the Gulf of Finland: a review for 1997-2007. Oceanologia 50 (3), 287–362.

Suhhova, I., Liblik, T., Madis-Jaak, L., Urmas, L., 2018. A descriptive analysis of the linkage between the vertical stratification and current oscillations in the Gulf of Finland. Boreal Environmental Research 23, 83–103.
URL http://www.borenv.net/BER/pdfs/ber23/ber23-083-103.pdf

Talley, L. D., Pickard, G. L., Emery, W. J., Swift, J. H., 2011. Gravity waves, tides, and coastal oceanography: Supplementary materials. In: Talley, L. D., Pickard, G. L., Emery, W. J., Swift, J. H. (Eds.), Descriptive Physical Oceanography (Sixth Edition), sixth edition Edition. Academic Press, Boston, pp. 1–31.

Thomson, R. E., Emery, W. J., 2014. The spatial analyses of data fields. In: Thomson, R. E., Emery, W. J. (Eds.), Data Analysis Methods in Physical Oceanography, 3rd Edition. Elsevier, Boston, pp. 313 – 424.

Tuomi, L., Myrberg, K., Lehmann, A., 2012. The performance of the parameterisations of vertical turbulence in the 3D modelling of hydrodynamics in the Baltic Sea. Continental Shelf Research 50, 64–79.

Vancoppenolle, M., Fichefet, T., Goosse, H., Bouillon, S., Madec, G., Maqueda, M. A. M., 2009. Simulating the mass balance and salinity of Arctic and Antarctic sea ice. 1. Model description and validation. Ocean Modelling 27 (1), 33–53.

Vankevich, R. E., Sofina, E. V., Eremina, T. E., Ryabchenko, V. A., Molchanov, M. S., Isaev, A. V., 2016. Effects of lateral processes on the seasonal water stratification of the Gulf of Finland: 3-D NEMO-based model study. Ocean Science 12 (4), 987–1001.
URL http://dx.doi.org/10.5194/os-12-987-2016

Westerlund, A., Tuomi, L., Alenius, P., Miettunen, E., Vankevich, R. E., 2018. Attributing mean circulation patterns to physical phenomena in the Gulf of Finland. Oceanologia 60 (1), 16–31.
URL http://dx.doi.org/10.1016/j.oceano.2017.05.003

Williams, R. N., de Souza, P. A., Jones, E. M., 2014. Analysing coastal ocean model outputs using competitive-learning pattern recognition techniques. Environmental Modelling & Software 57 (Supplement C), 165 – 176.
URL https://doi.org/10.1016/j.envsoft.2014.03.001

Witting, R., 1912. Zusammenfassende Uebersicht der Hydrographie des Bottnischen und Finnischen Meerbusens und der Nördlichen Ostsee nach den Untersuchungen bis Ende 1910. Soc. Scient. Fenn., Finländische Hydr.-Biol. Untersuchungen (7), in German.

**Table 1.** Modelled daily average temperatures and salinities from the NEMO model compared against CTD observations, 2007-2013. Three depths for three frequently sampled stations in the study area, from east (Haapasaari) to west (Längden). Model RMS errors and biases (°C, PSU) are shown. Positive biases indicate that the observational mean is larger than the model mean. N is the number of observations for each point.

| 2007-2013 | T | | S | | |
|---|---|---|---|---|---|
| Haapasaari | RMSE | Bias | RMSE | Bias | N |
| 5 m | 1.5 | -0.96 | 0.60 | 0.030 | 91 |
| 10 m | 1.4 | -0.50 | 0.47 | -0.17 | 91 |
| 20 m | 2.5 | -1.3 | 1.3 | -1.1 | 91 |
| Länsi-Tonttu | RMSE | Bias | RMSE | Bias | N |
| 5 m | 1.5 | -0.84 | 0.53 | -0.30 | 98 |
| 10 m | 1.7 | -0.40 | 0.57 | -0.37 | 99 |
| 20 m | 1.8 | -0.19 | 1.1 | -0.92 | 99 |
| Längden | RMSE | Bias | RMSE | Bias | N |
| 5 m | 1.6 | -0.84 | 0.64 | -0.54 | 121 |
| 10 m | 1.6 | -0.64 | 0.66 | -0.57 | 125 |
| 20 m | 2.0 | -0.62 | 1.0 | -0.88 | 125 |

**Table 2.** Wind forcing, RMS errors and biases (m/s). Positive biases indicate that the observational mean is larger than the forcing mean. N is the number of observations for each point.

| Kalbådagrund | Wind speed | | |
|---|---|---|---|
| 2013 | RMSE | Bias | N |
| FMI-HIRLAM | 1.9 | 0.8 | 9699 |
| EURO4M | 3.1 | 2.6 | 9699 |

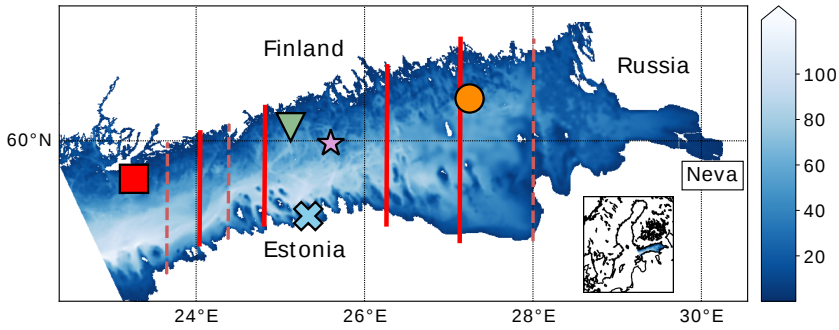


**Figure 1.** The model domain and bathymetry (in metres). CTD stations referenced in the article (from the east): Haapasaari (orange circle), Länsi-Tonttu (green triangle) and Längden (red square). Kalbådagrund weather station is marked with a magenta star. Station 18A used in analysis is marked with a blue X. Red lines show the location of the transects used in the analysis. Solid, darker lines indicate transects that were used for plots in this article. The map also indicates the approximate location of the Neva river mouth at the eastern end of the basin. The inset is the location of the model domain on a map of the Baltic Sea.

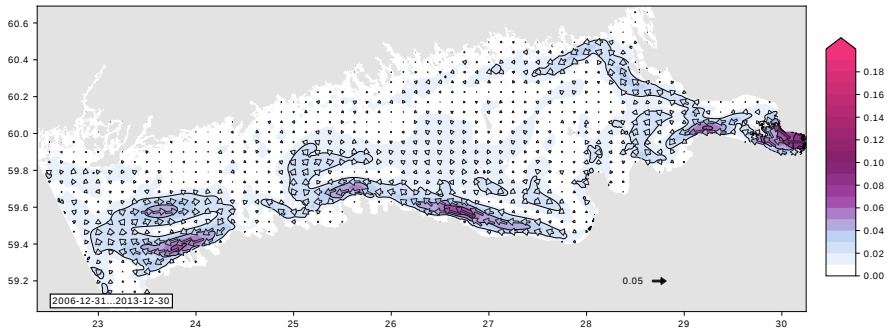


**Figure 2.** Annual mean circulation averaged from 0 m to 7.5 m depth for the years 2007-2013. Velocities are in m/s. Vector arrows are drawn for every 15 grid points in the longitudinal direction and every 13 grid points in the latitudinal direction.

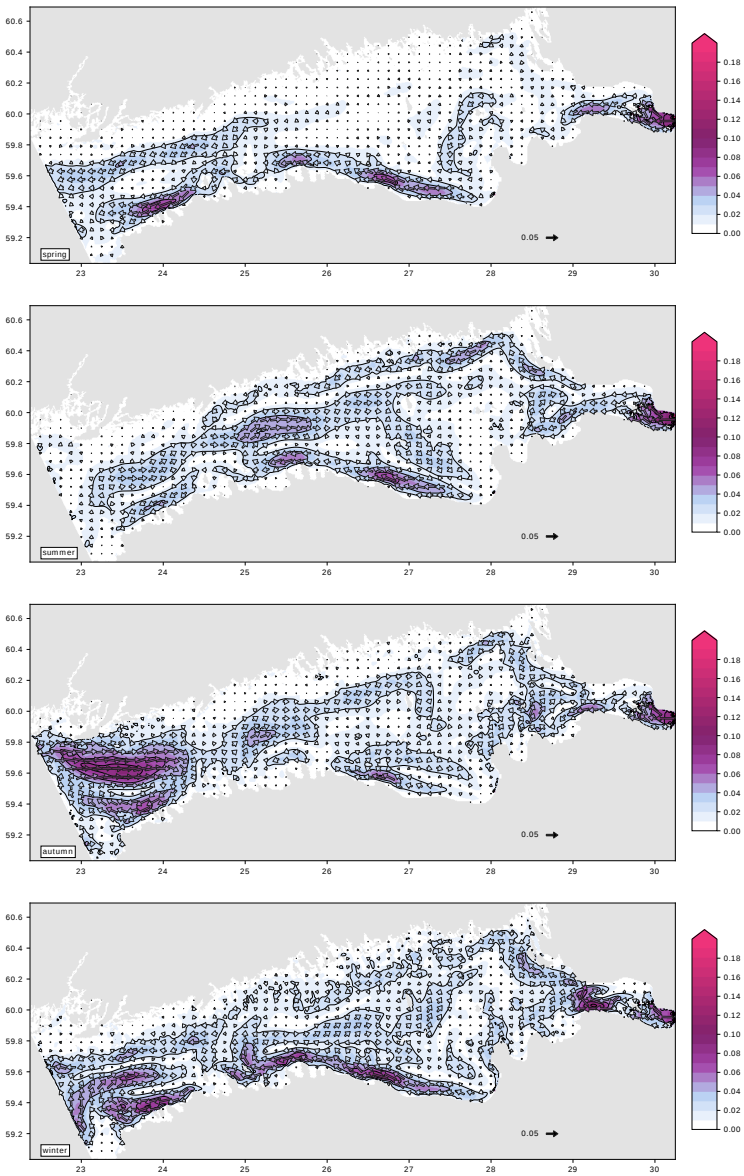


**Figure 3.** Mean circulation in 2007-2013 averaged from 0 m to 7.5 m depth for spring (top), summer, autumn, and winter (bottom). Velocities are in m/s. Vector arrows are drawn for every 15 grid points in the longitudinal direction and in every 13 grid points in the latitudinal direction.

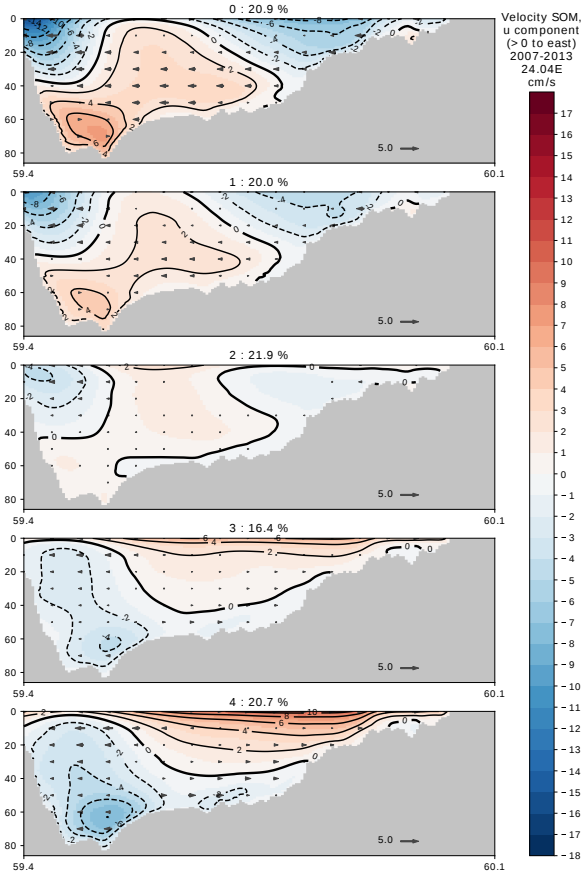


**Figure 4.** SOM patterns for modelled currents at a north-south section at 24.04 °E. Data covers the years 2007-2013. Nodes are numbered from 0 to 4. Frequency of occurrence as percentages is indicated for each node. Colour contours indicate the u component of velocity, with positive values (red hues) for eastward velocities (into the page). Grey vector arrows show the v component of the velocity field, with every tenth vector displayed. Velocities are in cm/s.

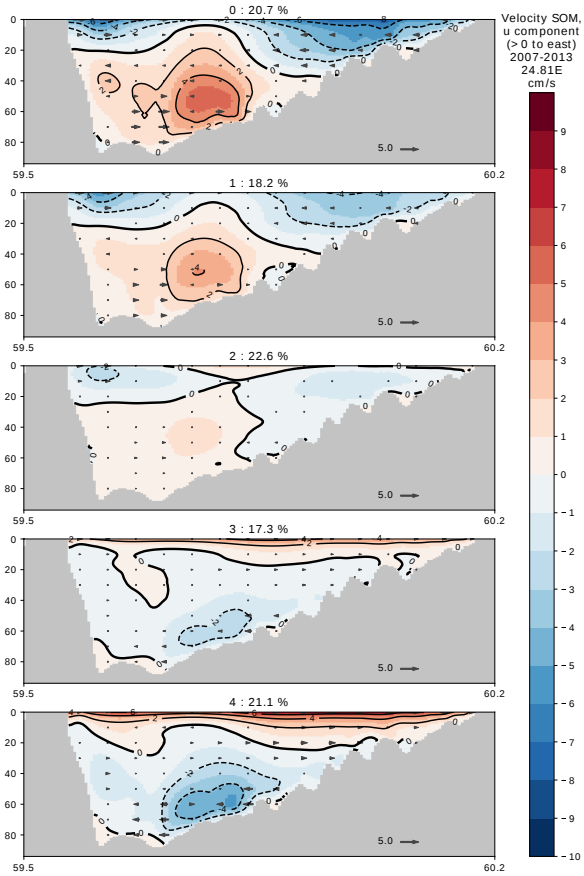


**Figure 5.** Like Fig. 4, but at 24.81 °E.

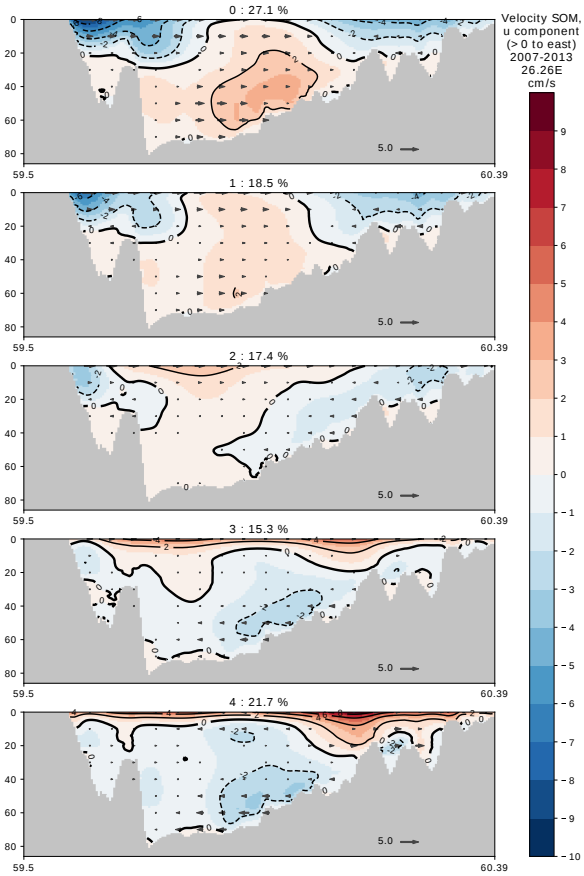


**Figure 6.** Like Fig. 4, but at 26.26 °E.

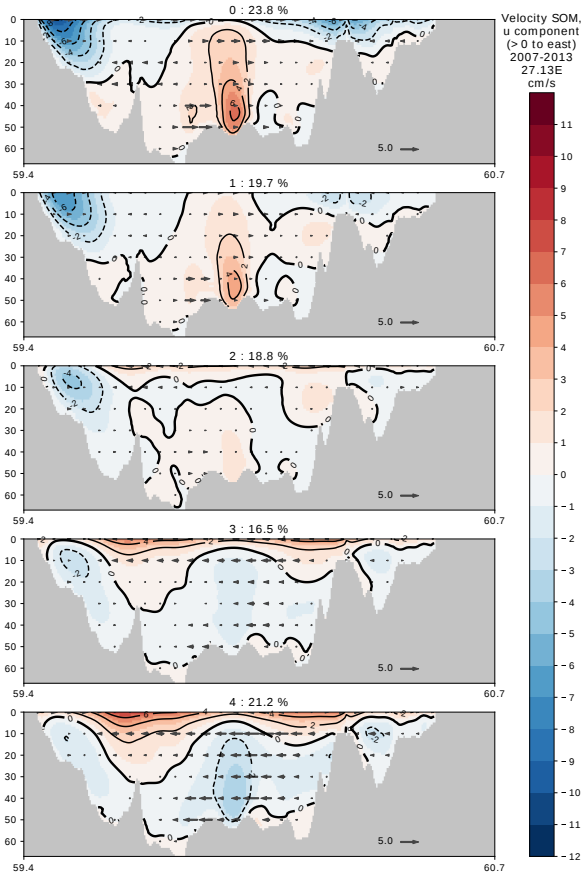


**Figure 7.** Like Fig. 4, but at 27.13 °E.

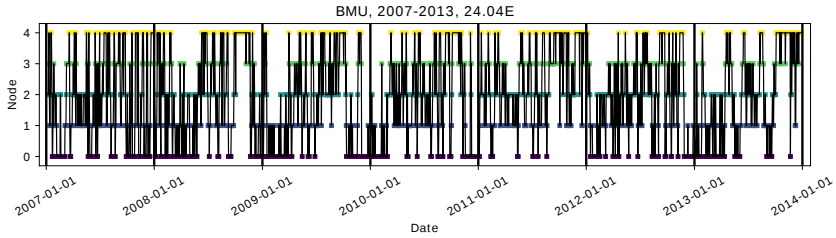


**Figure 8.** SOM BMU time series for the section in Fig. 4. Node numbers are the same as in Fig. 4.

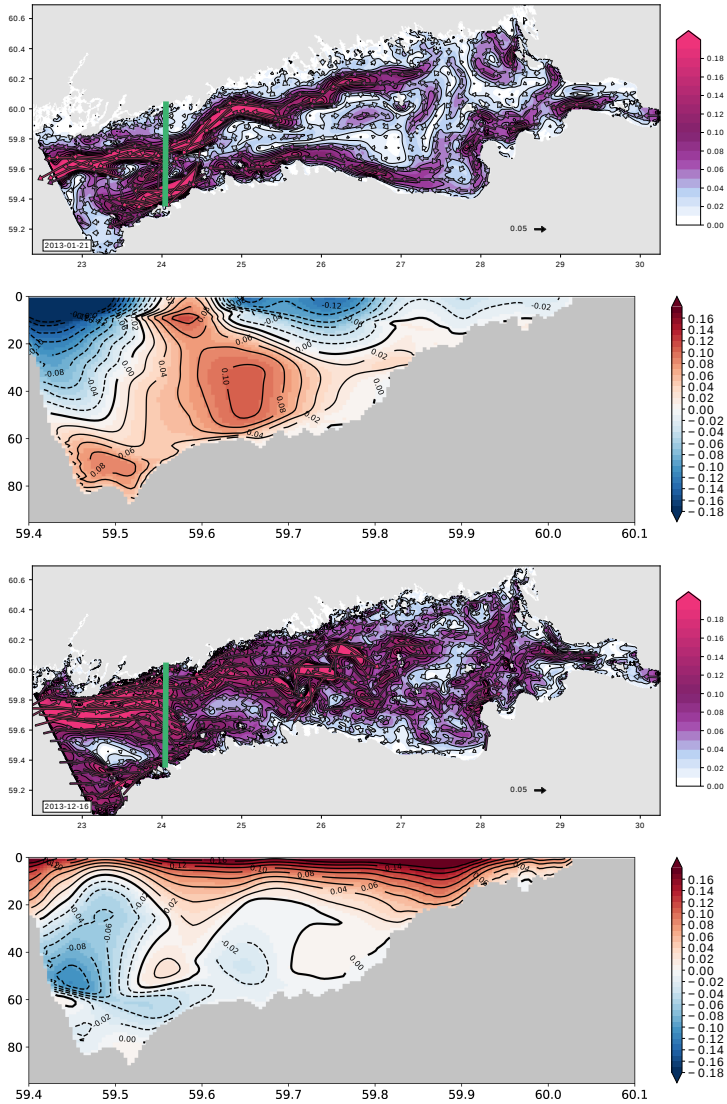


**Figure 9.** Daily mean velocity maps and zonal component of velocity at north-south section at 24.04 °E for 2013-01-21 (normal estuarine circulation) and 2013-12-16 (reversed estuarine circulation). Vector arrows are drawn for every 19 grid points in the longitudinal direction and every 17 grid points in the latitudinal direction. Location of the north-south section is indicated by a green line on the velocity maps.

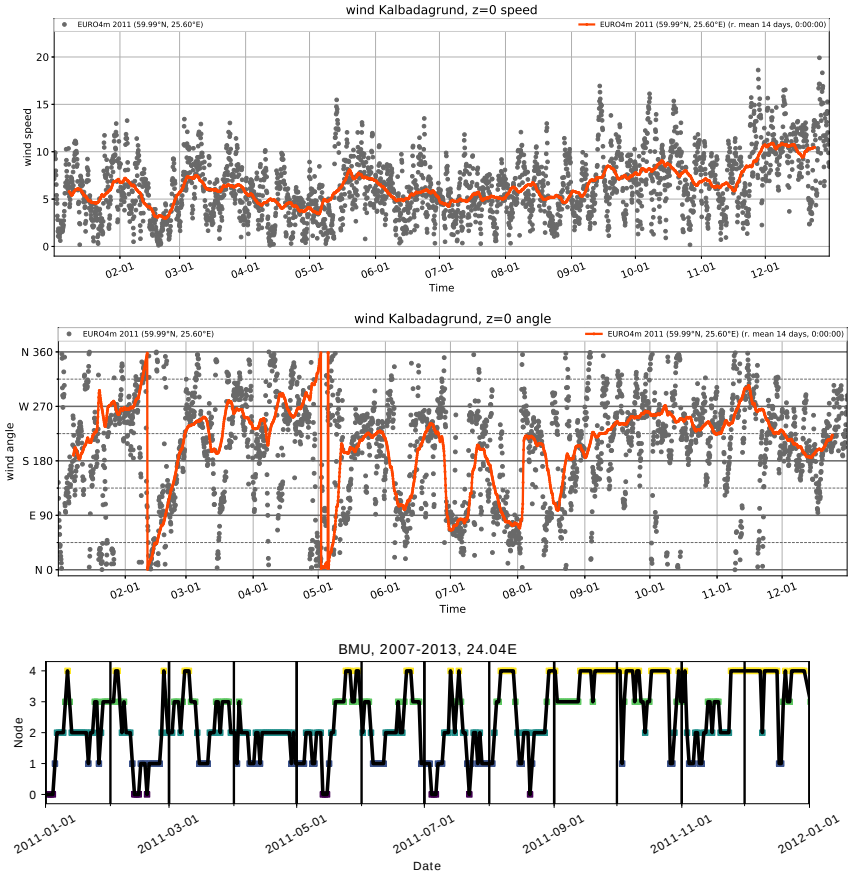


**Figure 10.** Top: wind speed and direction used as model forcing at Kalbådagrund, 2011 (black dots). 14-day running mean overlay (red line). Bottom: the BMU timeseries at 24.04 °E for the same period. Wind vector averages were calculated component-wise.

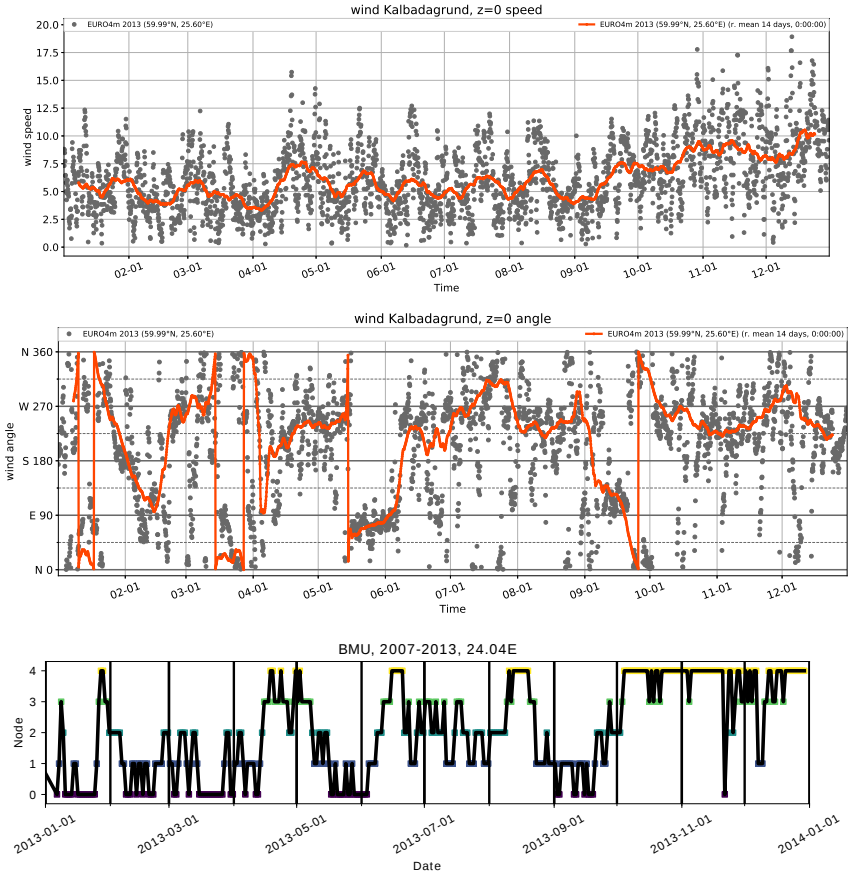


**Figure 11.** Like Fig. 10, but for 2013.

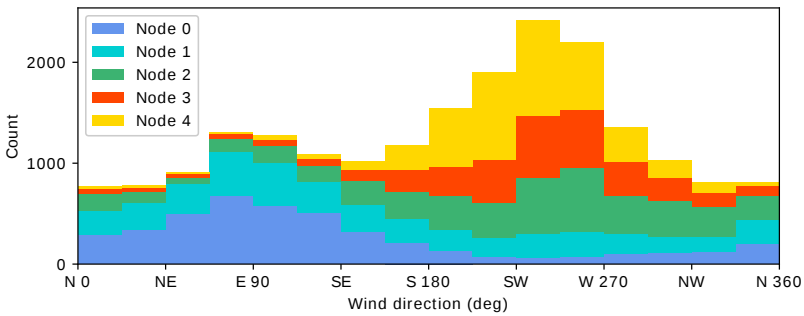


**Figure 12.** Wind direction distribution for BMU's of SOM nodes as a stacked histogram, 2007-2013. Wind direction taken from the model forcing at the Kalbådagrund station. BMU from the section at 24.04 °E.

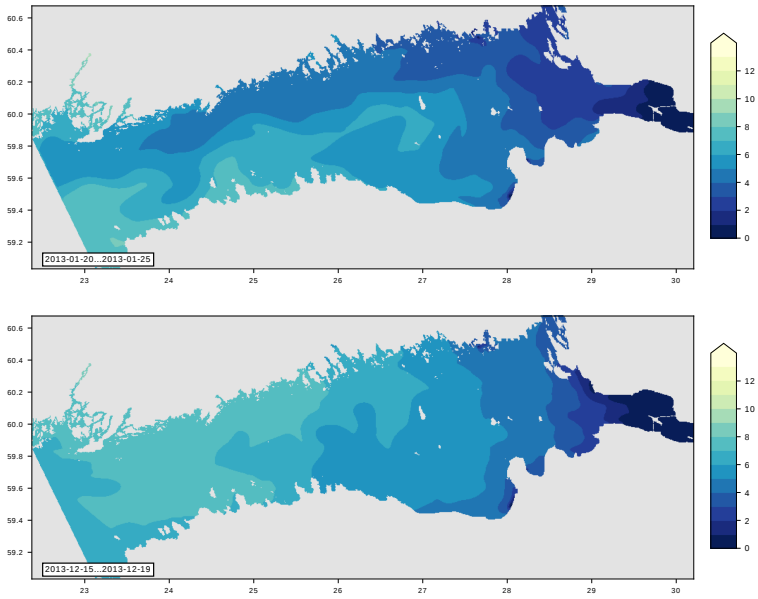


**Figure 13.** Mean surface salinity (PSU) in the model for late January 2013 and mid-December 2013 (cf. Fig. 9).

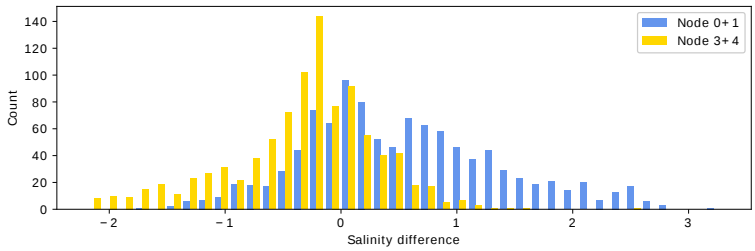


**Figure 14.** Histogram of modelled salinity (PSU) difference $\Delta S$ between northern and southern coast of GoF at 5 m depth, 2007-2013. Nodes 0 and 1 (standard estuarine circulation) and 3 and 4 (reverse estuarine circulation) are combined in this Figure. $\Delta S = S_{18A} - S_{LT}$, where $S_{18A}$ is salinity at station 18A near the southern coast and $S_{LT}$ at station Länsi-Tonttu near the northern coast (locations in Fig. 1).

**FINNISH METEOROLOGICAL INSTITUTE**
Erik Palménin aukio 1
P.O. Box 503
FI-00101 HELSINKI
tel. +358 29 539 1000
**WWW.FMI.FI**

FINNISH METEOROLOGICAL INSTITUTE
CONTRIBUTIONS No. 145
ISBN 978-952-336-054-9 (paperback)
ISSN 0782-6117
Erweko
Helsinki 2018

ISBN 978-952-336-055-6 (pdf)
Helsinki 2018